FILM FABRICATION USING CORNCOB AS LIGNOCELLULOSIC BIOMASS

A THESIS SUBMITTED TO
THE GRADUATE SCHOOL OF NATURAL AND APPLIED SCIENCES
OF
MIDDLE EAST TECHNICAL UNIVERSITY

BY

EYLÜL GÖKÇE ERGÜN

IN PARTIAL FULFILLMENT OF THE REQUIREMENTS
FOR
THE DEGREE OF MASTER OF SCIENCE
IN
CHEMICAL ENGINEERING

SEPTEMBER 2014

Approval of the thesis:

FILM FABRICATION USING CORNCOB AS LIGNOCELLULOSIC BIOMASS

submitted by **EYLÜL GÖKÇE ERGÜN** in partial fulfillment of the requirements for the degree of **Master of Science in Chemical Engineering Department, Middle East Technical University** by,

Prof. Dr. Canan Özgen ______________
Dean, Graduate School of **Natural and Applied Sciences**

Prof. Dr. Halil Kalıpçılar ______________
Head of Department, **Chemical Engineering**

Assist. Prof. Dr. Pınar Zeynep Çulfaz Emecen ______________
Supervisor, **Chemical Engineering Dept., METU**

Prof. Dr. Ufuk Bölükbaşı ______________
Co-Supervisor, **Chemical Engineering Dept., METU**

Examining Committee Members:

Prof. Dr. Levent Yılmaz ______________
Chemical Engineering Dept., METU

Assist. Prof. Dr. Pınar Zeynep Çulfaz Emecen ______________
Chemical Engineering Dept., METU

Prof. Dr. Ufuk Bölükbaşı ______________
Chemical Engineering Dept., METU

Assoc. Prof. Dr. Çerağ Dilek Hacıhabipoğlu ______________
Chemical Engineering Dept., METU

Assist. Prof. Dr. Mecit Öztop ______________
Food Engineering Dept., METU

Date: 01.09.2014

I hereby declare that all information in this document has been obtained and presented in accordance with academic rules and ethical conduct. I also declare that, as required by these rules and conduct, I have fully cited and referenced all material and results that are not original to this work.

Name, Last name: Eylül Gökçe Ergün

Signature :

ABSTRACT

FILM FABRICATION USING CORNCOB AS LIGNOCELLULOSIC BIOMASS

Ergün, Eylül Gökçe
M. S., Department of Chemical Engineering
Supervisor : Assist. Prof. Dr. Pınar Zeynep Çulfaz Emecen
Co-Supervisor: Prof. Dr. Ufuk Bölükbaşı

September 2014, 133 pages

Renewable biopolymer resource, lignocellulosic biomass, has emerged as an alternative raw material to petroleum-based resources for the sustainable production of materials, fuels and chemicals. In this study, the main focus was to constitute a novel and eco-friendly process to fabricate films from low value lignocellulosic agricultural residues in the absence of any additional film-forming compounds. In this scope, raw lignocellulosic biomass, namely corn cobs, was turned into films using the ionic liquid 1-ethyl-3 methylimidazolium acetate ([EMIM][Ac]) as solvent. Solution preparation conditions were 140°C dissolution temperature at 1 h dissolution time. Films were also fabricated from the fractions (cellulose and hemicellulose rich portions) of corn cob. Resultant corn cob based films were evaluated and compared in terms of their morphological and physical properties. Nodular, layered and macrovoid-free structure throughout the whole cross-section of the films was observed via SEM. Films were essentially transparent, hygroscopic and absorbed significant amount of moisture, which ranged from 46% to 104% in 100% relative humidity environment. Water sensitivity of the films was reduced by heat treatment performed at 200°C. On the other hand, heat treatment was found to decrease optical transparency and increase the stiffness of the films. Among the films, the lowest water vapor permeability (WVP) value (3×10^{-12}g.m^{-1}.Pa^{-1}.s^{-1}) was measured for the corn cob film coagulated in ethanol/water mixture. The ultimate tensile strength, elastic modulus and elongation at break values of the films were in the range of 36.9-56.0 MPa, 1700-3449 MPa and 1.4-3.8%, respectively.

Keywords: Ionic liquid, 1-ethyl-3-methylimidazolium acetate, Corn cob, Cellulose, Film

ÖZ

MISIR KOÇANINDAN FİLM ÜRETİMİ

Ergün, Eylül Gökçe
Yüksek Lisans, Kimya Mühendisliği
Tez Yöneticisi : Yrd. Doç Dr. Pınar Zeynep Çulfaz Emecen
Ortak Tez Yöneticisi: Prof. Dr. Ufuk Bölükbaşı

Eylül 2014, 133 sayfa

Yenilenebilir biyolimer kaynağı, lignoselülozik biyokütle, son zamanlarda malzeme, yakıt ve kimyasalların sürdürülebilir üretiminde petrol bazlı kaynakların yerine kullanılacak alternatif hammadde olarak ortaya çıkmıştır. Bu çalışmada, temel odak noktası düşük değerli lignoselülozik tarımsal atıklardan, film oluşumuna katkı sağlayacak herhangi bir katkı maddesi kullanılmadan, film üretilebilecek özgün ve çevre dostu bir süreç tasarlanmasıdır. Bu amaçla, ham lignoselülozik biyokütleden (mısır koçanı) iyonik sıvının, 1-etil-3 metilimidazolyum asetat ([EMIM][Ac]), çözücü olarak kullanılmasıyla filmler üretilmiştir. Optimum film üretimi koşulları 140°C çözdürme sıcaklığı ve 1 saat çözdürme zamanı olarak belirlenmiştir. Filmler ayrıca mısır koçanının alkali özütleme yoluyla ayrıştırılan selüloz ve hemiselülozca zengin kısımlarından da üretilmiştir. Elde edilen filmler fiziksel özellikleri ve morfolojileri açısından değerlendirilmiş ve karşılaştırılmıştır. Nodüler, katmanlı ve büyük gözeneklerin bulunmadığı yapı, filmlerin bütün kesit yüzeyleri boyunca taramalı elektron mikroskobu aracılığıyla gözlemlenmiştir. Transparan filmlerin higroskopik özellik gösterdiği ve %100 bağıl nem içeren ortamda önemli miktarda, %46-%104 aralığında, nem tuttuğu sonucuna varılmıştır. Filmlerin suya olan hassasiyetinin 200°C de uygulanan ısıl işlemle azaltıldığı sonucuna varılmıştır. Diğer yandan, ısıl işlemin filmin optik transparanlığını azalttığı, rijitliğini ise arttırdığı görülmüştür. Üretilen filmler içinde en düşük su buharı geçirgenliğine (3×10^{-12} $g.m^{-1}.Pa^{-1}.s^{-1}$) sahip filmin etanol/su karışımında çöktürülen film olduğu saptanmıştır. Maksimum çekme gerilimi, elastisite modülü ve kopma anındaki uzama değerleri sırasıyla 36.9-56.0 MPa, 1700-3449 MPa ve %1.4-3.8 aralığında bulunmuştur.

Anahtar kelimeler: İyonik sıvı, 1-etil-3-metilimidazolyum asetat, Mısır koçanı, Selüloz, Film

Anne ve babama

ACKNOWLEDGEMENTS

I acknowledge my advisors, Asst. Prof. Dr. Zeynep Çulfaz Emecen and Prof. Dr. Ufuk Bölükbaşı, who have provided guidance throughout my graduate studies with their patience, knowledge, and criticisms that helped to formulate new ideas along the way. I would like to express my gratitude to them for giving me the opportunity to be a part of this study.

I would like to thank my family for their patience, continued love and support. To my parents, Sevim and Metin, who are a constant source of inspiration and have always been a support mechanism. To my sister, Gülce, who always stands by me, and cheers me up when the times got rough. My completion of this work could not have been accomplished without them. My heartfelt thanks.

Finally, I am grateful to colleagues and friends for their friendship and support.

TABLE OF CONTENTS

CHAPTERS

APPENDICES

LIST OF TABLES

TABLES

LIST OF FIGURES

FIGURES

NOMENCLATURE

CC: corn cob
[EMIM][(MeO$_2$)PO$_2$]: 1-ethyl-3-methylimidazolium methyl phosphate
[EMIM][Ac]: 1-ethyl-3-methylimidazolium acetate
[Bz(m-ome)MIM][Cl]: 1-methyl-3-m-methoxylbenzylimidazolium chloride
[EMIM][XS]: 1-ethyl-3-methylimidazolium xylenesulphonate
[BzMIM][N(CN)$_2$]: 1-methyl-3-benzyl-imidazolium dicyanamide
[Bz(m-me)MIM][Cl]: 1-methyl-3 methylbenzylimidazolium chloride
[BMIM][SCN]: 1-butyl-3-methylimidazolium thiocyanate
[EOHMIM][Cl] 1-(2-Hydroxylethyl)-3-methylimidazolium chloride
[AMIM][Cl]: 1-allyl-3-methylimidazolium chloride
[BMIM][Cl]: 1-butyl-3-methylimidazolium chloride
[BMIM][OAc]: 1-butyl-3-methyltmidazolium acetate
[C$_4$MIM][Cl]: 1-n-butyl-3-methylimidazolium chloride
[EMIM][Ba]: 1-ethyl-3-methylimidazolium benzoate
[BMIM][Ba]: 1-butyl-3-methylimidazolium benzoate
[BMIM][Ac]: 1-butyl-3-methylimidazolium acetate
[AMIM][Br]: 1-allyl-3-methylimidazolium bromide
[HeMIM][Cl]: (2-hydroxyethyl)-3-methylimidazolium chloride
[DiMIM][MeSO$_4$]: 1,3-methylimidazolium dimethyl sulfate
[C$_2$MIM][OAc]: 1-ethyl-3-methylimidazolium acetate
RG cellulose: Regenerated cellulose
WVP: Water vapor permeability
MUP: Moisture uptake
PWP: Pure water permeability
DP: Degree of polymerization
RH: Relative humidity
UTS: Ultimate tensile strength
E: Elastic modulus
e_b: elongation at break
TGA: Thermal gravimetric analysis
FT-IR: Fourier transform infrared spectroscopy
XRD: X- ray diffraction
SEM: Scanning electron microscopy
LPDE: Low-density polyethylene
PS: Polystyrene
PET: Polyethylene terephthalate

PLA: Poly (lactic acid)
PP: Polypropylene
BSA: Bovine serum albumin
NMMO: N-methylmorpholine-N-oxide
DMAc/LiCl: N,N-Dimethylacetamide/lithium chloride
Water_CC: Water coagulated corn cob film
ETOH/Water_CC: 50-50 wt% ethanol-water coagulated corn cob film
1D_CC: Corn cob film conditioned 1 day in desiccator (RH=100%) before coagulated in water
2D_CC: Corn cob film conditioned 2 days in desiccator (RH=100%) before coagulated in water
5D_CC: Corn cob film conditioned 5 days in desiccator (RH=100%) before coagulated in water
Hemicellulose film: Hemicellulose (extracted from corn cob by alkaline extraction) based film
Cellulose film: Cellulose (extracted from corn cob by alkaline extraction) based film
Heated_CC: Water_CC film heated to 200°C for 24 hours

CHAPTER 1

INTRODUCTION

Petroleum based resources used for years as a starting material for chemicals, materials and biofuels had concerns for their future use associated with limited resources, increasing prices, and environmental issues (Sun et al., 2012). An intense interest has grown to find alternative starting materials for sustainable large-scale production of chemicals and biofuels (Hou et al., 2012). Lignocellulosic biomass has attracted attention as abundant, renewable and biological alternative resource to substitute petroleum based resources (FitzPatrick et al., 2012).

1.1. Lignocellulosic Biomass

Lignocellulosic biomass is a natural composite, synthesized by plant cells, comprised of three main biopolymers, cellulose, hemicellulose and lignin as well as other minor components (Harmsen et al., 2010; Brandt et al., 2013; Chen et al., 2014).

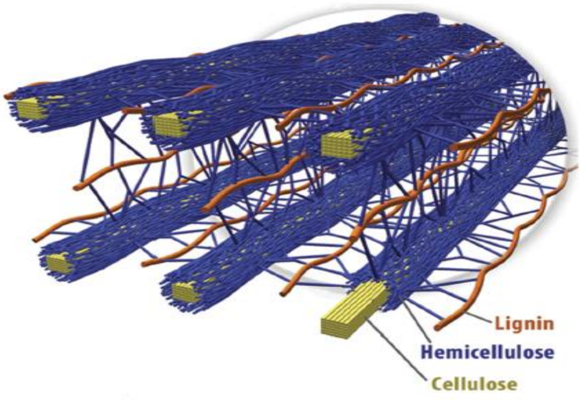

Figure 1.1. The structure of lignocellulosic biomass (http:// genomics.energy.gov)

It is available in high quantities as being the most plentiful material on the planet that makes up the cell walls of woody plants (Brandt et al., 2013). Lignocellulosic biomass intended for use in industry can originate from miscellaneous resources, such as agricultural and forest residues (Brandt et al., 2013). Depending on the plant species, plant parts, and growth conditions, structure and composition of lignocellulose can vary from one plant species to another (Zhang et al., 2007). Lignocellulose composition data in several agricultural residues and wastes is provided in Table 1.1.

Table 1.1. Lignocellulose composition of several agricultural residues and wastes (Sun and Cheng, 2002)

Lignocellulosic materials	**Cellulose (%)**	**Hemicellulose (%)**	**Lignin (%)**
Hardwoods stems	40-55	24-40	18-25
Softwood stems	45-50	25-35	25-35
Nut shells	25-30	25-30	30-40
Corn cobs	45	35	15
Grasses	25-40	35-50	10-30
Paper	85-99	0	0-15
Wheat straw	30	50	15
Sorted refuse	60	20	20
Leaves	15-20	80-85	0
Cotton seed hairs	80-95	5-20	0
Newspaper	40-55	25-40	18-30
Switch grass	45	31.4	12

1.1.1. Cellulose

Cellulose is an abundant and renewable polymer which makes up a large fraction (30-35%) of lignocellulosic biomass found in nature almost exclusively in plant cell walls. Cellulose is also known to be produced by a few bacteria (Lynd et al., 2002; Dadi et al., 2006; Brandt et al., 2013). Cellulose is a linear polymer composed of solely glucose units with the chemical formula of $(C_6H_{10}O_5)_n$. D-anhydroglucopyranose units are linked together through 1-4-β glycosidic bonds. A network of inter and intra-molecular hydrogen bonding and van der Waals forces joins together individual cellulose chains into flat sheets. Cellulose is reported to be in both crystalline and non-crystalline structure by Harmsen et al. (2010). Hydrogen bonds and van der Waals interactions between adjacent cellulose fibrils create a crystalline nature in cellulose which is unusual among polysaccharides (Lynd et al., 2002; Dadi et al., 2006). The structural order is observed by the location of atoms in discrete positions relative to each other in the crystalline cellulose.

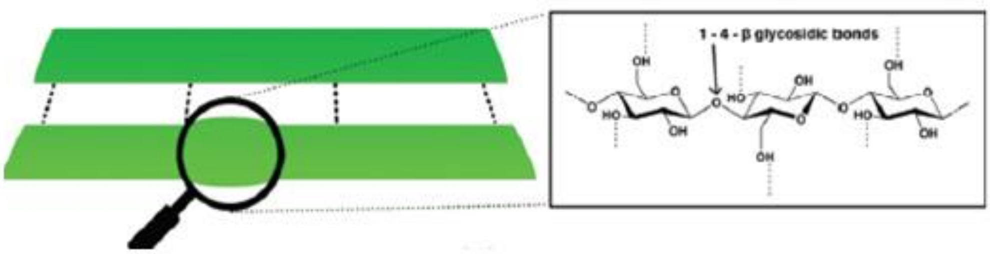

Figure 1.2. Structure of cellulose chain observed for cellulose with β-configuration (http:// genomics.energy.gov)

Tight packaging created between the molecules of micro fibrils avoids the penetration of molecules, such as enzymes or water and makes the hydrolysis process of cellulose to manufacture simple sugars for fermentation to produce ethanol fuel and other bio-based products difficult (Lynd et al., 2002; Dadi et al., 2006).

Properties of cellulose were reported to be altered depending on its degree of polymerization (DP) which is defined as the number of glucose units that form one polymer molecule and commonly, a number of 800-10000 units is encountered for the DP of cellulose (Harmsen et al., 2010).

Under typical atmospheric conditions, i.e. 20°C, 60% relative humidity (RH), cellulose behaves as a hygroscopic material by absorbing 8-14 % water. Although glucose monomer is water-soluble, cellulose is insoluble in water due to its high molecular weight and comparatively low flexibility of its chains (Harmsen et al., 2010; Brandt et al., 2013). The decomposition of cellulose is also reported to initiate at 180°C, although the melting of it is not possible by heating (Thermowoodhandbook, 2003).

1.1.2. Hemicellulose

Hemicellulose is a group of polysaccharides and another constituent of lignocellulosic biomass that makes up roughly 25 wt% of it (Brandt et al., 2013). It behaves as an amorphous matrix material to hold stiff cellulose fibrils together by binding non-covalently to the cellulose fibril surfaces (Brandt et al., 2013). Harmsen and coworkers (2010) also defines the hemicellulose as a collective term since it represents a group of polysaccharides like arabino-xylans, gluco-mannans, galactans, and others that exist in the plant cell wall with different composition and structure depending on the source and method of extraction. In general, hemicellulose is a carbohydrate polymer comprised of hexose and pentose sugars whose structures shown in Figure 1.3 (the C6 sugars glucose, mannose, galactose and the C5 sugars xylose and arabinose). These carbohydrate polymers could be categorized as xylans (β-1,4-linked ᴅ-xylose units), mannans (β-1,4-linked ᴅ-mannose units), galactans (β-1,3-linked ᴅ-galactose units) and arabinans (β-1,5-linked L-arabinose units) depending on sugar units substituted with side chains (Spiridon and Popa, 2008).

For instance, galactoglucomannan is a branched hemicellulose found in softwood and its backbone is established by β-1, 4-linked ᴅ-glucopyranose ᴅ-mannopyranose units arbitrarily distributed in the main chain (Figure 1.4). Partial substitutions are possible with α -ᴅ-galactose side groups, which can be joined to both glucose and mannose units by an α-1,6- linkage (Sipiridon and Popa, 2008). Schematic representation of arabinoxylan is also provided in Figure 1.5.

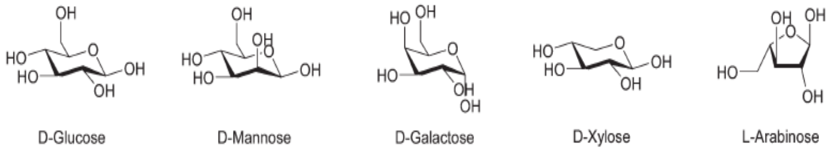

Figure 1.3. Common hexoses and pentoses existed in hemicellulose (Brandt et al., 2013

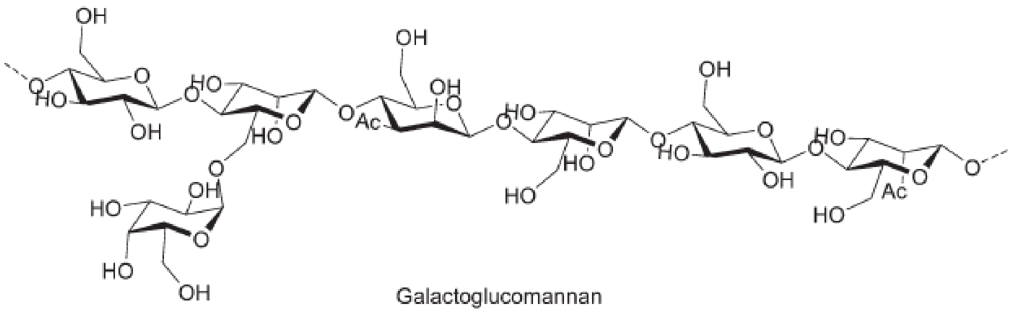

Figure 1.4. A schematic representation of branched-hemicellulose, galactoglucomannan (Brandt et al., 2013)

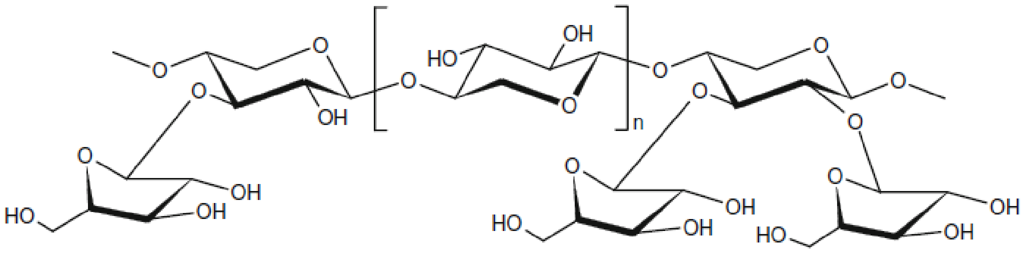

Figure 1.5. A schematic representation of rye arabinoxylan (Stevanic et al., 2012)

A significant characteristic of the structure of hemicellulose is the lack of crystalline structure as a consequence of the presence of highly branched structure and the acetyl groups connected to the polymer chain (Kirk-Othmer, 1983). Non-crystalline nature of hemicellulose makes it more susceptible to depolymerization as compared with cellulose. Molecular weight of hemicellulose is lower than that of cellulose (degree of polymerization around 150-200) (Harmsen et al., 2010; Brandt et al., 2013). Furthermore, unlike cellulose, hemicellulose is water-soluble at elevated temperatures (Thermowoodhandbook, 2003).

1.1.3. Lignin

Lignin is an aromatic, amorphous and three-dimensional macromolecule with phenolic monomers which becomes part of the composite after plant growth has finished. Predominant building blocks of lignin often encountered are p-coumaryl alcohol, coniferyl alcohol and sinapyl alcohol (Figure 1.6) (Harmsen et al., 2010; Brandt et al., 2013).

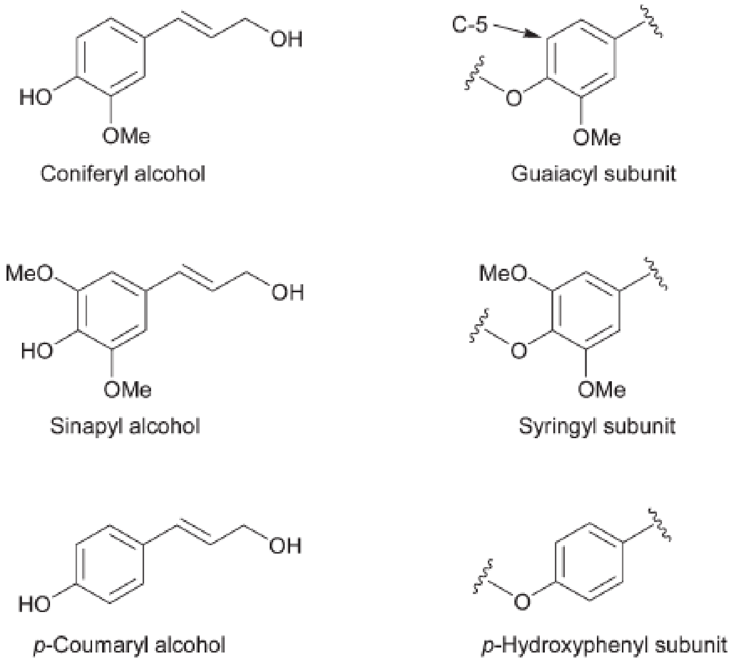

Figure 1.6. Building blocks of three-dimensional polymer lignin (Brandt et al., 2013)

It builds up the plant cell wall structure together with cellulose and hemicellulose and plays an important role in the cell's endurance and development by regulating the transport of water, nutrients and metabolites. Lignin provides a noticeable resistance against impact, compression, bending behaving as a binder between cells, and microbial decomposition. Following figure (Figure 1.7) represents the structure of lignin.

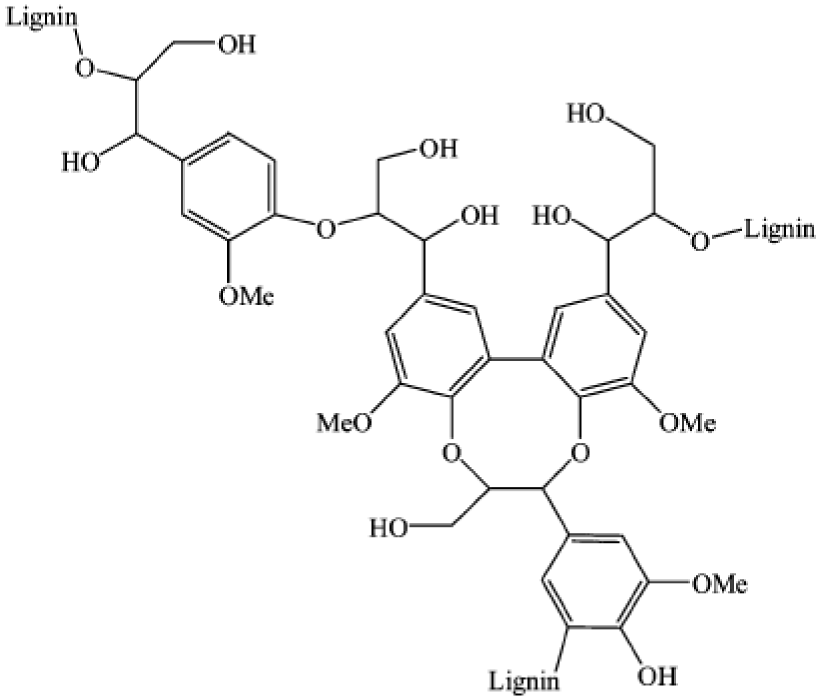

Figure 1.7. Representative structure of lignin (Sun et al., 2009)

1.2. Ionic Liquids

Ionic liquids, composed of entirely ions, are salts that melt below 100°C (Sun et al., 2011). Interest in ionic liquids stems from their properties such as non-volatility, non-flammability, and ease of recycling, thermal stability and could be traced back to mid-1990s (Sun et al., 2011; Muhammad et al., 2012; Brandt et al., 2013). These compounds are also called as "designer solvents" due to the existence of vast number of cation and anion combinations that can equate up to 10^{12} (Ni, 2012). Therefore, solvent properties of ionic liquids (such as viscosity, polarity, and hydrogen bond basicity) are reported to be tailored to specific applications (Mora-Pale et al., 2011; Ni, 2012). They have been subject of study of electrochemistry, extraction, organic synthesis, polymer chemistry, and biocatalysts, and more recently as solvents for the processing of lignocellulosic biomass.

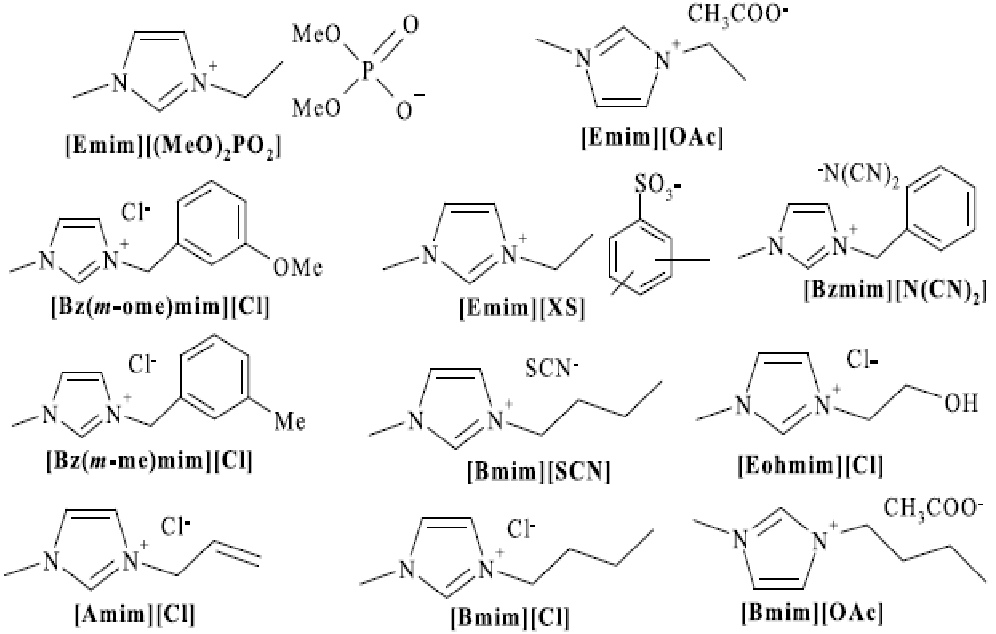

Figure 1.8. Abbreviations and structures of some ionic liquids, [EMIM][(MeO$_2$)PO$_2$]: 1-ethyl-3-methylimidazolium methyl phosphate [EMIMOAc]: 1-ethyl-3-methylimidazolium acetate, [Bz(m-ome)MIM][Cl]: 1-methyl-3-m-methoxylbenzylimidazolium chloride, [EMIM][XS]: 1-ethyl-3-methylimidazolium xylenesulphonate, [BzMIM][N(CN)$_2$]: 1-methyl-3-benzyl-imidazolium dicyanamide, [Bz(m-me)MIM][Cl]: 1-methyl-3 methylbenzylimidazolium chloride, [BMIM][SCN]: 1-butyl-3-methylimidazolium thiocyanate, [EOHMIM][Cl] 1-(2-Hydroxylethyl)-3-methylimidazolium chloride [AMIM][Cl]: 1-allyl-3-methylimidazolium chloride, [BMIM][Cl]: 1-butyl-3-methylimidazolium chloride, [BMIM][OAc]: 1-butyl-3-methyltmidazolium acetate (Muhammad et al., 2012)

Ionic liquids enable the production of biopolymer-based materials with the benefits of high solubility of biopolymers that cannot be dissolved with conventional organic solvents, greener procedures and easy fabrication of composites consisting of biopolymers and synthetic polymers (Lee et al., 2010). Therefore, ionic liquids are green solvents to prepare biodegradable cellulose and wood biomass derivatives and composites (Muhammad et al., 2012). As shown in Tables 1.2 and 1.3, ionic liquids are good solvents for different types of cellulose as well as for different biopolymers such as chitin and chitosan (Lee et al., 2010).

1.3. Biodegradable Polymers

Albertsson and Karlsson (1994) defines the term ‘biodegradation’ as an event that takes place through the action of enzymes and/or chemical decomposition related with living organisms (bacteria, fungi, etc.) and their secretion products. Polymers that undergo microbially induced chain scission leading to mineralization are called biodegradable polymers (Sinha et al., 2005). Certain conditions, such as pH, humidity, oxygenation and the presence of some metals are required to assure biodegradation of polymers. Biodegradable polymers may be originated from bio-resources (corn, wood cellulose, etc.) and petroleum sources as well as from mixed sources of biomass and petroleum. They can also be synthesized by bacteria from small molecules (polyhydroxyalkanoates, PHA and

Table 1.2. Cellulose solubility in ionic liquids (Zavrel et al., 2009; Lee et al., 2010; FitzPatrick et al., 2012)

Ionic Liquids	Type of cellulose	Solubility
[BMIM][Cl]	Avicel (DP 286)	18% (80^{o}C)
	Spruce sulfite pulp (DP 593)	13% (80^{o}C)
	Cotton linters	10% (80^{o}C), 10 wt% (ultrasound)
	Microcrystalline cellulose(Aldrich, 20 µm)	8 wt % (ultrasound)
[AMIM][Cl]	Microcrystalline cellulose(Aldrich, 20 µm)	2-11 wt% (80-100 ^{o}C), 27 wt% (ultrasound)

Table 1.2. Cellulose solubility in ionic liquids (Zavrel et al., 2009; Lee et al., 2010; FitzPatrick et al., 2012) (continued)

Ionic Liquids	**Type of cellulose**	**Solubility**
[AMIM][Cl]	Cotton linters	13 wt% (ultrasound)
	Kraft pulp (0.35 μm)	8 wt% (ultrasound)
	Cellulose	8-15t% (80^{o}C)
[EMIM][Ac]	Microcrystalline cellulose, Avicel	5%(w/w)(90°C,12 h)
	α-cellulose (typical fiber structure)	5%(w/w)(90°C,12 h)
	cellulose (Avicel PH-101)	4%(w/w)(75°C,1 h)
	Eucalyptus pulp (DP 569)	>14%
[EMIM][Cl]	Avicel (DP 286)	12% (10^{o}C above mp.)
	Spruce sulfite pulp (DP 593)	6% (10^{o}C above mp.)
	Cotton linters (DP 1198)	4% (10^{o}C above mp.)
	Eucalyptus pulp (DP 569)	>16% (vertical kneader)

Table 1.3. Some biopolymer solubility's in ionic liquids (Lee et al., 2010; Gao et al., 2012)

Ionic Liquids	**Biopolymer**	**Solubility**
[EMIM][Ba]	Heparin (imidazolium salt)	7.0% (35^{o}C)
[BMIM][Ba]		7.0% (35^{o}C)
[EMIM][Ac]	Corn starch	10%(w/w)(100°C,45 min)
	Corn starch	10%(w/w)(120°C,30 min)
[BMIM][Ac]	Chitin	6% (α-chitin, 110 ^{o}C),6-7% (low MW β-chitin, 110^{o}C), %3 (high MW β-chitin, 110^{o}C)
[BMIM][Cl]		partially soluble (α-chitin & low MW β-chitin, 110^{o} C), >10% (110^{o}C)
[BMIM][Ac]	Chitosan	12% (110^{o}C)
[BMIM][Cl]		10% (110^{o}C, DAC=5%), <10% (110^{o}C, DAC=12%)
[AMIM][Cl]		8% (110^{o}C)

polyhydroxybutyrates, PHB) (Sinha et al., 2005). Starch, cellulose or chitosan and proteins, such as casein and gluten could be given as the examples of nature based biodegradable polymers extracted from biomass. Polymers derived from renewable resources (such as, polylactides, PLA), are gaining much more attention due to their inherent eco-friendly properties as compared to fully petroleum-source derived biodegradable polymers (aliphatic polyester or aliphatic-aromatic copolyesters) (Sinha et al., 2005). Renewable sources of polymeric materials have recently attracted interest due to their potential to bring solutions to waste-disposal problems caused by conventional petroleum-based plastics (Mohanty et al., 2000). Research and innovations for the use of such polymers are expected to allow the reduction in the volume of garbage and compost-ability in the natural cycle, preservation of fossil-based raw materials, reduction of carbon dioxide release and the production of bio/green materials (Mohanty et al., 2000). Biodegradable polymers are estimated to compete with commodity plastics in the near future; however, brittleness, low heat distortion temperature, high gas permeability, low melt viscosity for further processing etc., are drawbacks that restrict their utilization in a wide-range of applications (Sinha et al., 2005). The production of ‘next generation materials’ seems to be possible with the formidable modifications to be done through innovative technology to biodegradable polymers (Sinha et al., 2005). Current research on biodegradable polymers is connected with many areas of use, such as biodegradable plastics, biomedical applications (e.g. wound dressings, drug delivery applications, and surgical implants); agricultural uses (e.g. controlled release of fertilizers and pesticides), applications in the automotive industry and as surfactants (Amass et al., 1998).

Biopolymer based materials prepared with ionic liquids are also reported to have the potential to be used in a variety of application areas. They can be employed in biomedical applications owing to their biocompatibility and biodegradability (Lee et al., 2010). On the other hand, biodegradable materials processed with ionic liquids have also the potential to be employed in the packaging market instead of synthetic petrochemical-based packaging materials due to the concerns on limited natural resources and the environment. Packaging materials, after finishing their lifetime, are needed to biodegrade within a reasonable period of time to prevent waste disposal problems. In this sense, production of natural biopolymer based films that can replace their non-biodegradable petrochemical-based counterparts have been investigated through the studies in the literature.

The main objective of this study is to constitute a novel and environmentally benign process to fabricate films from low value lignocellulosic agricultural residues in the absence of any additional film-forming additives. For this purpose, films from raw lignocellulosic biomass, namely corn cob, were fabricated using ionic liquid, 1-ethyl-3 methylimidazolium acetate ([EMIM][Ac]) as solvent. On the other hand, the fractions of corncob (cellulosic and hemicellulosic portions) isolated from this agricultural waste via alkaline extraction were used to prepare corn cob cellulose and hemicellulose based films. Films fabricated directly from corn cob or its fractions were compared in terms of their morphological and physical properties. Utilization of the corncob cellulose based film as a membrane was also investigated via pure water permeance and retention of bovine serum albumin and sodium alginate.

CHAPTER 2

LITERATURE SURVEY

2.1. Cellulose based materials

Consumption and over-exploitation of non-renewable resources have motivated researchers to focus on the development and utilization of natural polymers in recent decades (Feng and Chen, 2008).

Cellulose derivatives are a class of natural polymers prepared via swelling and dissolving cellulose by means of a solvent prior to further processing to films, fibers, coatings, membranes or filaments (Paunonen, 2013). In the literature, cellulose derivatives are often produced and employed as an important raw material of biomaterials. Cellulose was reported to be functionalized in a solvent with various side groups to form derivatives, such as cellulose esters (cellulose acetate, cellulose triacetate, and cellulose acetate butyrate) and cellulose ethers (methylcellulose, hydroxypropyl methylcellulose, ethylcellulose, hydroxyethyl methylcellulose, carboxymethylcellulose, and hydroxyethylcellulose) as highlighted by Paunonen (2013).

Regenerated cellulose materials including fibers and films have existed on the market for one hundred years (Cao et al., 2009; Wawro et al., 2014). However, the traditional viscose route utilized to fabricate cellulosic materials necessitates the use of toxic and harmful chemicals detrimental to the environment and human health (Cao et al., 2009; Paunonen, 2013; Wawro et al., 2014).

Alternative solvent systems are sought throughout the world for efficient utilization of cellulose and its derivatives to diminish the consumption of limited fossil resources and to protect the environment accordingly (Pang et al., 2013; Wawro et al., 2014). N-methylmorpholine-N-oxide (NMMO) used as a new environmentally friendly, organic solvent for cellulose during the last three decades; however this dissolution process facing certain challenges related with its utilization, such as requirement of activation before dissolution, instability, and difficulty of recycling in addition to its high cost (Cao et al., 2009; Liu et al., 2011). Cellulose degradation, the demand for high temperatures and formation of by-products were also pointed as drawbacks of this solvent (Liu et al., 2011). As well as NMMO, a limited number of solvents have been employed to dissolve cellulose, such as N,N-dimethylacetamide (DMAc)/LiCl, NaOH/urea, dimethyl sulfoxide (DMSO)/tetrabutylammonium fluoride. However, these solvents have certain limitations; for instance, the recovery of NaOH/urea is difficult as the recovery is a common problem of binary solvent systems, whereas DMAc is volatile and harmful and tetrabutylammonium fluoride is toxic (Liu et al., 2011). To sum up, conventional production processes for cellulose derivatives are reported to require solvents with high ionic strength and harsh conditions such as alkalis, acids and high temperature. (Feng and Chen, 2008).

Therefore, the search for a new class of solvent that is environmentally benign with high cellulose solubility performance continues. Recently, ionic liquids have drawn a remarkable interest by being efficient solvents for the dissolution and pretreatment of cellulose which is revealed for the first time by Swatloski and coworkers (2002). The recent studies in the literature have been focused on the preparation of cellulosic materials using ionic liquid as solvent during the past several years (Li et al., 2011).

Turner et al. (2004) proposed a model system to investigate the entrapment of enzyme, laccase from *Rhus* V*ernificera* into cellulosic films fabricated by [C_4MIM][Cl]-cellulose dissolution and regeneration process, in an attempt to produce biologically active membranes. In the study it was aimed to eliminate chemical attachment employed in conventional procedures for the encapsulation or entrapment of an enzyme or a protein. Formation of thin cellulose films incorporating dispersed laccase enzyme revealed that active enzyme-encapsulated films can be fabricated following the methodology described. Ionic liquid precoating of enzyme prior to dispersion in the cellulose/ionic liquid solution was proven to increase the enzyme activity compared to that of untreated films. The finding was attributed to the stabilized microenvironment provided by the ionic liquid treatment.

Cao and coworkers (2009) obtained cellulose from corn husks via chemical extraction and regenerated the extracted cellulose using the ionic liquids viz., 1-allyl-3-methylimidazolium chloride [AMIM][Cl] and 1-ethyl-3 methylimidazolium acetate [EMIM][Ac] to cast regenerated corn husk cellulose (RCC) films. [AMIM][Cl] and [EMIM][Ac] were proven to be direct solvents for cellulose by means of FT-IR analysis. Resultant films regenerated both in [AMIM][Cl] and [EMIM][Ac] displayed relatively homogeneous macrostructure from the interior to the surface, indicating a rough and dense texture, through the SEM micrographs. RCC films prepared with [AMIM][Cl] outperformed the films cast from [EMIM][Ac] in terms of mechanical properties. Maximum strength of the RCC films prepared in [AMIM][Cl] was higher than films regenerated in [EMIM][Ac] (112 MPa vs. 47 MPa). Young’s modulus of RCC films prepared from [AMIM][Cl] was also found to be higher than that of regenerated cellulose films from [EMIM][Ac]. The study also showed that ionic liquids could be effectively recycled after regeneration of cellulose.

Takegawa et al. (2010) reported the fabrication and characterization of chitin/cellulose composite gels and films utilizing [AMIM][Br] and [BMIM][Cl] ionic liquids. Cellulose and chitin were dissolved in the two ionic liquids individually prior to mixing in the desired ratios at 100°C to get homogeneous mixtures. For the film production, obtained mixture was cast on glass plates, then soaked in water and finally left to dry. Miscibility among the polysaccharides and the ionic liquids in the materials was reported to be good and proven by means of TGA measurements. Mechanical behavior of the films was reported to be depending on the ratios of chitin to cellulose in the films. Films were found to be more brittle with the increasing ratio of chitin to cellulose in the film content. The fracture stresses and strains were measured in the range of 7.5–9.0 MPa and 3.7–11.0%, respectively.

All-cellulose nanocomposite films consisting of nanocrystalline cellulose (NCC) as fillers and regenerated cellulose as matrix were fabricated by Ma et al. (2011) via adding NCC to the cellulose ionic liquid ([HeMIM][Cl]) solution. NCC suspension was prepared by using a sulfuric acid solution (60 wt %) and then the resultant NCC was stored in the ionic liquid for further use. The presence of reinforcement material with increasing concentrations was found to improve optical transparency, thermal stabilities and mechanical properties of the films fabricated. Increasing NCC content (0 vs. 10 wt %) caused a marked enhancement in tensile strength (from 34.87 to 51.37 MPa). On the other hand, decomposition temperature and elongation at break of the films decreased with the increasing content of NCC from 5% to 25%. (elongation at break; from 15.90% to 2.11%, decomposition temperature; from 304.0°C to 294.2°C).

Regenerated cellulose fibers extruded from bagasse cellulose and wood cellulose solutions in ionic liquid (1-butyl-3-methylimidazolium chloride) [BMIM][Cl] were prepared via dry-jet and wet spinning method using water as precipitant by Jiang and coworkers (2011). A comparison between the properties of bagasse-based fibers and wood pulp based fibers was provided in the study. Ionic liquid regenerated cellulose exhibited improved heat resistant properties compared to raw cellulose powder. Bagasse cellulose and regenerated film was found to decay at low temperature, but with slow decomposition rate. This finding was explained with the lower polymerization degree of cellulose molecules in bagasse compared to that of cellulose molecules in wood (800-1200 vs. 1800-2000). Low molecular weight cellulose was reported to have a lower decomposition rate. The regenerated bagasse fibers illustrated a higher degree of crystallinity than the regenerated wood fibers fabricated under the same condition. Water washing during the fiber spinning was found to be necessary to eliminate ionic liquid residue from fibers through FT-IR analysis.

Stefanescu et al. (2012) prepared biocomposite films from cellulose and chitosan blends in ionic liquid solvent media (1-butyl-3-methylimidazolium acetate [BMIM][Ac]). Characteristic bands of cellulose and chitosan observed in FT-IR were also observed for the FT-IR spectra of their blends. The presence of chitosan was found to increase the thermal stability of cellulose by decelerating its thermal degradation. Furthermore, XRD results revealed that blending cellulose and chitosan caused to fabricate more amorphous materials. Observed morphology of the cellulose/chitosan blend film monitored via SEM was found to be quite different than that of pure chitosan film and reported to be depend on chitosan/cellulose weight percent ratio. Chitosan film had very porous and disorganized structure, whereas cellulose film had well-organized fiber-like network with voids ranging from 1.9 µm to 13.5 µm. Cracks with no particular order were observed in the cross section of blend films. A more compact structure with fewer parallel voids was observed for the films had 25 wt % chitosan compared to that of films with less than 25 wt% chitosan in their composition.

Mahmoudian and coworkers (2012) presented an environmentally friendly method to prepare regenerated cellulose/montmorillonite (RC/MMT) nanocomposite films by incorporating MMT into cellulose matrix using ionic liquid, 1-butyl-3-methylimidazolium chloride [BMIM][Cl] as solvent. Thermal stability, gas barrier properties, water absorption and mechanical properties of the films were also investigated to understand the effect of MMT loading. MMT incorporation to cellulose matrix was found to enhance the thermal stability of RC. 12% and 40% improvements were observed with the addition of 6 wt % MMT for the tensile strength and Young’s modulus of RC films. However, higher contents of MMT were found to be detrimental to tensile strength of the nanocomposite films as a result of aggregation of MMT particles. The elongation at break values of the films was measured to decrease from 7.5% to 4.5% as the

MMT content increased from 0 to 8 wt.%. A linear increase was observed for the Young's modulus of RC films with the increasing MMT loadings. O_2 and CO_2 permeability values were found to be decreased with increasing MMT concentration. Lowest O_2 and CO_2 permeability values measured were reported as 0.82 and 1.34 $*10^{-18}$ $m^3.m/m^2.s.Pa$ for RC film with the highest (8 wt %) MMT loading. MMT also improved the water absorption resistance of RC films as the 24 h water absorption of the nanocomposite films decreased from 90.2% to 61.3% when the MMT content in cellulose increased from 0 to 8 wt %.

Pang et al. (2013) employed different plasticizers to enhance mechanical properties of regenerated cellulose films using 1-allyl-3-methylimidazolium chloride [AMIM][Cl] as the solvent. Film was prepared by dissolving cotton fiber (5% weight of the ionic liquid) in [AMIM][Cl] prior to addition of plasticizers to film forming solutions. After that, mixture was cast on a glass plate and immersed in de-ionized water and washed thoroughly to get rid of ionic liquid. Obtained films were dried in atmosphere for 48 hours. Complete miscibility between cellulose and plasticizers was confirmed by SEM micrographs. All regenerated cellulose films displayed smooth and homogeneous structures with typical granular morphology and no sign of phase separation. It was also noted from the XRD measurements that regeneration in ionic liquid transferred the crystalline structure of cellulose from cellulose I to cellulose II. In addition, tensile strength and hydrophobicity of cellulose films blended with plasticizers were reported to be improved. Sorbitol, glycerol and carboxymethyl cellulose (CMC) were found to improve tensile strength of fabricated films by 44%, 46% and 58%, respectively. Furthermore, glycerol-plasticized regenerated cellulose film exhibited better thermal stability compared with other cellulose films.

Wawro and coworkers (2014) prepared films by casting solutions of cotton linters and a hydrothermally treated (HT) wood cellulose pulp in ionic liquid 1-ethyl-3-methylimidazolium acetate ([EMIM][Ac]). The impact of cellulose concentration in ionic liquid solution upon film casting process was investigated as well as the influence of composition of the coagulation bath *(*demineralised water-ethanol mixtures) and solution and coagulation bath temperature on the mechanical properties and morphology of the resultant cellulose films. Low cotton linter concentrations (2 wt %) were found to be not adequate to prepare a suitable film for analysis since samples were weak, brittle and opaque regardless of the precipitant employed at 20°C. Therefore, further trials were continued with 5 wt% solution of cotton linters in [EMIM][Ac]. High viscosity of 10 wt% cotton linter solution in ionic liquid made difficult to evenly spread the solution on the glass plate; therefore temperature was increased up to 80 °C. Transparent film with tensile strengths up to 103 MPa and elongation of 30% were fabricated by arranging the conditions. Thermally treated dissolving pulp was found to be appropriate to form cellulose films with high tensile strength. Dissolution time was found to be shortened (15 minutes) with the adequate processing of HT cellulose that avoids degradation of cellulose upon ionic liquid treatment.

2.2. Hemicellulose based films

Hemicellulose extracted from wood and agricultural resources have been shown as another future biorefinery product and studied as the raw material of value-added products such as biodegradable and edible films due to the growing needs to renewable raw materials in packaging applications. (Mikkonen et al., 2009; Mikkonen and Tenkanen, 2012). The applicability of these films is often measured with their thermal, barrier and mechanical features (Mikkonen et al., 2009).

Commonly, plasticizers (sorbitol, xylitol, glycerol and propylene glycol, etc.) are added or polymers (wheat gluten, carboxyl methyl cellulose, nanofibrillated cellulose and chitosan, etc.) are compounded along with hemicellulose to enhance film forming and other properties of these films in the literature.

Peroval and coworkers (2002) proposed to use industrial byproduct arabinoxylan which was extracted from maize bran as the raw materials of edible coatings and films. Four different fats which were palmitic acid, oleic acid, triolein, or a hydrogenated palm oil (OK35) were emulsified to fabricate composite arabinoxylan-based films with glycerol content. The effect of lipid addition was investigated through water barrier and mechanical properties. Lipid addition resulted to improve the water barrier efficiency of arabinoxylan based films. Ultimate tensile strength, elastic modulus and percent elongation values were measured as 26.5±4.1 MPa, 72.4±35.2 MPa, and 7.4±2.9% for the arabinoxylan based films, respectively. Arabinoxylan-based film emulsified with triolein fat illustrated the best mechanical behavior for ultimate tensile strength and percent elongation features.

Kayserilioglu et al. (2003) conducted a study where xylan was blended with wheat gluten at different ratios to produce biodegradable composite films. As well as the effect of xylan addition, it was aimed to examine the effect of different wheat gluten to xylan ratio, pH of the film-forming solution and drying conditions on mechanical and water vapor transfer rates of the films produced. The results revealed that films produced at pH 11 resulted in higher tensile strength value than the films prepared at pH 4. On the other hand, tensile strength was found to be not affected to same extent by addition of xylan and different drying conditions. Since xylan addition did not cause to measure lower tensile strength value for the films tested, at pH 11 up to 40% (w/w) xylan was found to be appropriate for use as an additive. Furthermore, drying under controlled conditions was proven to be ineffective in terms of tensile strength; therefore, room temperature drying was preferred at the situations where high tensile strength values are desirable. Increasing amount of xylan added to film forming solutions caused to produce less stretchable films. Elastic modulus of the films decreased when drying temperature was increased at pH 11. Film prepared with 9:1 wheat gluten to xylan ratio at pH 11 and dried under 80^{o}C at 35% RH gave the smallest water vapor transmission rate among all the films produced in this study. Additive xylan was found to have no effect on water vapor transmission rate.

Arabinoxylan-based thin edible films were fabricated by Zhang and Whistler (2004). Sorbitol, propylene glycol and glycerol were added as plasticizers to the film forming solutions at 0-20 wt % to study mechanical properties, and water vapor permeability as a function of these added plasticizers. Tensile strengths of propylene glycol, sorbitol and glycerol plasticized films were found to be varying between 53 to 61 MPa, 20-48 MPa and 10-47 MPa, respectively. Thus, tensile strength was reported to be changed much more with the changing sorbitol and glycerol content compared to the tensile strength of films with different propylene glycol content. Elongations were changing from 6 to 8%, 6 to 9% and 6 to 12%, respectively for the propylene glycol, sorbitol and glycerol plasticized arabinoxylan films. In this study, unplasticized hemicellulose based films had higher water vapor permeability values than those of films with low plasticizer content. High content of glycerol i.e., up to 10 wt. % caused an increase in water vapor permeability, which was attributed by the author to hygroscopic nature of the plasticizer. Sorbitol-plasticized film (13% sorbitol) was reported to have the best moisture barrier property with 23×10^{-12} g. m^{-1}.Pa^{-1}. s^{-1}.

Another study focused on the fabrication of oxygen barrier hemicellulose based films and coatings isolated from barley husks, was conducted by Höije et al. (2005). Comparative data was provided in the study on certain properties of the hemicellulose-rich fractions (AX1-AX4) gathered by four different isolation methods. Chlorite delignification was regarded as the most appropriate isolation method to fabricate films as the films produced from AX-3 fraction were light, homogeneous and transparent. Films produced from that fraction resulted in ultimate tensile strength (UTS) greater than 50 MPa, 2.5% elongation at break, and elastic modulus of 3000 MPa. Water content of the films was reported as 35.5±4.44% and 82.27±0.79%, respectively for 50% RH and 100% RH at which the water content measurements were carried out.

Hartman et al. (2006) manufactured new candidate renewable barrier films originated from the hemicellulose *O*-acetylgalactoglucomannan (AcGGM) which were intended to be used in food packaging applications. The hybrid films were fabricated from a physical blend of AcGGM and either alginate or carboxymethylcellulose (CMC). 21-25 wt% glycerol, sorbitol, and xylitol were added as plasticizer to the binary mixture of AcGGM/alginate or AcGGM /carboxymethylcellulose (CMC). Storage modulus of the films was measured under six different relative humidity environments up to 80%. AcGGM/alginate and AcGGM/carboxymethylcellulose (CMC) illustrated better mechanical behavior than the plasticized films that showed a drop in storage modulus with increasing humidity. On the other hand, films compounded with polymer blends maintained their mechanical behavior at elevated humidity environments. The highest elongation value was measured for the AcGGM film plasticized with glycerol which was reported as 195%, whereas AcGGM/CMC and AcGGM/alginate films gave 3 and 4% elongations, respectively. Lowest oxygen permeabilities were measured for AcGGM /CMC and AcGGM/alginate films as 1.28 and 0.55 (cm^3.µm)/ (m^2 .d. kPa), respectively. Sorbitol-plasticized AcGGM film had lower oxygen permeability than xylitol-plasticized film which was reported as 2 (cm^3.µm)/ (m^2.d.kPa). Highest oxygen permeability value was reported for glycerol-plasticized alginate-AcGGM film ((cm^3.µm)/(m^2.d.kPa)) whereas oxygen permeability measurements conducted at 50% RH could not be possible for glycerol-plasticized AcGGM film as glycerol started to soften the film at around 35% RH.

Goksu and coworkers (2007) produced composite films from cotton waste xylan with the addition of small amount of lignin. The study was reported to be the first that shows it is possible to fabricate the self-supporting continuous films from the least utilizable component of lignocellulosic biomass, xylan without introducing a plasticizer or an additive. Cellulose was separated from xylan and lignin by means of an alkaline solution, and then lignin was removed from xylan by ethanol washing. Continuous film formation could not be achieved using either pure cotton stalk xylan or commercial birchwood xylan, thus small amount of lignin was kept in xylan fraction during ethanol washing process for cotton stalk xylan film. Remaining lignin in the washing solution was introduced into commercial birchwood xylan film by evaporating ethanol. Cracks in film structure were disappeared when lignin was not completely removed from xylan and the presence of lignin was resulted in continuous and self supporting film formation. 1% (w/w lignin/xylan) was determined as the sufficient content for continuous film formation for both cotton stalk and birchwood xylan films. Ultimate tensile strength, strain at break and Elastic modulus of cotton stalk xylan film was found to be in a range of 1.08-1.39 MPa and 45-57%, and 0.11-0.49 MPa, respectively. Addition of glycerol caused to measure lower tensile strength as this value decreased from 1.34 to 076 MPa and much higher strain at break values. Increasing xylan concentration was reported to decrease water vapor transfer rates, whereas glycerol addition caused to measure higher water vapor transfer rates.

Another study conducted by Mikkonen et al. (2009) was focused on film forming properties oat spelt arabinoxylan for packaging purposes. Plasticizers, namely, glycerol and sorbitol were added to film forming solutions at different concentrations. Self-supporting continuous film formation could not be achieved from oat spelt arabinoxylan itself without the presence of an external plasticizer. UTS of glycerol-plasticized film were higher than sorbitol-plasticized film when the plasticizer content was 10 wt%, however this result was reversed with 40 wt% plasticizer content. Highest UTS and elastic modulus values was measured for 10 wt% glycerol-plasticized film as 25-30 MP and 1000-1200 MPa, respectively. Highest elongation at break value was recorded as 10-12% for 40 wt% glycerol-plasticized film. On the other hand, sorbitol-plasticized film was found to be better to retain its mechanical features during 5 months of storage. Sorbitol-plasticized films gave lower WVP results than the films plasticized with glycerol. At RH gradient of 0-54%, films with 10 wt% sorbitol content had WVP value of 1.1 g mm/(m^2.d.kPa).

Edlund et al. (2010) fabricated bio-based free-standing films and coatings from a wood hydrolysate and characterized the samples in terms of their tensile properties and water vapor transmission. A polysaccharide component either carboxymethyl cellulose (CMC) or chitosan was mixed to films prepared from wood hydrolysate. Free-standing smooth and transparent film production was reported to be possible with 10% (w/w) of CMC co-component content and all other wood hydrolysate/chitosan mixtures except the film with the highest chitosan content due to higher viscosity. An increase was observed for both tensile strength and strain values with the addition of polysaccharide co-components. Films containing co-component chitosan was found to have higher strength and strain at break values than CMC contained films. UTS value was measured up to a maximum of 62 MPa for chitosan co-component films. Elastic modulus of the films was also reported to increase with the increasing amount of co-component introduced. An application of the wood hydrolysate based material as a coating onto commercially used packaging PET films was also provided in the study. Coating was found not to effect tensile properties that would be detrimental to intact structure of PET films in packaging applications. Water vapor transmission rate of PET coated with wood hydrolysate containing 50% (w/w) of CMC and chitosan were recorded as 0.168 and 0.159 $g.day^{-1}. m^{-2}$, respectively which were lower than that of uncoated PET film (0.217 $g.day^{-1}. m^{-2}$).

Peng et al. (2011) proposed a method to fabricate hemicellulose based biomaterials of high quality by incorporating cellulose nano-fibers (CNFs) into xylan-rich hemicelluloses. Continuous self-supporting films were produced with the addition of CNF. Incorporation of 5 wt% CNF was found sufficient to improve film formation without cracks. Disappearance of cracks was interpreted to stronger mechanical strength and this was proven by the tensile testing results of composite films. Tensile strength and Young’s modulus reached up to 39.5 MPa and 3404 MPa, respectively with 20 wt% CNF content. Reported values were much higher than those of xylan film. Improvement in tensile strength was attributed to the high aspect ratio and strong interactions between CNF and the xylan-rich matrix.

Bahcegul et al. (2012) investigated the effect of alkaline pretreatment temperature with a multi-product perspective. The fractions of cotton stalks pretreated with alkaline at three different temperatures (25, 60 and 90°C) were used for the co-production of hemicellulose based films and glucose. Pretreatment temperature effect was evaluated in terms of glucose yield and properties of hemicellulose based films for cellulosic and hemicellulosic portions, respectively. The results revealed that hemicellulosic portion of cotton stalk was more sensitive to the alteration of alkaline pretreatment temperature. The films fabricated from fractions pretreated at higher temperatures had undesired features in terms of film formation property and the color of the films which was observed most apparently for pretreatment temperature at 90°C. This pretreatment temperature was also declared as bad choice considering the tensile properties since lower UTS and elongation at break values were measured compared to room temperature and 60°C pretreatments.

A comparative data on mechanical and barrier properties of arabinoxylan films was presented by Sárossy et al. (2013). Films were cast from water-extractable arabinoxylan from rye (WEH) or the fractions of WEH which were identified as WE-AX and β-glucans (BG). Furthermore, blended films of WE-AX and BG were fabricated with varying amounts of added BG (20:80; 50:50; 80:20 ratios). BG addition was found to significantly improve the tensile strength and elongation at break of rye WE-AX film and this finding was ascribed to intermolecular or physical interactions between the blended polysaccharides. Presence of BG resulted in an increase in average tensile strength from 15.7 to 32.8 MPa of WEH films; on the other hand, water content of the WE-X films at 98% RH did not change significantly with BG addition. Highest water content was reported as 55.6 wt% at 98% RH for one-component rye WEH film. In addition, the water vapor permeability was reported to increase with addition of increasing amounts of BG to WE-AX. At 0/52% RH gradient, lowest WVP value was measured for WEH films as 2.8±0.4 g.mm/(m^2.kPa.day).

Egüés and coworkers (2014) studied the preparation of arabinoxylan films extracted from agricultural waste, corn cobs, by solvent casting method. Three different samples which were corncob arabinoxylan (CCAX), washed CCAX (indicated as W), bleached CCAX (indicated as B) were prepared to fabricate films. Purification process employed for arabinoxylan samples which was the raw material of the films produced was found to enhance the tensile properties of the films produced. Tensile strength and Elastic modulus were increased from 9 to 53 MPa and from 293 to 1600 MPa, respectively while elongation at break remained constant at around 8% for both untreated and purified CCAX. Further acetylation step was applied on washed and bleached CCAXs and highest values of tensile strength (67 MPa), elongation at break (13.4%) and Elastic modulus (2241) was recorded for bleached-acetylated CCAX film. Storage modulus of the films was scanned under different relative humidity environments and this value was found to be highly sensitive to RH changes. Acetylation process was proven to make the storage modulus of the films independent of humidity changes and the presented hydrophobic character was ascribed to attached acetyl groups on hemicelluloses during this process.

Heikkinen et al. (2013) studied the influence of long-term storage on physical stability of plasticized hemicellulose based films. Oat spelt arabinoxylan (OsAX) and spruce galactoglucomannan (GGM) films plasticized with 40 wt% of glycerol, sorbitol, or their blends and the physical stability of these films was examined for four months. An alteration on mechanical properties was reported during storage and glycerol-plasticized films were less stable than sorbitol-plasticized films. However, plasticizing effects was reported as might not be stable under long-term storage conditions and migration of the plasticizer in or out of the film matrix which may cause alterations in mechanical or barrier properties, was cited as possible. Sorbitol migration was not occurred in this study, whereas the opposite was reported for glycerol. Glycerol-plasticized films were reported to be less stable than sorbitol-plasticized films, accordingly. However, films became stronger, stiffer and water vapor permeability decreased after glycerol migration. Drastic changes were monitored for WVP properties of OsAX film during storage; more than a 40% decrease was observed when plasticizer blends contained 50% or more glycerol.

2.3. Converting lignocellulosic biomass into value-added products via ionic liquids

Lignocellulosic biomass can be fabricated into films, coatings, fibers and membranes due to the potential of ionic liquids to dissolve biomass (Lee et al., 2010). Lignocellulose based materials prepared with ionic liquids are reported to have the potential to be used in a variety of applications owing to their inherent biocompatibility and biodegradability (Lee et al., 2010).

Simmons and coworkers (2011) mimicked the real wood sample by preparing a synthetic wood solution consisting of 5% (wt/wt) cellulose fiber, 3% (wt/wt) hemicelluloses (xylan from birchwood), and 2% (wt/wt) kraft lignin in room temperature ionic liquid solvent, 1-ethyl-3-methylimidazolium acetate, [EMIM][Ac]. Synthetic wood films at given ratios were spin-coated from [EMIM][Ac] and reconstituted with water and then dried. Higher tensile strength value (61.7±5.6 MPa) was measured for synthetic wood film compared to xylan and functionalized cellulose films of the literature, indicating that presence of lignin improved the mechanical properties by behaving as a cross-linker among other wood components, cellulose and xylan. Various synthetic wood composites were also prepared by dissolution process of wood components (5/3/2 wt %), polyethylene glycol (5% PEG MW 400), 0.5% chitosan, and multi-wall carbon nano-tubes (0.025 or 0.1 wt % MWNTs) in ionic liquid. The results revealed that numerous materials could be prepared by the compounds to be added to the synthetic wood composites, with unique properties, such as high tensile strength, conductivity, and antimicrobial properties.

Sun et al. (2011) employed shorter dissolution times (10-30 min)/higher temperatures (temperatures above the glass transition temperature of lignin) method which was defined as ‘one pot process’ in the article to direct dissolution of raw lignocellulosic biomass in ionic liquid, 1-ethyl-3-methylimidazolium acetate ([C_2MIM][OAc]). Lignocellulosic biomass composite fibers were prepared with a dry-jet wet spinning process by defined method and the study was the first in the literature that produce such composite fibers directly from raw lignocellulosic biomass which were pine, oak and bagasse. Utilizing different dissolution conditions, a total of 12 different spinning solutions were prepared and bagasse fibers fabricated by the higher temperature/shorter time were found to be stronger with higher stress compared to those of made with the lower temperature method. (125 MPa for fibers prepared at 185°C, 10 min vs. 86 MPa for fibers prepared at 110°C, 16 h). The tensile testing results were explained by the cellulose content and polymer degradation. It was reported that cellulose content of the fibers prepared under higher temperature and shorter dissolution time conditions were higher than those of fibers obtained by lower temperature/ longer time method (63.5% for fibers prepared at 185°C, 10 min vs. 57.3% for fibers prepared at 110°C, 16h). Thus, the fibers spun from biomass sources with higher cellulose content were reported to be stronger. On the other hand, higher temperature/shorter time heating methods were reported to result in less polymer degradation. Furthermore, the fibers subjected to NaOH pretreatment before dissolution that results in higher cellulose content of wood, gave the highest strength results. The recovered pine after 15% NaOH, 4 h pretreatment (with 61% cellulose content) illustrated an UTS value of 336 MPa, whereas those pretreated 10% NaOH, 4 h (with 57% cellulose content) exhibited UTS of 222 MPa.

Abdulkhani et al. (2013) utilized two imidazole-based ionic liquids (1-butyl-3-methyl-1-imidazolium chloride ([BMIM][Cl]) and 1,3-methyl imidazolium dimethyl sulfate ([DiMIM][$MeSO_4$])) to dissolve lignocellulosic materials, namely, ball-milled poplar wood (PW), chemi-mechanical pulp of poplar wood (CMP), and cotton linter (CEL) to fabricate composite films. The results revealed the inability of [DiMIM][$MeSO_4$] in complete dissolution of lignocellulosic materials. On the other hand, [BMIM][Cl] were reported to dissolve all used lignocellulosic materials in the study. Physical properties of the films produced were characterized by means of optical transparency (OT), water absorption (WA), water vapor permeability (WVP) and tensile strength (σ_b). Optical transmittance of CEL film was much higher than those of CMP and PW film (40% and 20%, respectively), ascribed to the better miscibility of the lignocellulosic material and ionic liquid. The WA values were ranged from 32% to 42% for CEL film, from 100 to 110% for CMP film, and from 114% to 120% for PW film. The highest WVP value (0.25×10^{-9}g.m^{-1}.Pa^{-1}.s^{-1}) was recorded for PW film, while CEL film illustrated the lowest WVP value (0.17×10^{-9}g.m^{-1}.Pa^{-1}.s^{-1}) and the decrement in WVP value was considered to be associated with the increasing cellulose content of the film. Tensile strength of CEL film was found to be much higher than other composites fabricated in the study.

Chen et al. (2014) aimed to fabricate novel, green, renewable and biodegradable films by directly transforming the raw lignocellulosic biomass in DMSO/LiCl solution without any additional film-forming additives. Facile and environmentally friendly film production was followed by coagulation either in an acetone/water mixture or in water and concluded with a freezing treatment step. The bagasse film coagulated in the acetone/water (9:1, v/v) mixture was named as Film 1 and the acetone was added to coagulation bath to avoid the film from shrinking upon drying. Film 2 was prepared by coagulating the film in water. Freezing-thawing treatment step was reported to enhance physical cross-linking and thus made the film stronger to resist cracks occurred during drying upon the removal of water. Therefore, a freezing-thawing treatment step was employed in fabrication of Film 2 to compensate any problem that could arise from coagulation in water. Cross-sectional morphology of the films were characterized by scanning electron microscopy (SEM), and Film 1 illustrated a relatively dense structure, while freezing process led to observe some micro pores in the cross-section of Film 2. Light transmittance of the films was determined by means of a UV/vis spectrophotometer, roughly as 44.5 ± 0.5% at 600 nm. Film 2 showed higher tensile strength (38.3 MPa for Film 1 vs. 30 MPa for Film 2) together with improved elastic modulus, except the decreased elongation at break those that of Film 1.

Environmentally benign processes become inevitable for the future fabrication of membranes as well as other biomaterials due to the environmental issues as highlighted by Xing et al. (2011). Currently cellulose membranes are prepared from cellulose derivatives obtained through the utilization of heavily toxic and hazardous chemicals that lead to produce a mass of air and water pollutants (Chen et al., 2012). Lignocellulosic biomass and its components could also be utilized as the abundant, biodegradable and inexpensive raw material in the research area of membrane separation technologies together with green solvents, ionic liquids.

For the first time, ionic liquids were utilized to replace conventional organic solvents to fabricate flat sheet and hollow fiber membranes by Xing and coworkers (2010). 1-butyl-3-methylimidazolium thiocyanate ([BMIM][SCN]) was used as solvent to produce cellulose acetate (CA) membranes via phase inversion in water. CA membranes were also prepared by other solvents, namely, *N*-methyl-2-pyrrolidinone (NMP) and acetone for comparison. CA membranes cast or spun from CA/[BMIM][SCN] solution had macro-void free, dense cross-sections full of nodules, while membranes cast or spun from CA/NMP and CA/acetone solutions had relatively porous cross-sections. Distinctive morphology observed for membranes fabricated from CA/[BMIM][SCN] solution was ascribed to ionic liquid's unique nature of high viscosity and the high ratio of [BMIM]]SCN] outflow to water inflow. CA/[BMIM][SCN] membrane had nodular structure along the entire membrane cross-section due to the slow diffusion of water into the membrane. Using the same casting thickness, thicknesses of the CA/[BMIM][SCN] membranes were found to be thinner (8.72 μm) than that of CA/acetone (11.61 μm) and CA/NMP (55.7 μm) membranes. The resultant CA/[BMIM][SCN] flat sheet membrane was reported to have pure water permeability (PWP) of 114.1 L/(m^2.h.bar). The study also provides the demonstration of recovery and reuse of [BMIM][SCN] and fabricated membranes from recovered [BMIM][SCN] exhibited similar morphology and flux characteristics to that of membranes produced from fresh [BMIM][SCN].

Another study conducted by Xing and coworkers (2011) focused on cellulose acetate (CA) hollow fiber membrane fabrication by phase inversion method using ionic liquid as the solvent. CA/[EMIM][SCN] flat sheet membranes were also prepared and coagulated in different non-solvents, namely, water and isopropanol (IPA), with different hydrogen bonding strengths to investigate the molecular effects of CA/[EMIM][SCN] solutions on membrane formation. The membrane coagulated in water was thinner (14 µm) and exhibited a dense packed nodular structure; whereas the one coagulate in IPA had a thickness of 48µm with a closed-cell porous cross-section. Nodular structure observed was explained by the diffusion of different amounts of [EMIM][SCN] and water inside or outside the membrane structure. Pore evolution was said to be allowed by the slower phase inversion rate in IPA before solidification of the membrane. The resultant hollow fibers cross-sections exhibited an asymmetric structure with a porous inner surface but a relatively dense outer surface without macro-voids. Absence of macro-voids was attributed to the high dope viscosity and high ratio of ionic liquid outflow to water inflow. It was found out that higher dope temperature caused to fabricate slightly more porous cross-sections and inner surface as a result of reduced shear viscosity, and improved diffusion flow between the solvent and non-solvent. PWP value was also reported to increase in accordance with the altered morphology observed at elevated dope temperature.

Li et al. (2011) used phase inversion method to fabricate cellulose nanofiltration membranes cast from 8 wt% of cellulose/[AMIM][Cl] solutions on a PET non-woven fabric support. A macro-void free and dense layered structure was observed via SEM images due to the distinctive effect of [AMIM][Cl] on phase inversion process. Pure water flux of the composite membrane was reported as

128.5 L/(m^2.h) under 0.4 MPa. The rejection of dye molecules was given as 100%, 99.7% and 22.7% for Brilliant Blue R (MW: 826), Congo Red (MW: 697) and Methyl Orange (MW: 327), respectively. Accordingly, cellulose composite membrane molecular weight cut-off (>700) was said to be in the range of a nanofiltration membrane. It was also investigated that how performance of the fabricated membrane effected under different operation pressures. Water flux of the membranes was found to increase at elevated operation pressures and rejection of membrane to Congo Red stabilized at around 99.4–99.8% and did not change with changing the operation pressure. Furthermore, produced membranes exhibited good stability and anti-fouling ability.

Ma et al. (2011) used regenerated cellulose, chitin, and a cellulose-chitin blend with an ionic liquid, 1-ethyl-3-methylimidazolium acetate [EMIM][Ac] to fabricate thin-film nano-fibrous composite (TFNC) membranes with cellulose or chitin barrier layers. Polymer/ionic liquid (barrier layer) solution was coated on a composite fibrous support composed of electrospun polyacrylonitrile (PAN) scaffold (mid-layer) and PET non-woven substrate (bottom substrate) and then immersed in water. Resultant membranes were intended to use for the purification of a model of bilge water (oil/water emulsion). Cellulose and chitin were proven to be miscible and form a homogeneous solution in the chosen ionic liquid by TGA. Regenerated cellulose and chitin blend was cited as a new material to combine individual features of both chitin and cellulose. No apparent difference was observed via SEM for the morphology of cellulose, chitin, and cellulose-chitin blend barrier layers in TFNC membranes. It was seen from the SEM images that top barrier layer and the support were adhered excellently and the barrier layer was relatively thin for all three membranes. Average pore size distribution of TFNC membranes based on cellulose, chitin and cellulose-chitin blend were around 25, 27 and 14 nm, respectively. A narrower pore size distribution was observed for cellulose-chitin blend barrier layer compared to other two membranes fabricated. TFNC membrane had chitin as its barrier layer exhibited a permeation flux of 239 L/m^2.h and a rejection ratio of 99.6% after 24 h of filtration operation. The oil concentration in permeate was reported to meet the environmental standards for the wastewater discharge. 6.7 and 4.6-fold increase in permeation flux was reported for TFNC membrane with chitin (with 99.9% retention ratio) and cellulose (with 99.8% retention ratio) barrier layers, respectively compared to commercial membrane, PAN10. In addition, TFNC membranes based on the cellulose-chitin blend was reported to have 10 times higher permeation flux when compared to permeation flux of commercial ultrafiltration membrane (PAN10, Sepro) with similar (high) and stable rejection ratio (above 99.5%) over a long time period of filtration operation, i.e., up to 100 h.

Wheat straw cellulose (WSC) fractionated from wheat straw after steam explosion was used as the raw material of the membranes prepared in the study of Chen and coworkers (2012). Regenerated WSC membranes prepared via phase inversion process using water as coagulant and ionic liquid, 1-butyl-3-methylimidazolium chloride ([BMIM][Cl]) as solvent. Membrane raw material, WSC extracted from wheat straw, was reported to have 93.6% α-cellulose content. An asymmetric porous structure was observed through SEM and surface layer was reported to be much denser than the inner layer due to the earlier conversion of surface to gel when contacted with the precipitant. The inner layer (with big pores) was determined to be thicker than the surface layer (with small pores). Resultant membrane cast from WSC/[BMIM][Cl] solution, illustrated good mechanical and permeability properties. The tensile strength and elongation at break were reported to be 170 MPa and 6.4%, respectively. At 0.3 MPa pressure, pure water flux permeability was 238.9 L/(m^2.h) and furthermore, BSA rejection was reported to be stabilized around 97%. After regeneration of cellulose, [BMIM][Cl] was recycled by vacuum distillation owing to its extremely low vapor pressure and the recovery ratio was reported as 95.2%.

In this study, lignocellulosic agricultural waste, corn cobs, were dissolved in ionic liquid, 1-ethyl-3 methylimidazolium acetate ([EMIM][Ac]) for the fabrication of corn cob based films. Resultant films could be classified into three different categories which are films based on the corn cob itself that is unfractionated corn cob, films based on cellulose extracted from corn cob via alkaline extraction and films based on hemicellulose extracted from corn cob via alkaline extraction. Fabricated corn cob based films were evaluated and compared in terms of their morphological and physical properties.

CHAPTER 3

MATERIALS AND METHODS

3.1. Materials

Corn cobs supplied from Hatay (Turkey) were milled to pass an 80 mesh (177µm) sieve to use in this study. Ionic liquid 1-ethyl-3 methylimidazolium acetate ([EMIM][Ac]>97%) was obtained from Sigma–Aldrich (St. Louis, MO, USA) Potassium hydroxide, acetic acid, sulfuric acid, and were purchased from Merck (Darmstad, Germany). Ethanol, sodium hydroxide, bovine serum albumin (BSA, mol wt ≅ 66 kDa), sodium alginate and the phosphate buffered saline (PBS, pH 7.4) were purchased from Sigma-Aldrich (St. Louis, MO, USA).

3.2. Experimental Methods

3.2.1. Isolation of cellulosic and hemicellulosic portions of corn cobs

Corn cobs were milled to a particle size of less than 177 µm and hemicellulosic and cellulosic portions of it were extracted from grounded corn cobs according to the previously reported procedure in the study of Zilliox and Debeire (1998). Corn cobs were swollen in water for half an hour at room temperature. Swollen corn cobs were added to 10 wt% NaOH at 60°C with magnetic stirring for 3 hours. The suspension was filtered with a filtering cloth and alkaline insoluble fraction of the solution, cellulosic portion, was removed. pH of extracted cellulose was adjusted by means of acetic acid and subsequently, cellulosic portion was desalted by washing 3 times with de-ionized water and the desalted cellulose (cellulose containing no salt) was left to dry at ambient conditions. Alkaline soluble fraction (liquid fraction) was precipitated by mixing with refrigerated 250 mL acetic acid-ethanol solution in 1:10 volumetric ratio. Following the addition of acetic acid-ethanol solution, the precipitated polymers (hemicellulosic portion) were removed by filtration from the suspension with a filtering cloth. Hemicellulosic portion was dissolved in 200 ml of water and re-precipitated with 600 ml of ethanol addition for 3 times and finally recovered hemicellulosic portion was left to dry at ambient conditions.

3.2.2. Lignocellulose (corn cob) based film fabrication

3.2.2.1. Corncob film fabrication

Corn cob films (Water_CC, ETOH/Water_CC, 1D_CC, 2D_CC and 5D_CC) were fabricated directly from corn cob without additional film-forming additives (Table 3.1). Corn cobs were milled to a particle size less than 177 µm. Moisture content of grounded corn cob was determined and corn cobs dried at 110°C for 20 minutes by using a Mettler Toledo HS 153 Moisture Analyzer. Grinded dry corn cobs (4 wt%) were added to 1-ethyl-3-methylimidazolium acetate ([EMIM][Ac]) under magnetic stirring for 1 hour at 140°C by IKA C-MAG HS7 equipped with an electronic contact thermometer (IKA ETS- D5).

A homogeneous solution was prepared with 4 % weight ratio of corncob. The corncob-ionic liquid solution was cast onto a glass plate and immersed in coagulation bath (water and water/ethanol) directly or after conditioning in 100% RH desiccator at different time periods in the range of 1-5 days. The corn cob solution cast on the glass plate was washed further two times with de-ionized water with an interval of 24 hours until residual [EMIM][Ac] was removed and left to dry at ambient temperature. Finally, a series of corncob films (Water_CC, EtOH/Water_CC, 1D_CC, 2D_CC and 5D_CC) were obtained by this method (Figure 3.1).

The following table provides the information of types of the films produced in this study and briefly explains the differences in their production process.

Table 3.1. Descriptions of the films prepared in the present study

TYPE OF FILM	**ABBREVIATIONS USED**
WATER_CC	Water coagulated corn cob film
ETOH/WATER_CC	50-50 wt% ethanol-water coagulated corn cob film
1D_CC	Corn cob film conditioned 1 day in desiccator (RH=100%) before coagulated in water
2D_CC	Corn cob film conditioned 2 days in desiccator (RH=100%) before coagulated in water
5D_CC	Corn cob film conditioned 5 days in desiccator (RH=100%) before coagulated in water
HEMICELLULOSE	Hemicellulose (extracted from corn cob by alkaline extraction) based film
CELLULOSE	Cellulose (extracted from corn cob by alkaline extraction) based film
HEATED_CC	Water_CC film heated to 200°C for 24 hours

3.2.2.2. Corn cob cellulose based film fabrication

Alkaline-extracted cellulose from corn cobs were milled to a particle size less than 177 µm. Moisture content of milled cellulose corn cob was determined and extracted cellulose dried at 110°C for 20 minutes by using a Mettler Toledo HS 153 Moisture Analyzer. Grounded dry corncob cellulose was added to ionic liquid ([EMIM][Ac]) under magnetic stirring for 1 hour at 140°C and a homogeneous solution was prepared with 4 % weight ratio of corncob cellulose. The corn cob cellulose-ionic liquid solution was cast onto a glass plate and immersed in coagulation bath (water). The corncob cellulose solution cast on the glass plate was washed further two times with de-ionized water with an interval of 24 hours to remove [EMIM][Ac]. Films were allowed to form at ambient conditions and finally, a corncob cellulose film (cellulose film) (Table 3.1) was obtained by this method (Figure 3.2).

3.2.2.3. Corn cob hemicellulose based film fabrication

0.5 grams of alkaline-extracted hemicellulose from corn cob was dissolved in 20 ml of de-ionized water under magnetic stirring at room temperature for 24 hours. The suspension was ultrasonicated at 40% amplitude for 8 minutes for the better dispersion of solid particles. The resultant solution was then poured into a polystyrene petri dish 9 cm in diameter and left to dry at controlled atmosphere (Medcenter 111 Climacell, MMM Group, Munich, Germany) that is 23°C and 50% relative humidity, for 3 days. Following the drying of the solution, water evaporated and left behind the hemicellulose film (Figure 3.2).

3.2.3. Corn cob cellulose based membrane fabrication

Corn cob cellulose based membranes were fabricated via phase inversion technique using ionic liquid as solvent. Alkaline-extracted cellulose from corn cobs were milled to a particle size less than 177 µm. Moisture content of milled corn cob cellulose was determined and they were dried at 110°C for 20 minutes by Mettler Toledo HS 153 Moisture Analyzer. Milled dry corn cob cellulose was added to ionic liquid ([EMIM][Ac]) under magnetic stirring for 1 hour at 140°C and a homogeneous solution was prepared with 4 % weight ratio of corn cob cellulose. The corn cob cellulose-ionic liquid solution was cast onto a nonwoven support with 250 µm casting knife and immersed in coagulation bath (water). The corn cob cellulose gel cast on nonwoven support was washed further two times with water with an interval of 24 hours to remove [EMIM][Ac]. Membranes were allowed to form at ambient conditions.

3.3. Characterizations

3.3.1. Optical Microscopy

Leica CM E optical transmission light microscope was employed to monitor the dissolution of peanut shell and corn cob in ionic liquid, [EMIM][Ac]. The samples were taken from biomass-ionic liquid solution at different periods of time and placed between microscope slides to monitor the biomass dissolution. Films produced were also monitored via optical microscopy. Optical micrographs were taken with a digital camera prior to or following the complete biomass dissolution. All images were taken at 40X magnification.

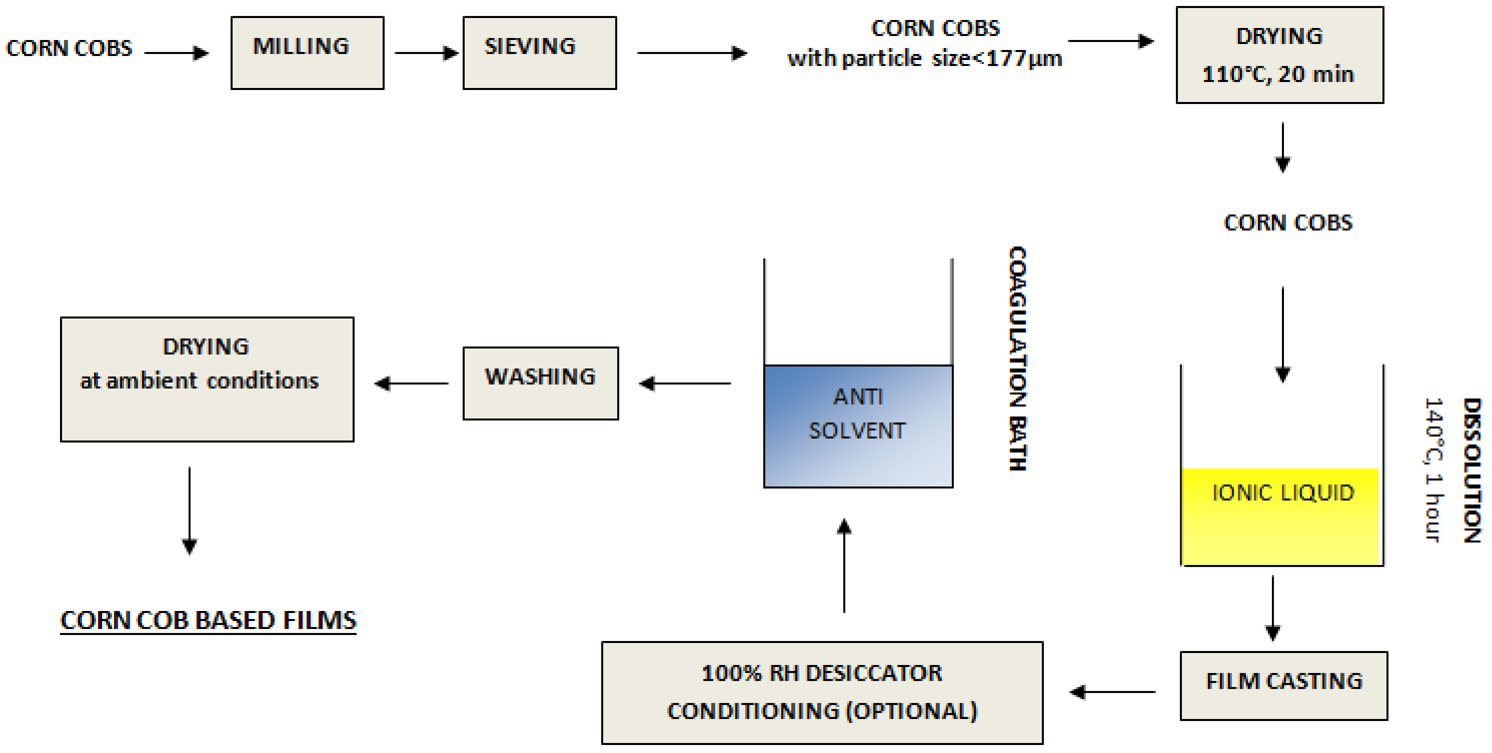

Figure 3.1. Flowchart of corn cob film fabrication

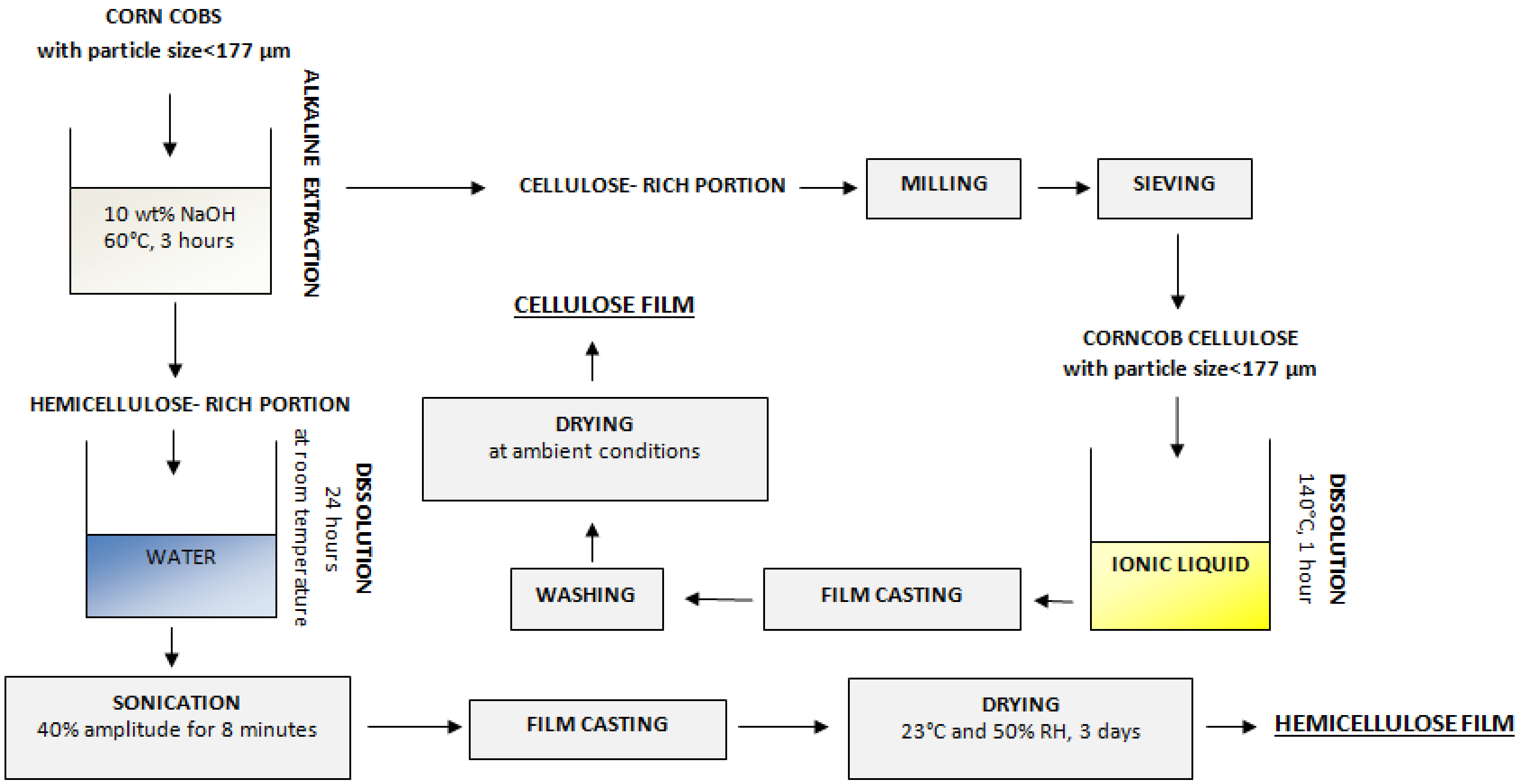

Figure 3.2. Flowchart of corn cob cellulose and hemicellulose based film fabrication

3.3.2. Scanning Electron Microscopy (SEM)

Prepared samples were frozen in liquid nitrogen, fractured, coated with gold/palladium and the cross-sectional morphologies were examined via scanning electron microscope (SEM) (Quanta 400F). The acceleration voltage was set to 5-10 kV.

3.3.3. Light transmittance

The percentage light transmittance of the samples was measured via an experimental set up of light source (halogen light bulb) and light meter (Figure 3.3). Samples on a glass substrate were placed under the light source and the light transmittance value was measured by means of a light meter kept in the dark. At least two replicate specimens were tested from each sample. Percent light transmittance value was calculated by taking the light transmittance value of glass substrate as the reference. Opaqueness for unit thickness values of the films were calculated by the formula represented below.

$$\frac{Opaqueness}{Film\ thickness} = \frac{1 - \frac{Light\ transmittance\%}{100}}{Film\ thickness}$$

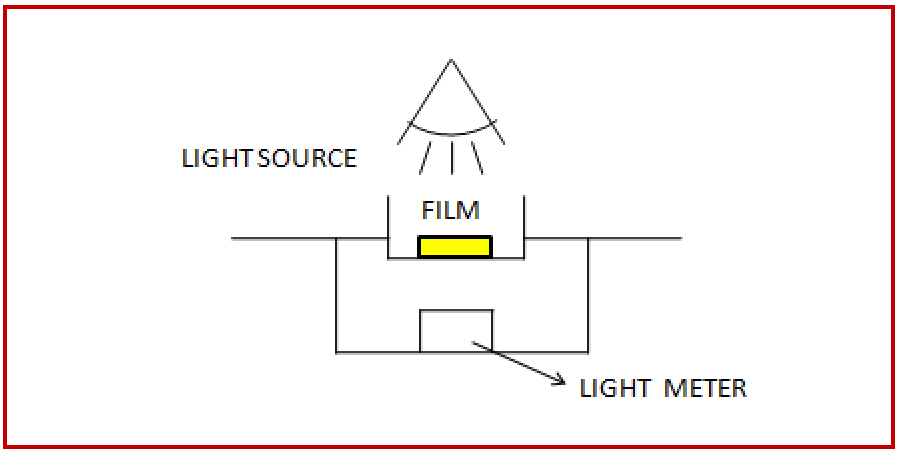

Figure 3.3. Light transmittance experimental setup

3.3.4. Water vapor permeability (WVP)

The water vapor permeability tests were conducted in accordance with ASTM E96/E96M – 12. Prior to testing, films were cut into circles, conditioned at 50°C for 24 h, weighed and sealed with epoxy on a test dish where zero relative humidity was maintained using a zeolite (Zeolite A). Zeolite A was dried by keeping at 300°C for 3 h before the test. Following the sealing, test assemblies are placed in a controlled atmosphere (100% RH desiccator at 30°C) as shown in Figure 3.4. 100% RH was maintained by filling the bottom of the desiccator with water. Total vapor transferred is calculated by the weight gain of each test assembly and recorded as a function of time. Slopes of total vapor transferred vs. time graphs were determined by linear regression. The water vapor transpiration rates (WVTR) were calculated by dividing the slopes (g/s) to the water vapor transfer area (m^2). WVPs were calculated according to the given formula below where P is the saturation vapor pressure of water (Pa) at 30°C, R_1 is the RH in the controlled atmosphere and, R_2 is the RH in test assembly and X is the film thickness (m).

$$WVP = \frac{WVTR}{P * (R_1 - R_2)} * X$$

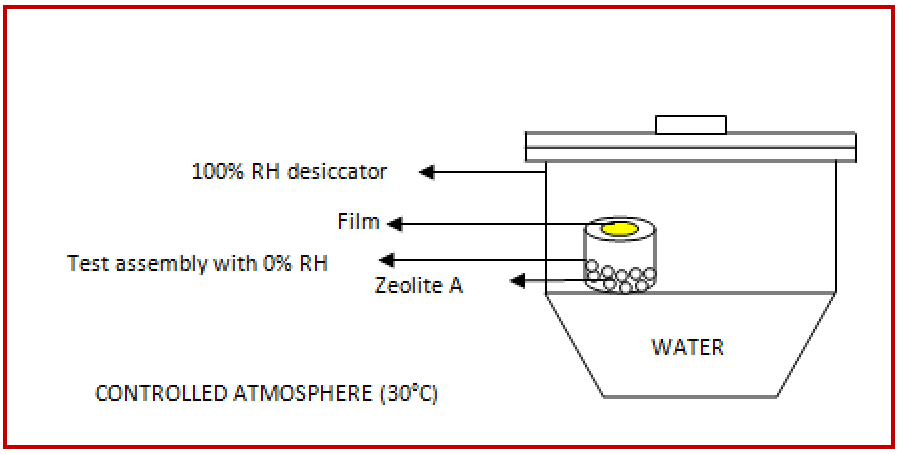

Figure 3.4. Water vapor permeability experimental setup

3.3.5. Moisture Uptake (MUP)

Prior to testing, all the samples were conditioned at 50°C for 24 hours and weighed subsequently. Conditioned samples of each type of film were placed in 100% RH desiccator at room temperature. Weight gain of the film upon exposure to moisture was recorded against certain time periods. A minimum of two samples was tested for each type of film. Percent moisture uptake was calculated according to the given formula below where W_{sample} (gr) is the weight of sample at the time of exposure to moisture, $W_{conditioned}$ (gr) is the weight of the conditioned sample.

$$MUP = \frac{W_{sample} - W_{conditioned}}{W_{conditioned}} * 100$$

3.3.6. Tensile testing

The samples were conditioned within a climatic chamber (MMM Medcenter Climacell 111) at 23°C and 50% RH for 24 hours prior to tensile testing while adjusting the atmospheric condition of the tensile testing room identical to the conditions of climatic chamber. Prior to performing the test, dog bone shaped specimens were obtained from the films by means of a manual cutting press (ZCP 020, Zwick GmbH & Co., Ulm, Germany).The mechanical properties of the samples including ultimate tensile strength (UTS), elongation at break (e_b) and Elastic modulus (E) were measured with a universal testing machine (Zwick/Roell Z250, Zwick GmbH & Co., Ulm, Germany) equipped with a 100 N load cell and pneumatic grips. All tensile testing data were collected by adjusting the crosshead speed as 5 mm/min. The results were obtained via the software (testXpert 2) accompanying the universal testing machine. At least three repeated measurements of each film were used to determine mechanical properties.

3.3.7. Pure Water Permeability (PWP)

The pure water permeability (PWP) tests were conducted using ultrapure water (18MΩ.cm) under pressure differences of 1-2 bars regulated by exit valve of pressure vessel at room temperature as shown in Figure 3.5. Membrane with effective membrane area 0.0015 m^2 was stored in an aqueous solution of sodium bisulfide at room temperature prior to testing. PWP was calculated by the following equation where Q, A and ΔP denote the water permeation rate (L/h), effective filtration area of membrane (m^2) and pressure difference (bar), respectively.

$$PWP = \frac{Q}{A * \Delta P}$$

3.3.8. Retention test

Membranes fabricated were kept in aqueous sodium bisulfide solution at room temperature prior to retention test. Retentions of membrane were tested using probe molecules, namely Bovine serum albumin (BSA) with 66 kDa and sodium alginate with 0.01-0.1µm in diameter (Ven et al., 2008). The concentrations of the feed and permeate solutions were determined by UV-vis spectrophotometer (Nicolet Evolution 100, Thermo Electron Corporation, WI, USA) at room temperature. Wavelengths for BSA and sodium alginate were 220 and 260 nm, respectively. The membrane supported on nonwoven surface was placed into

Millipore 50 mL solvent resistant stirred cell. The effective membrane area was 0.0015 m^2.

The solute rejection was calculated by the following equation where C_p and C_f are the solute concentrations in permeate and feed solutions, respectively.

$$Rejection\ (R) = \left(1 - \frac{C_P}{C_F}\right) * 1$$

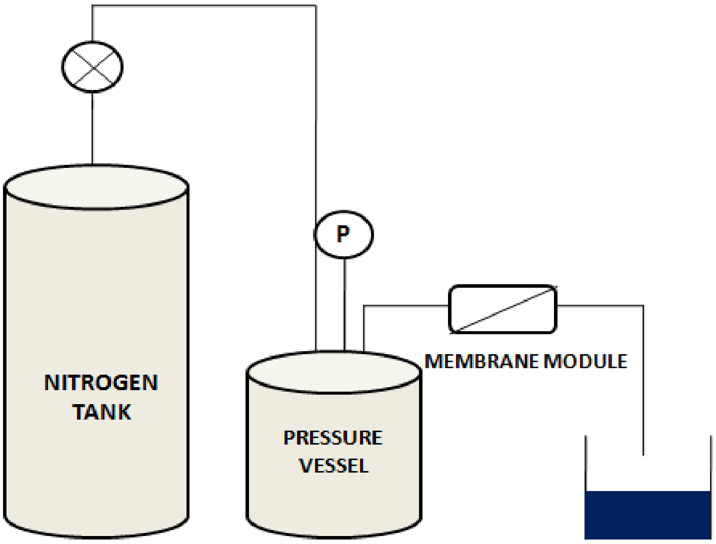

Figure 3.5. Pure water permeability experimental setup

CHAPTER 4

RESULTS AND DISCUSSION

This study presents the fabrication of corn cob based films that can be classified into three different categories which are films based on the corn cob itself that is unfractionated corn cob, films based on cellulose extracted from corn cob via alkaline extraction and films based on hemicellulose extracted from corn cob via alkaline extraction. For corn cob cellulose based film production, cellulose extracted from corn cob is dissolved in ionic liquid, [EMIM][Ac] and cast on a glass plate before coagulated in water and subsequently dried at room temperature to manufacture cellulose films. Hemicellulose based film production includes the steps of suspending hemicellulose in water followed by solvent casting. Films fabricated from unfractionated corn cob are further separated into six categories in themselves. All of them produced by dissolving the entire corn cob in [EMIM][Ac] at specified conditions. Water_CC and ETOH/Water_CC films were coagulated directly in water and 50/50 wt% ethanol water solution, respectively after casting the film forming solution onto glass plates. On the other hand, 1D_CC, 2D_CC and 5D_CC films are conditioned in 100%RH desiccator for 1, 2 and 5 days, respectively before coagulated in water. Heated_CC film was fabricated following the same route in the case of Water_CC film only includes an additional heating step for 24 hours at 200°C after drying in room temperature. Totally, 8 different films are fabricated to investigate the physical, morphological and mechanical properties as well as the effect of film production parameters in this work.

4.1. Solubilization of lignocellulosic biomass in ionic liquids

Lignocellulosic biomass has gained remarkable increase of interest as alternative and sustainable resource to produce chemicals, materials, and fuels due to the unavoidable depletion of petroleum based resources (Rogers et al., 2009; Zavrel et al., 2009). However, the recalcitrance of lignocellulosic biomass due to the crystalline nature of cellulose, three dimensional network structure of lignin and complicated cross-linkages between hemicellulose and lignin in the plant cell wall makes the dissolution of biomass in common solvents difficult (Hou et al. 2012; Muhammad et al. 2012). This complex structure also limits the widespread use of lignocellulosic biomass as reported by Lynd et al. (2002). Methods to manipulate its features for a variety of applications require the deconstructing the three-dimensional structure of lignocelluloses and further biomass processing (Muhammad et al., 2012). Conventional approaches to utilize biomass employed so far have drawbacks as they require a considerable amount of money and time, energy, high temperatures and pressures (Muhammad et al., 2012). Therefore, it is inevitable to find alternative and efficient solvent and process technologies for cost effective and sustainable utilization of lignocellulosic biomass (Rogers et al., 2009). Dissolution of lignocellulose in ionic liquid could be pointed out as a green and energy efficient pretreatment for lignocellulose based processes (Zavrel et al., 2009). Ionic liquids have gained tremendous increase of attention due to their high thermal stability and electric conductivity, negligible vapor pressure, polar nature and tunable properties to specific applications as highlighted by Mora-Pale and coworkers (2011). As uncovered for the first time by Rogers et al. (2002) that ionic liquids are able to dissolve cellulose, ionic liquids have been used as promising solvents for lignocellulosic biomass by disrupting three dimensional network of biomass components (Hou et al., 2012; Mora-Pale et al., 2011). Therefore, in this study ionic liquid is selected to dissolve the lignocellulosic biomass.

A homogeneous solution comprised of lignocellulosic biomass and ionic liquids was required for the film production. First, two sources of biomass were tried which are peanut shell and corn cob. 5 wt% peanut shells was tried to dissolve in the ionic liquid, [EMIM][Ac] at predetermined conditions for other biomass, namely corn cob. In order to investigate whether the homogeneous solution is achieved at the conditions tried; the samples were taken at different periods of

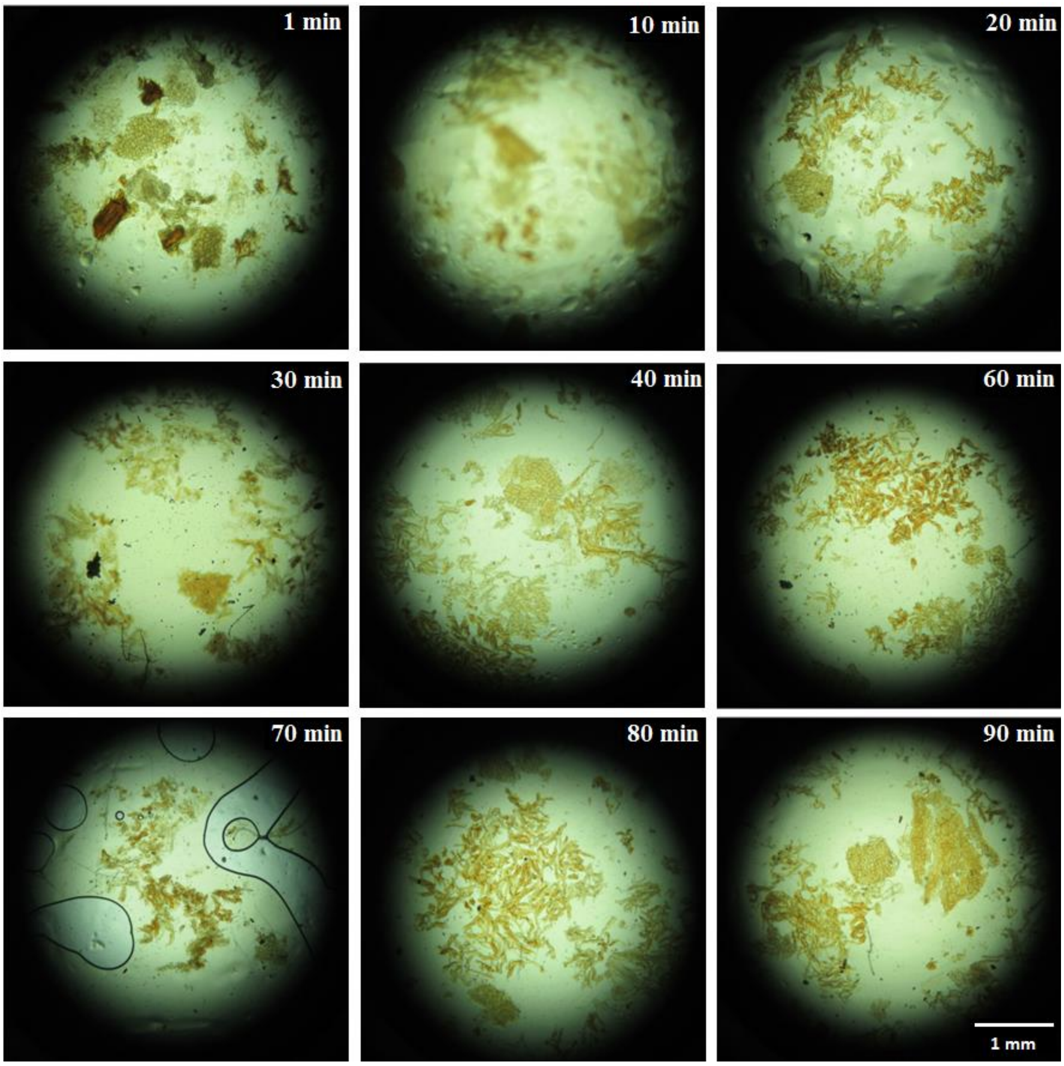

Figure 4.1. Optical microscopy images of the peanut shell particles in ionic liquid [EMIM][Ac] (0.21:4, w/w) at 140°C for different periods of time

time from the solution of IL and biomass. Figure 4.1 illustrates the observed images at different times of the solution prepared with peanut shell and [EMIM][Ac] with the optical microscopy. Peanut shell was not soluble even after 90 min stirring at 140°C in [EMIM][Ac] as proven by the optical microscopy images. Darker fibril like structures observed with the optical microscopy confirmed the existence of undissolved components in the solution prepared.

In order to obtain a complete dissolution, homogeneous solution of ionic liquid lignocellulosic biomass was tried to be prepared by using corn cobs instead of peanut shells. Homogeneity of the solution was investigated in the same manner with the optical microscopy and the images observed at different time intervals were provided for the solution of 5 wt% corn cob and [EMIM][Ac] in Figure 4.2 that provides the complete dissolution conformation. After certain amount of time, the fibril-like structures seen as darker started to swell and disappear in the case of corn cob. After 40 min, a homogeneous solution was observed with the complete disappearance of these darker structures. For this reason, corn cob is chosen as the lignocellulosic biomass to fabricate the films. Solubility and solubility rates of lignocellulosic biomass in ionic liquid can be affected by different means; source of lignocellulose, water content of biomass, particle size and initial biomass load (Kilpeläinen et al., 2007; Sun et al., 2009; Zavrel et al., 2009). The only parameter related with the corn cob and peanut shell that could affect their solubility in ionic liquid was different source of biomass since other parameters were eliminated to avoid any influence in the results. For instance, in a study of Zavrel et al. (2009), spruce was found to be fully dissolved in [EMIM][Ac] whereas silver fir was found to dissolve partially under same dissolution conditions. The result was attributed to the more recalcitrant structure of silver fir as compared to spruce. Furthermore, red oak was found to dissolve better than southern yellow pine by Sun and coworkers (2009). Different rate of dissolution of the biomass was reported to be related to the existence of fractions harder to dissolve that could belong to more strongly inter or intra molecularly bonded or interacting polymers or higher molecular weight polymers (Sun et al., 2009).

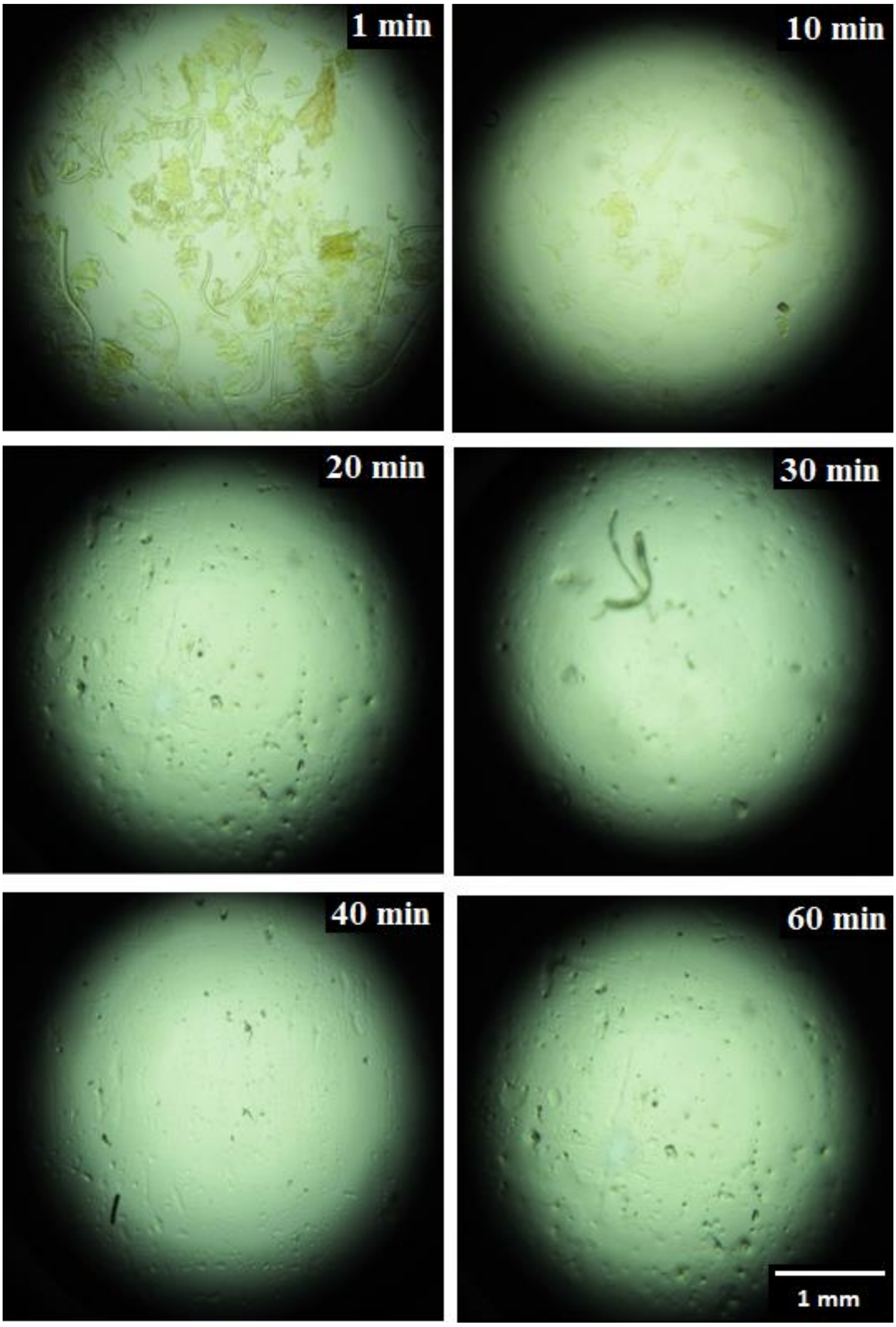

Figure 4.2. Optical microscopy images of corn cob particles dissolved in ionic liquid [EMIM][Ac] (0.21:4, w/w) at 140°C for different periods of time

On the other hand, considering the dissolution temperature, in order to avoid any possible polymer degradation and to improve the economical feasibility of the process, dissolution of corn cob at a lower temperature that is 90°C was also investigated. However, even 3 days stirring in [EMIM][Ac] at specified temperature was not sufficient to prepare a homogenous solution (Figure 4.3).

Different from the approaches involved in biomass dissolution and fractionation, Rogers and coworkers (2011) proposed alternative higher temperature and shorter time dissolution procedure to see whether such conditions facilitate biomass dissolution in ionic liquid and further fractionation. The possibility of this was investigated by choosing the lignin transition temperature as the dissolution temperature while trying to keep the dissolution time less than 30 min.

Lignocellulosic biomass was found to dissolve and separate more efficiently when the dissolution temperature was selected above the glass transition temperature of lignin that is 150°C approximately (Rogers et al., 2011). Based on these results and considering the energy demand of long lasting heating, all the lignocellulosic biomass based films were produced using 140°C as the dissolution temperature.

4.2. Compositional analysis of Water_CC film

Compositional analysis was conducted by alkaline lignocellulosic biomass fractionation and alkaline soluble portion (hemicellulose and lignin) of the film produced from corn cob itself was found to be 53 wt%, whereas alkaline insoluble portion (cellulose rich portion) of the Water_CC film was determined as 47 wt%. The composition of the corn cobs themselves was given approximately as 33% cellulose, 36% hemicellulose, 24% lignin and others (protein, acetyl, uronic acids, ash, etc.) by dry weight by Toraman (2012) where the composition was analyzed through HPLC analysis. The cellulose content of the film was higher compared to corn cob itself since this portion may also contains small amounts of hemicellulose and lignin when alkaline fractionation was employed to separate into constituents of lignocellulosic biomass. In addition, portion of hemicellulose

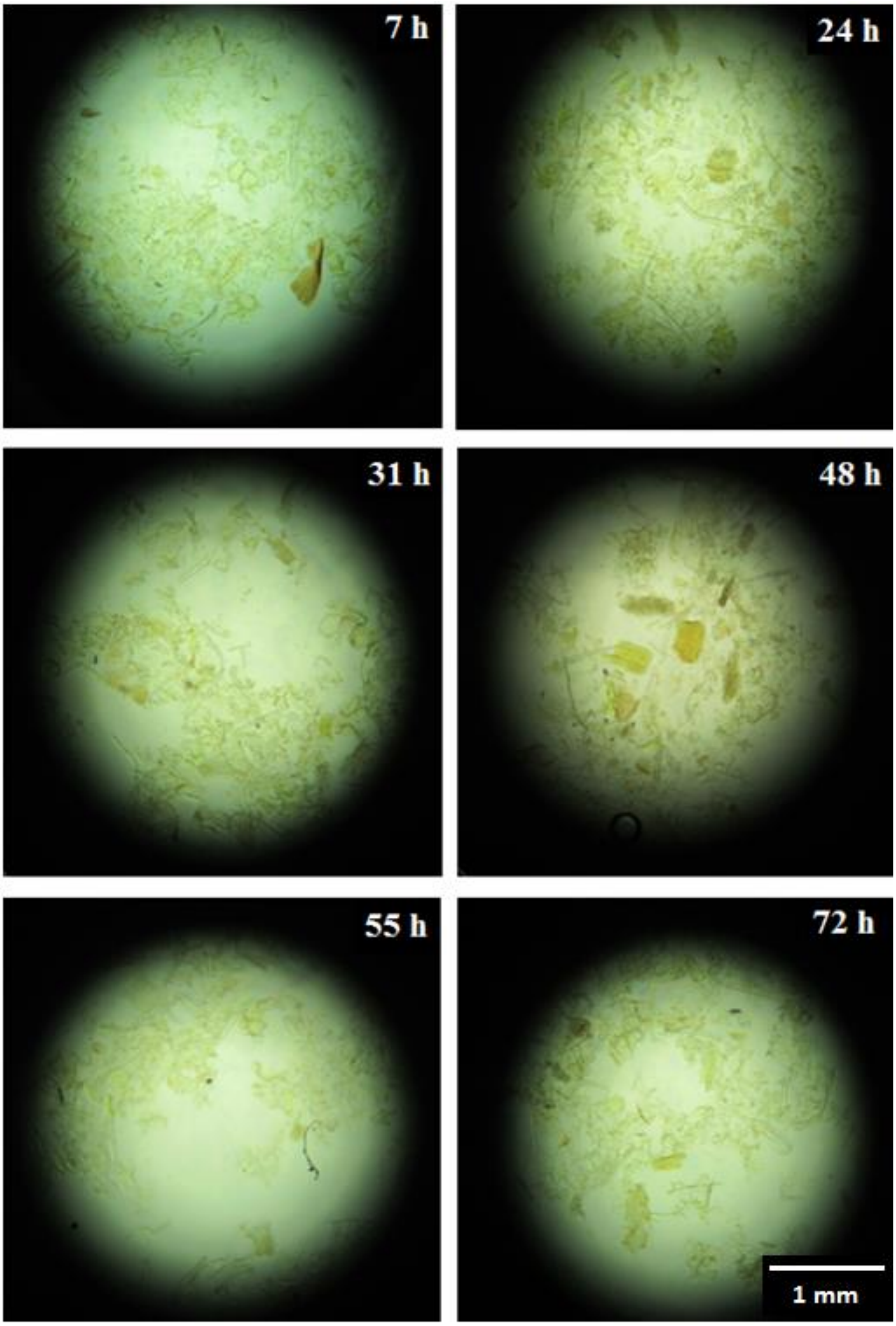

Figure 4.3. Optical microscopy images of corn cob particles dissolved in ionic liquid [EMIM][Ac (0.21:4, w/w) at 90°C for different periods of time

and lignin in the film forming solution may also be transferred into coagulation bath during washing steps.

4.3. Structure of the corn cob based films produced via different techniques

Structure of the films produced from unfractionated corn cob was monitored by means of optical microscopy with 40X magnification. Optical microscopy images of Water_CC, ETOH/Water_CC, 2D_CC and 5D_CC films are given in Figure 4.4. It is apparent from the figure that, conditioning the films at 100% RH independently from the conditioning time resulted in the disappearance of 'bubble-like' features monitored in optical microscopy. Desiccator conditioned corn cob films were more uniform in color than corn cob films coagulated directly in water without conditioning in 100% RH desiccator. These 'bubble-like' features observed for Water_CC and ETOH/Water_CC films were considered to be due to thickness variation or phase separation of lignocellulosic biomass constituents during coagulation, i.e., the separation of cellulose, hemicellulose and lignin that was presented in the cast solution, from each other in the precipitated film during coagulation. The dissociation of the biomass components in the precipitated film may give rise to observe local color differences. Darker areas were referred to lignin and hemicellulose-rich regions; whereas lighter areas observed referred to cellulose-rich regions of the film produced. On the other hand, water vapor was found to retard or prevent these bubble-like features that cause local color differences disappeared in the observed optical microscopy images of 1D_CC, 2D_CC and 5D_CC films.

As different coagulation baths could lead to different structures, structure of the ETOH/Water_CC film was also investigated through optical microscopy. Coagulating the film in 50/50 wt% ethanol/water solution had no obvious effect on the structure of the film as the observed image was similar to the structure of Water_CC film (Figure 4.4). The existence of 'bubble-like' features for Water_CC film was also confirmed for ETOH/Water_CC film by optical microscopy.

Apart from bubble-like features, the structures appeared as small dark particles in the optical microscopy images of corn cob based films was probably formed when the film precipitated in the coagulation bath since these structures were absent in the optical microscopy images of the initial film forming solutions.

Structure of the films produced in this study was also investigated via scanning electron microscopy (SEM). Thicknesses of the films represented in Figure 4.5 are 12,7,13 and 15µm, respectively. Desiccator conditioning did not lead to a significant difference in terms of cross section morphologies of the films produced and all the films exhibited a layered structure as shown in Figure 4.5.

Figure 4.6 shows the effect of heating, different coagulant and fractioning the corn cob on the cross sectional morphology of the films with thicknesses 11,5,20 and 24 µm, respectively. Heating corn cob film to 200°C did not cause an alteration in the morphology of the film. Different coagulant (50/50 wt% ethanol/water) effect was also inspected with SEM as well as optical microscopy. Cross sectional morphology of ETOH/Water_CC film was similar to Water_CC, 1D_CC, 2D_CC, 5D_CC and Heated_CC films as given in Figure 4.6b.

Layered structure observed with SEM for other corn cob based films was also observed when cellulose and hemicellulose which are fractionated from corn cob by alkaline extraction were used as the raw material of the films (Figure 4.6c-d).

Average film thicknesses were determined via cross-sectional SEM images of corn cob based films and varied between 6.9 and 20.8 µm as represented in Figure 4.7.

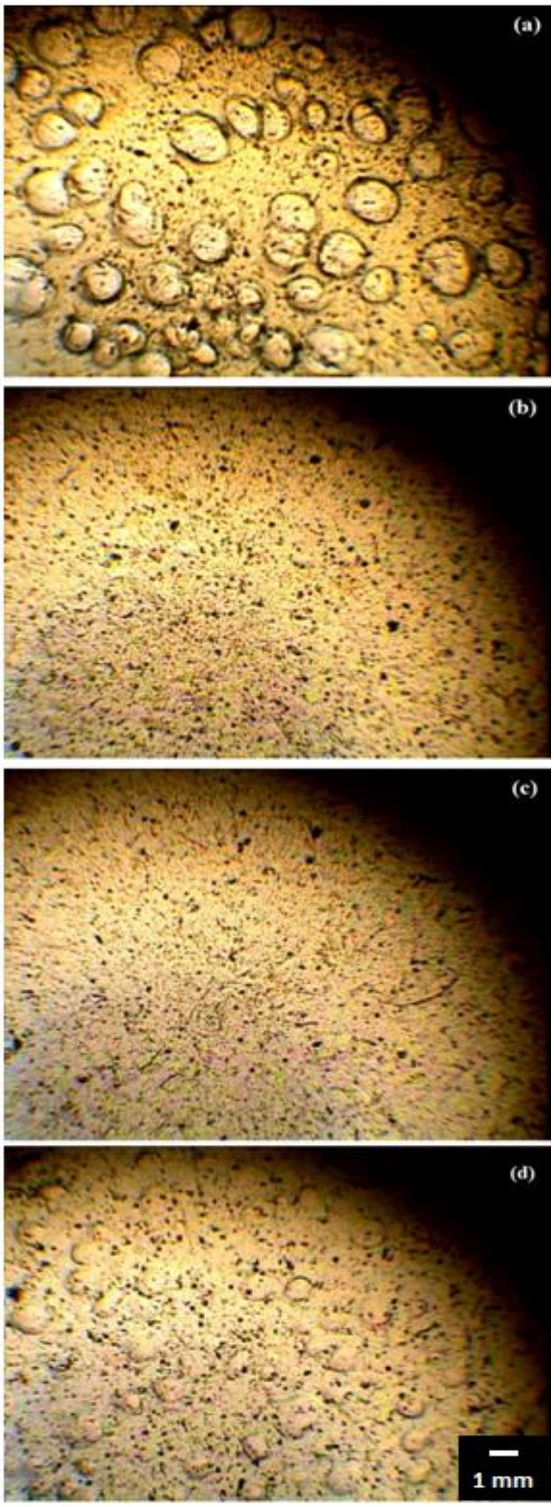

Figure 4.4. Optical microscopy images of the corn cob based films coagulated in water (a), conditioned in 100%RH desiccator for 2 days (b), for 5 days (c) and ethanol-water mixture (d)

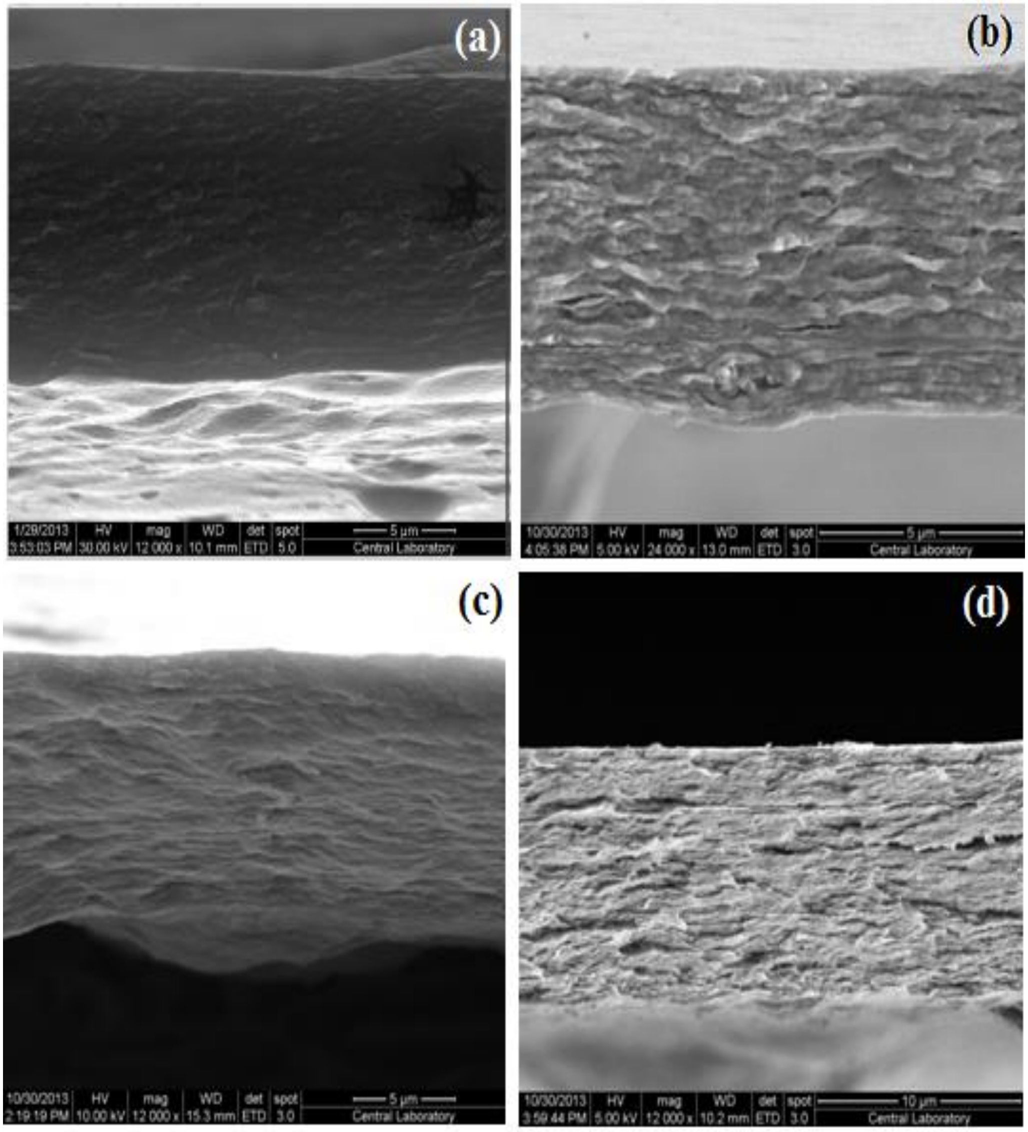

Figure 4.5. Scanning electron microscopy cross-sectional images of the corn cob based films coagulated in water (a), conditioned in desiccator for 1 day (b), 2 days (c) and 5 days (d)

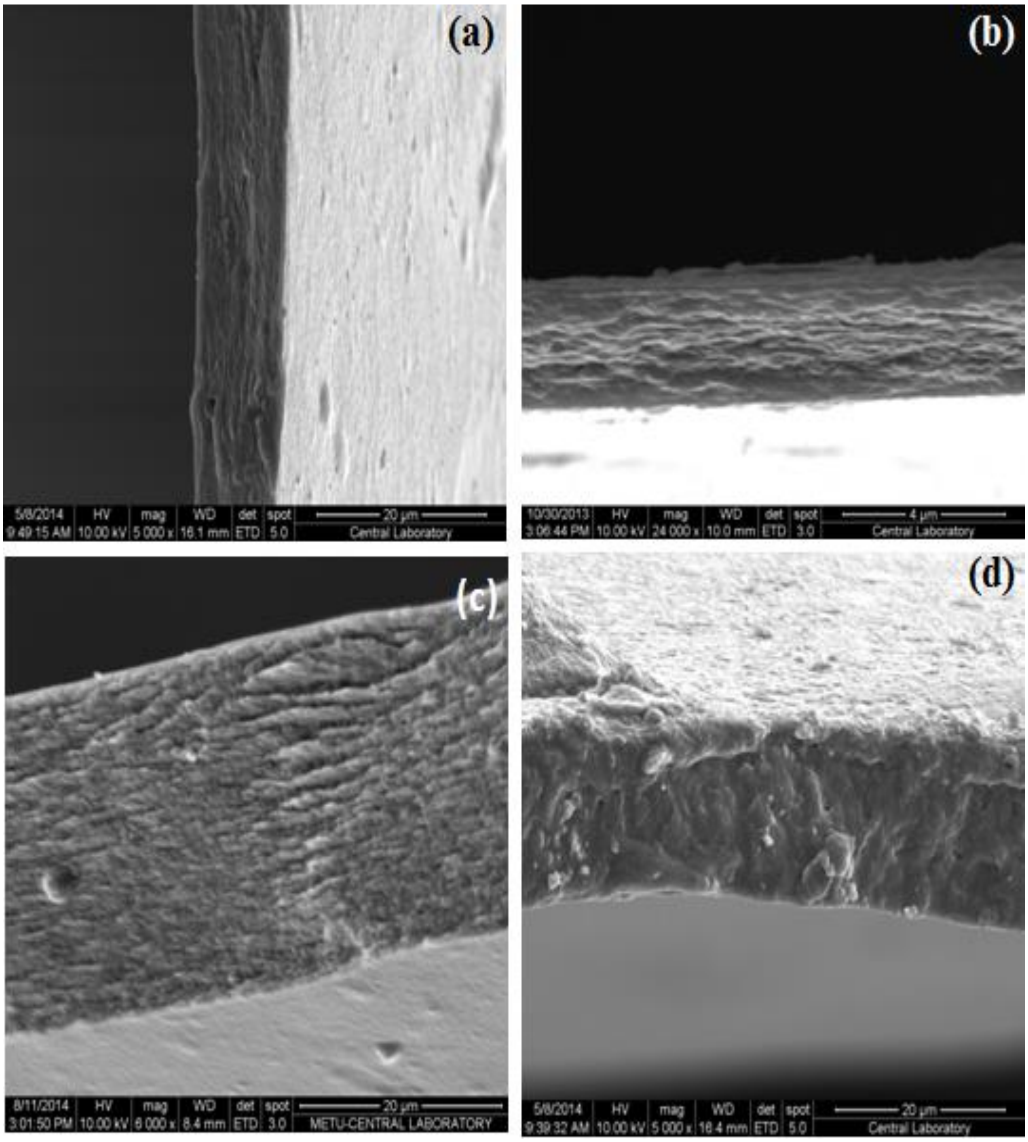

Figure 4.6. Scanning electron microscopy images of corn cob film heat treated at 200°C (a), corn cob film coagulated in ethanol/water mixture (b), cellulose film (c) and hemicellulose film (d)

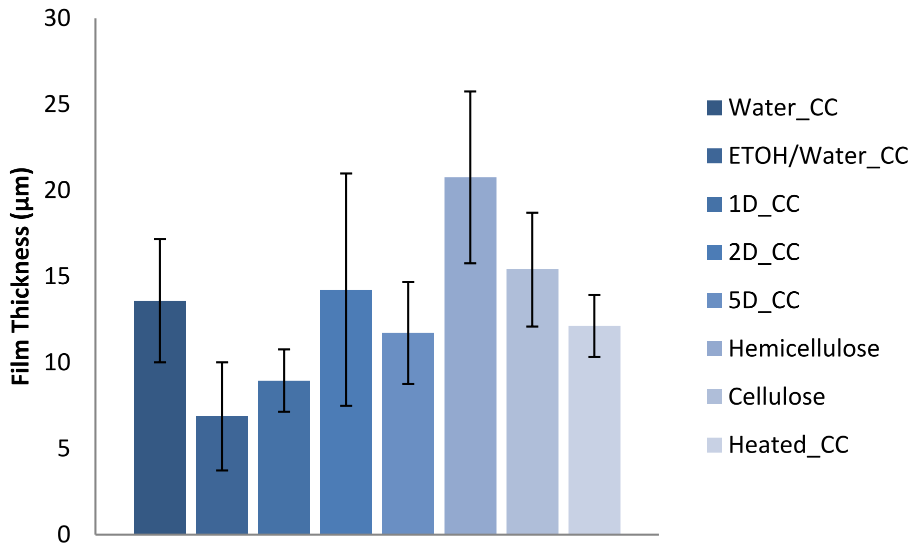

Figure 4.7. Average film thicknesses of corn cob based films

4.4. Effect of heat treatment on the water sensitivity of corn cob films

Biodegradable films on one hand are expected to be water-resistant in some food packaging applications where the film should be in contact with water through the processing of the packaged product. On the other hand, lower water resistance is considered as a sign of biodegradability of the films as packaging material (Bourtoom and Chinnan, 2008).

In order to examine the water sensitivity of the produced corn cob based films, films were immersed into water and were stirred with a vortex mixer at specific time intervals during the day. At the end of a week, films produced from corn cob could not maintain their integrity and broke apart in water as illustrated in Figure 4.8 a,b. In an attempt to reduce the water sensitivity of the films and accordingly facilitate their use in food packaging applications, Water_CC film was heated to

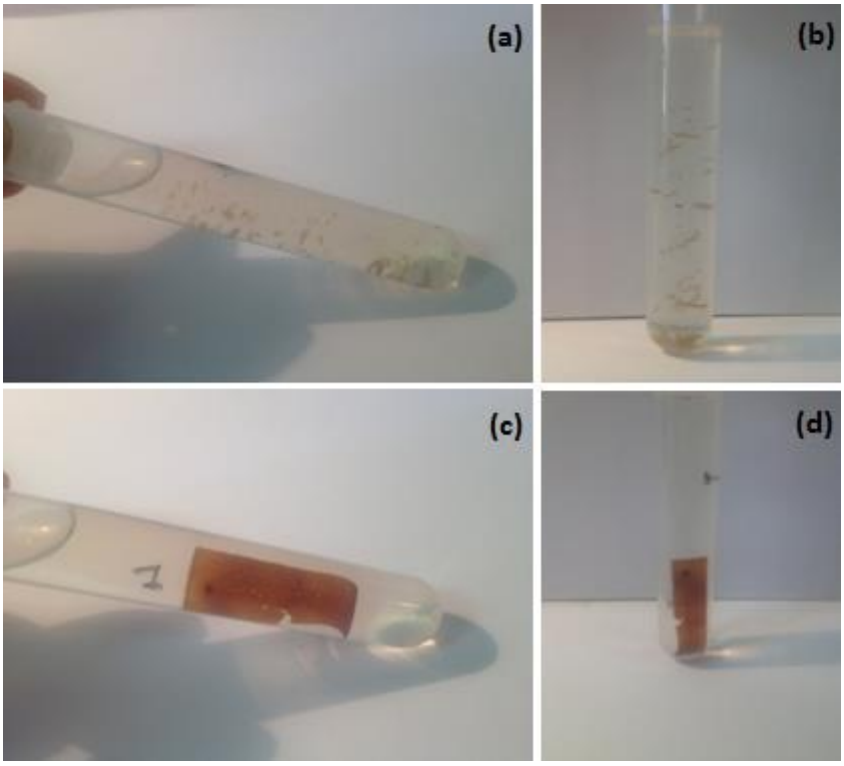

Figure 4.8. Appearance of corn cob films (Water_CC) in water upon stirring. Untreated films (a,b) and films treated at 200°C for 24 h (c,d)

120°C, 160°C and 200°C for 24 h and same procedure was applied to the heat treated sample (Heated_CC) to examine its behavior in water. It was found out that heat treatment performed at 200°C for 24 h helped the film to maintain its intact structure even after one week of immersion in water upon stirring (Figure 4.8 c,d). Heat treatment conducted at 120°C and 160°C were not sufficient to protect intact structure of the corn cob based films upon stirring in water.

4.5. Light transmittance of corn cob based films

The optical features could give the films the potential in various applications, such as food packaging, coating, biomedical applications, drug delivery, etc. Desired optical features were observed to change according to the application. Optical features were pointed out as a targeted property for food packaging and coating applications. For packaging purposes, for example on one hand, it should be advantageous to have films that slow down unwanted reactions that lead to fat and oil oxidation, formation of off-flavors, loses of vitamins depending on the application. This requirement is necessary to package foods containing light sensitive nutrients (Sahbaz et al., 2001). On the other hand, transparency of the films is considered as a prerequisite in terms of optical properties when priority is given to aesthetics and consumer demand accordingly. Transparent packaging films give companies opportunity to compete according to their product appearance (Farris et al., 2008).

Figures 4.9 and 4.10 illustrate the percent light transmittance and opaqueness/thickness values of the films produced in the present work. The following figures show that the percentage transmittance was in the range of 66-89% except for the Heated_CC film that had 30% light transmittance. Opaqueness/thickness values of the films varied between 0.007-0.03μm^{-1} roughly for the all the films except for Heated_CC film that had the highest opaqueness/thickness value.

Heating the films produced from unfractionated corn cob at 200^{0}C for 24 hr caused discoloration of the film therefore among all the films fabricated in this study, Heated_CC film was the least transparent by transmitting only 30% of incident light. The reason of darkening of the film colors could be attributed to polymer degradation. Cellulose is known to be sensitive to mild heat as highlighted by Molton and Demmitt (1977). Their findings and results obtained by other authors in the literature were found to be in accordance with this explanation. They found out that cellulose with initial degree of polymerization (DP) of 800 degraded to a product with 300 DP after heating the sample at 202^{0}C for 30 hr. Pacault and Sauret (1958) conducted a study to show the effect of heating temperature & time on degradation of cellulose. Cellulose with initial DP of 800 was heated to 202^{0}C for 55 h, to 186^{0}C for 100 h and resulted in a product with final DP as 300 for both of the cases. DP of the cellulose that has 600 initial

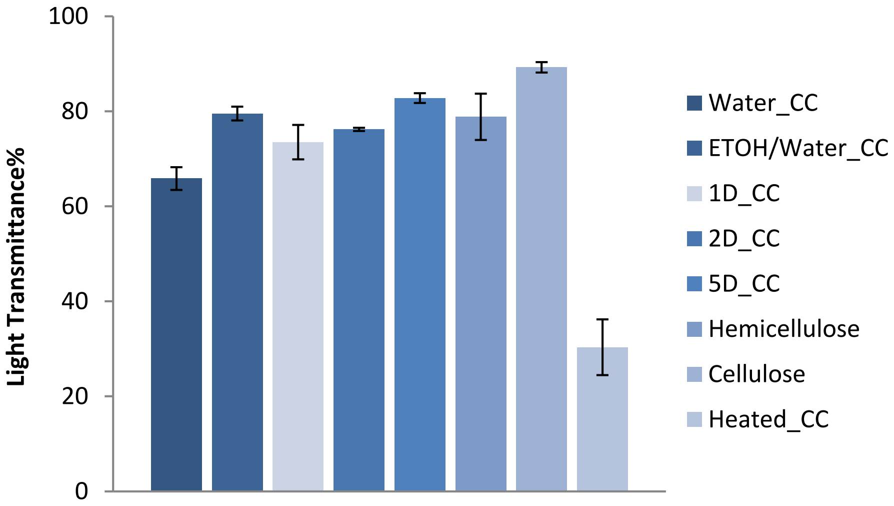

Figure 4.9. % Light transmittance of corn cob based films

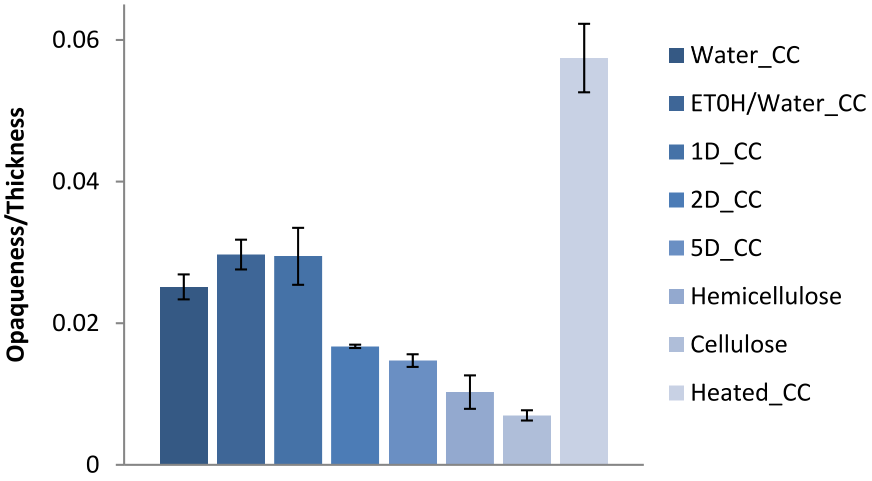

Figure 4.10. Opaqueness/thickness values of corn cob based films

DP decreased to 300 when heating temperature and time were 230^0C and 50 h. In order to show the heating temperature and time effect, Molton and Demmitt heated cellulose to 230^0C for 10 hr and its DP decreased to 300 from 600, further heating at this temperature did not cause a change in DP value. According to these results, they concluded that depolymerization of cellulose happens without of weight loss until DP of 300 is reached and their interpretation was also confirmed by the results of other studies reported in the literature. For instance, Brido and coworkers (1973) obtained a cellulose sample with DP of 455 after heating at 225^{0}C of cellulose with 2650 initial DP with less than 1% loss of weight.

Cellulose film illustrated the highest transparency as 89% followed by 5D_CC film. Cellulose and hemicellulose films transmitted more incident light compared to other films fabricated for unit thickness; therefore, it can be concluded that fractioning hemicellulose and cellulose from corn cob with the intention of producing films caused to produce more transparent; in other words, less opaque films as opaqueness and transparency are inversely correlated with each other. Similar results were also reported by Chen et al. (2014) for the films fabricated by coagulation of bagasse-DMSO/LiCl solution either in water or acetone-water mixture. Chen and coworkers (2014) reported lower light transmittance values than the films produced from regenerated cellulose in the study of Zhang et al. (2001). This finding was attributed to the presence of hemicellulose and lignin in bagasse films (Chen et al., 2014).

Results also revealed that conditioning the films in 100% RH desiccator for different times did not affect the opaqueness of the films (1D_CC, 2D_CC and 5D_CC), since these values were actually similar as indicated in Figure 4.9. Decreasing trend observed in Figure 4.10 for the films conditioned in 100% RH desiccator arises from the lower thicknesses of 2D_CC and 5D_CC films than 1D_CC film.

4.6. Water vapor permeability (WVP) of corn cob based films

Low water vapor permeability is another desired property for the films to be used as packaging materials as they should impede moisture transfer between atmosphere and packaged material in order to prolong shelf life of the product (Hansen and Plackett, 2008). Water vapor permeability of the films produced from fractionated/unfractioned corn cob is shown in the Figure 4.11. Produced films had different WVPs ranging from 3.4 to 40.0×10^{-12} g.m^{-1}.Pa^{-1}.sec^{-1}). Commonly, total grams of water transferred in the film increase linearly in the first 24 hours while the slope decreased after 24 hours for all the films which have unfractionated and fractionated biomass as the raw material. The decreasing slope of total grams of water absorbed vs. time graph for after 24 hours was considered to be related with the saturation of the adsorbent to water vapor.

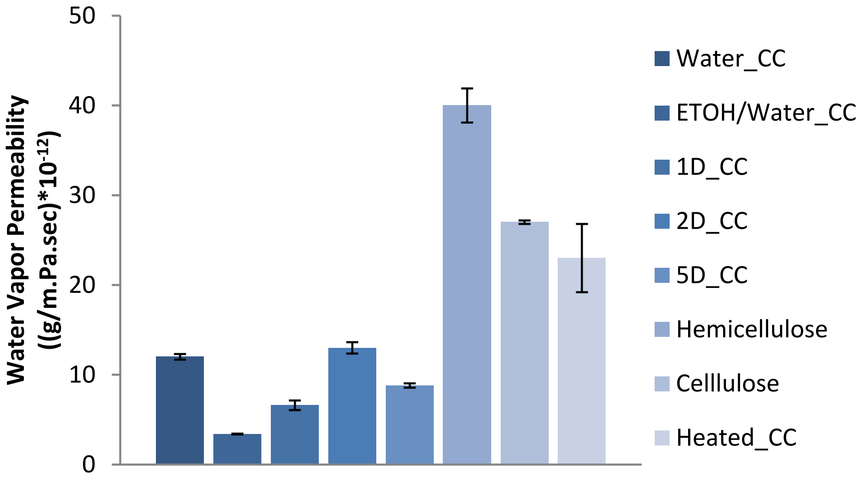

Figure 4.11. Water vapor permeability results of corn cob based films

Hemicellulose film had the highest water vapor permeability (WVP), and permeated water vapor approximately 10 times faster than ETOH/Water_CC film, which has the least water vapor permeability among all the films fabricated. WVP result of hemicellulose film is not surprising since it has a strong hydrophilic character inherently which is pointed out as one of the major obstacles by Yaich et al. (2014) that restrict their use in high volume packaging applications. Another prominent result gathered is that the fractionated corn cob films have higher water vapor permeability than films produced from unfractionated corn cob films. WVP values of fractioned corn cob films are in a range of 27-40×10^{-12} g.m^{-1}.Pa^{-1}.s^{-1} while these values range from 3 to 13×10^{-12} g.m^{-1}.Pa^{-1}.s^{-1} for unfractionated corn cob films.

Heated_CC film has about twice the WVP of Water_CC film. This result can be explained together with the moisture uptake (which is about 3.3 times higher for Water_CC) and morphology of these films. It can be assumed that the corn cob films have a microporous structure, which is due to the fabrication method used to obtain the films. The solvent exchange that takes place during film fabrication results in a certain level of porosity in the film. The porosity can also be inferred from the nodular appearance in the SEM images. Accordingly, vapor molecules can permeate more easily through the porous structure with less water vapor absorbed in Heated_CC film as compared to Water_CC film which has a higher affinity for water vapour, and probably has water condensed inside its pores due to this affinity.

Conditioning in 100% RH desiccator of the unfractioned corn cob films did not affect much WVP values since they show similar WVP as Water_CC films.

Table 4.1 is shown to be able to make a comparison of water vapor permeability performances of the films produced in this work and the films produced in the literature for similar purposes. The samples of this work give lower WVP results in terms of water vapor permeabilities than most of the films tabulated in the Table 4.1, reported in the literature. The result is expected since most of the studies included in the table measure the water vapor permeabilities of the films originated from inherently hydrophilic hemicellulose. Lowest WVP value among all hemicellulose films was measured as 30*10^{-12} g.m^{-1}.Pa^{-1}.s^{-1} (Sárossy, 2011) which is close to the WVP measured for hemicellulose film in this work. The WVP values measured in this study were also lower than reported WVP values for composite films from three different lignocellulosic materials which were given in Table 4.1 (Abdulkhani et al., 2013).

As mentioned, since their polymer matrix is hydrophilic in nature, hemicellulose based films have poor properties under high humidity conditions and as expected show little resistance to water vapor transfer. As well as plasticizers, in order to overcome these problems and make these films less compatible with water vapor, chemical modifications are also often employed as hemicellulose is a good candidate for chemical functionalization.

WVP values of three different composite lignocellulosic films manufactured from unfractionated lignocellulosic biomass reported by Abdulkhani et al. (2013) are also included Table 4.1 as well as hemicellulose based films. Reported WVP values are much higher compared to the WVP values of this work, varying between 170 and 250×10^{-12} $g.m^{-1}.Pa^{-1}.sec^{-1}$. The reason may be attributed to the different proportion of cellulose, hemicellulose, and lignin in biomass feedstock used since in this study corn cob is used whereas poplar wood (PW), chemi-mechanical pulp (CMP) and cotton linter (CEL) are used in the study of Abdulkhani et al. (2013) as the raw material of the films produced. Cotton linter was reported to be containing 99 % α-cellulose by the authors of the study (Abdulkhani et al., 2013), another raw material of composite films which was poplar wood reported to had approximately 42 to 49% cellulose, 16 to 23% hemicellulose and 21 to 29% lignin content (Sannigrahi et al., 2010). Final raw material of composite films was reported to be obtained by chemi-mechanical pulp of poplar wood that can be defined as the utilization of poplar wood to produce pulp to be further processed in paper industry by chemi-mechanical pulp (CMP) process. This final raw material could be considered to have higher cellulose content than poplar wood itself since pulp was defined as man-made cellulose obtained from lignocellulosic biomass sources by Akgül et al. (2006).

On the other hand, the raw material of the films produced in this study was corn cob and reported to contain 33%, 36% and 24% by dry weight cellulose,

Table 4.1. Water vapor permeability results of this work and biodegradable, edible and conventional polymer films in the literature

BIODEGRADABLE FILM TYPE	**WATER VAPOR PERMEABILITY ($g.m^{-1}.Pa^{-1}.s^{-1}$)$\times 10^{-12}$**	**REFERENCE**
Water_CC	12	
ETOH/Water_CC	3.4	
1D_CC	6.6	
2D_CC	13	
5D_CC	8.8	
Corn cob based hemicellulose	40	
Corn cob based cellulose	27	
Heated_CC	23	
Lignocellulosic composite film_- cotton linter(unfractionated biomass)	~170	Abdulkhani et al., 2013
Lignocellulosic composite film_- poplar wood(unfractionated biomass)	~250	Abdulkhani et al., 2013
Lignocellulosic composite film_- chemi-mechanical pulp (unfractionated biomass)	~200	Abdulkhani et al., 2013
Corn hull hemicellulose-based	48	Zhang et al., 2004
Rye bran hemicellulose-based	89	Sárossy et al., 2011
Rye endosperm hemicellulose-based	30	Sárossy et al., 2011
Corn hull hemicellulose-based (reinforced with sorbitol)	23	Zhang et al., 2004
Spruce wood hemicellulose-based (reinforced with 29wt% sorbitol)	23	Mikkonen et al., 2010
Spruce wood hemicellulose-based (reinforced with 19wt% sorbitol)	10	Mikkonen et al., 2012

Table 4.1. Water vapor permeability results of this work and biodegradable, edible and conventional polymer films in the literature (continued)

BIODEGRADABLE FILM TYPE	**WATER VAPOR PERMEABILITY ($g.m^{-1}.Pa^{-1}.s^{-1}$)×10^{-12}**	**REFERENCE**
Corn bran hemicellulose-based (reinforced with 15wt% glycerol)	120	Péroval et al., 2002
Barley oat hemicellulose-based (with 30-40wt% glycerol content)	680-1690	Tejinder et al., 2003
Maize bran hemicellulose-based (with 15wt% glycerol content)	77.2-137	Phan The et al., 2002
Corn bran hemicellulose-based (reinforced with 15wt% glycerol)	120	Rindlav-Westling et al., 1998
Poly lactic acid (PLA)	13.4	Auras et al., 2006
NON- BIODEGRADABLE FILM TYPE	**WATER VAPOR PERMEABILITY ($g.m^{-1}.Pa^{-1}.s^{-1}$)×10^{-12}**	**REFERENCE**
Polystyrene (PS)	4.2	Auras et al., 2006
Low-density polyethylene (LDPE)	1.9	Péroval et al., 2002
Polyethylene terephthalate (PET)	2.8	Auras et al., 2006

hemicellulose and lignin, respectively (Toraman, 2012). Besides, the type of hemicellulose in the biomass may also affect the water vapor transfer.

Furthermore, different ionic liquids which are [EMIM][Ac] and [BMIM][Cl] in the case of present work and the study of Abdulkhani et al. (2013) respectively were used to dissolve the biomass. [EMIM][Ac] is proven to be a better solvent for cellulose and wood types compared to [BMIM][Cl] (Zavrel et al., 2009). The reason that enable to measure lower WVP values in this present work might be due to the higher solubility performance of [EMIM][Ac] since better solubility of lignocellulosic biomass in ionic liquid may give a tighter structure.

On the other hand, film fabrication methods were different in some cases. For instance, composite films were prepared from suspension of ionic liquid and lignocellulosic material in the study of Abdulkhani et al (2013). Films produced with the exception of the cotton linter film were opaque, indicating that the films elements were not perfectly miscible with each other. In this study, films prepared from the solution of fractionated or unfractionated corn cob dissolved in [EMIM][Ac].

Abdulkhani et al, (2013) interpret the WVP results to amount of cellulose; hemicellulose and lignin content of the related biomass and regard the presence of cellulose as a blockage to water vapor. Accordingly, cotton linter composite film illustrated the best performance by permeating the least water vapor under the same conditions since it has the highest cellulose content by weight reported in the literature as more than 80 wt% (Sczostak et al, 2009; Morais et al., 2013) and reported to be containing 99 % α-cellulose in the study (Abdulkhani et al., 2013). As opposed to interpretation of Abdulkhani et al. (2013), Albertsson et al. (2010) reported that lignin included in the biomass composition enhances water vapor barrier properties of the films produced by decreasing that value. On the point of this view, the reason of lower WVP values measured in this study could be the higher lignin content of the corn cobs which is 24% by dry weight (Toraman, 2012). CEL and CMP had no or lower lignin content than corn cobs and the lignin content of PW used was not stated in the study by Abdulkhani et al. (2013).

Commercial nonrenewable polymer sources of the films often employed in food packaging are low-density polyethylene (LPDE), polystyrene (PS), polypropylene and polyethylene terephthalate (PET) (Hansen and Plackett, 2008). The WVP values of these commercial polymers range between (1.9-4.3) $\times 10^{-12}$ $g.m^{-1}.Pa^{-1}.s^{-1}$ (Auras et al., 2006; Péroval et al., 2002). Composite lignocellulosic films and most of the hemicellulose based films reported in the literature are not sufficient for rivaling the conventional nonrenewable raw materials of the films intended to use for packaging. It seems that different modifications applied for enhancing the water vapor barrier properties of hemicellulose based films are not adequate to replace commercial polymers. Films produced in this work are also insufficient to compete with commercial polymers in terms of WVP. However, films of this present study which are produced from unfractionated corn cob illustrated better barrier properties to water vapor compared to fractioned corn cob films and most of the films produced in the literature. Therefore, in the case of WVP, fractioning corn cob the biomass caused to measure higher WVP. WVP values of unfractionated corn cob films are 2-12 times; whereas, WVP values of fractionated corn cobs are 15-20 times higher than that of films from conventional polymers inspected to compare. Better WVP of the films manufactured from commercial polymers might be resulted from the better intense packaging or molecular interactions of the components of the films. The ETOH/Water_CC film produced in this study has shown lower WVP than biodegradable films reported in the literature and comparable WVP as commercial, non-biodegradable films, even without the support of additional film-forming additives or chemical modification.

4.7. Moisture uptake (MUP) of corn cob based films

As reported by Mikkonen and Tenkanen (2008), polysaccharides are hydrophilic materials and are sensitive to changes in RH due to the high content of hydroxyl groups. Hence, moisture uptake (MUP) is one of the major obstacles that restrict the application of biodegradable materials in various applications. For instance, in food packaging, the moisture uptake of the films should be within the certain limits under different circumstances that would not harm the packaged product (Guo et al., 2014). Damage to the product by water absorption of the packaging material can be observed by different means either by poor mechanical and chemical stability or dimensional stability (Abdulkhani et al., 2013).

The percent moisture uptake values of corn cob based films are given in the Figure 4.12. Moisture uptake of the films is studied by following the change of weight during exposure time at 100% relative humidity (RH).

MUP values for all the films ranged from 26% to 104%. Generally measured high MUP values confirms the films produced are quite hygroscopic and absorb significant amount of water in high humidity environment, which was set as 100% relative humidity in this study. Zhang and coworkers (2011) divided the RH scale into two regions and defined the high humidity conditions as the environment that has a RH value greater than 80%, where noticeable increase in weight gain values were observed. Stevanic et al. (2012) reached the same conclusion by reporting that the molecular interactions between the molecules of cellulose and hemicellulose become partly replaced by interactions of water molecules at relatively high humidity environments.

Considering the desiccator effect, weight gain due to the exposure to moisture decrease slightly with increasing conditioning time of the films' in 100% RH desiccator since MUP values are 77%, 100% and 81% for 1D_CC, 2D_CC and 5D_CC films, respectively. Still, conditioning in desiccator seem not to significantly reduce the moisture uptake of the films as Water_CC film's MUP value was determined as 86% approximately which is lower than the recorded MUP value for 1D_CC film. Overall, films produced from corn cob itself had similar MUP values with the exception of Heated_CC film.

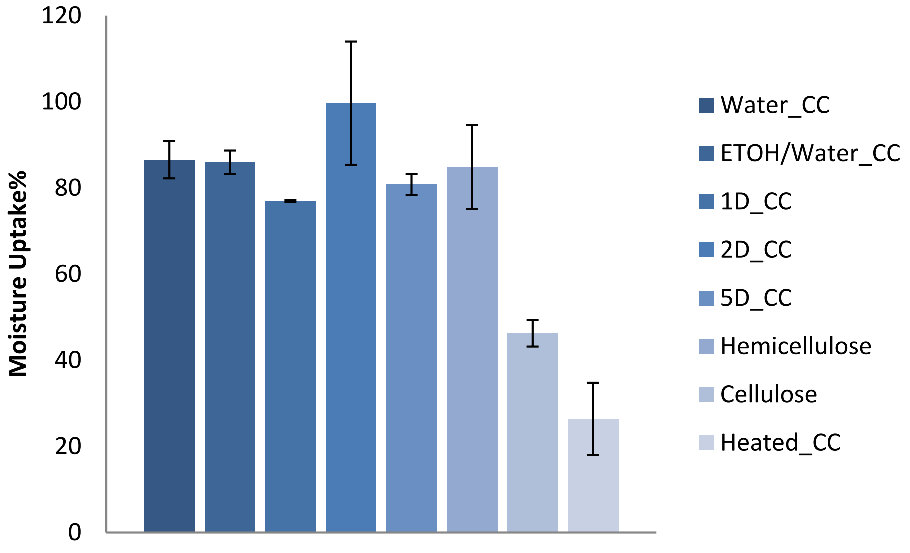

Figure 4.12. Moisture uptake of corn cob based films

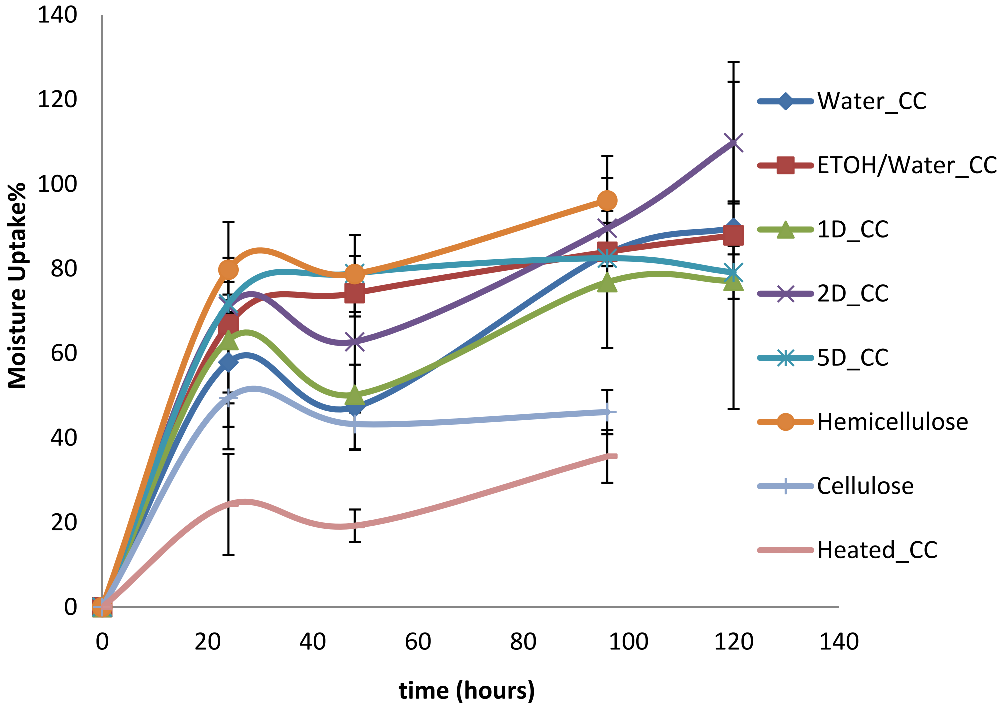

Figure 4.13. Moisture uptake of corn cob based films against time

Fractioning the hemicellulosic portion of the corn cob did not reduce the percentage of water absorbed. MUP value of hemicellulose film was similar to that of films produced from unfractionated corn cob. This result may reflect that films produced from unfractionated corn cob have a significant amount of hemicellulose content. High moisture uptake determined for hemicellulose film was expected and could be attributable to the strong hydrophilic character of hemicellulose reported also by Albertsson et al. (2014). Hemicellulose behaves as hygroscopic material and it is known to be water soluble at elevated temperatures (Huijgen and Bakker, 2010). On the other hand, isolation of the cellulosic portion of the biomass to fabricate the films reduced the moisture uptake by half reflecting the crystalline nature of the cellulose as reported by Stevanic and coworkers (2012) where they produced biocomposite films based on hemicellulose and nanofibrillated cellulose (NFC). Furthermore, unlike hemicellulose, cellulose is reported to be water insoluble due to the existence of large amount of intra and intermolecular hydrogen bonds that assemble cellulose fibers in its structure (Swatloski et al., 2002).

A greater difference in the measurement of moisture uptake of the films was seen for Heated_CC film as compared with other films tested in terms of MUP. This might be explained by cross-linking of biomass components upon heating that limits the affinity of the films towards water. The increase in the stability of the cellulose by inter chain cross-linking upon heating was also reported in the literature by Molton and Demmitt (1977). In a study of Keslter and Fennema (1986), it was reported that cross-linking could increase the resistance to vapor and gas transport by reducing the chain mobility of the polymer. Cross-linking upon chemical modification was studied by Coma et al. (2003) to allow an increase in hydrophobicity of the cellulose based packaging film. The cross-linking was reported by Coma et al. (2003) as an effective approach to hydrophobize cellulose derivatives which might be used as packaging materials.

As water sensitivity limits the utilization of biomass components for the packaging, coating purposes, it is possible to find many studies in the literature that investigate the moisture uptake of these materials under certain relative humidity environments. For instance, Zhang and coworkers (2011) found out that their hemicellulose films which are extracted from wheat bran absorbed 60-70% water at 90% RH. Stevanic et al. (2012); on the other hand, prepared rye arabinoxylan and nanofibrillated (NFC) cellulose films with different ratios and stated that at 90% RH, films absorb 25-30% moisture. They concluded that the results reflect the crystalline nature of cellulose and high amount of water sorption sites available in hemicellulose as NFC film displayed the lowest and pure hemicellulose film showed the highest content of moisture. Increasing the NFC content lead to a reduction in moisture sorption values and moisture-induce softening for composite films. In another study of Stevanic and coworkers (2011) they mixed two possible wood biorefinery products, hemicellulose and microfibrillated cellulose (MFC) to produce composite films and measured the moisture uptake of these films as 30-35% at 80% RH. Glycerol as plasticizer was also added to film forming solutions and it was found out that this substance affects the moisture uptake of the films depending on the RH value. At low RH, the existence of glycerol slightly decreased the moisture content by occupying the available water sorption sites but, increased that value at high RH. The reported effect of plasticizer on water uptake measurements by Stevanic et al. (2011) was also confirmed by Godbillot et al. (2006) for their plasticized starch based films. Similar to the former study of Stevanic et al. (2012) mentioned MFC addition caused to decrease in water content of the films reflecting that this substance somewhat made some of the water sorption sites unavailable when added to hemicellulose/plasticizer mixtures. Nanofibrillated cellulose (NFC) and microfibrillated cellulose (MFC) addition to hemicellulose caused to measure lower MUP values which are ranged from 25% to 35% at high RH than the WUP values measured in this present work. The lower MUP results of composite films reported by Stevanic et al. (2011 and 2012) could be explained by differing crystalline structure of cellulose contained in the film composition. On the other hand, differing compositions of the biomass components (cellulose, hemicellulose and lignin) in the film could lead to measure different MUP values since the moisture uptake contribution of each component is different. Based on this explanation, the film produced from cellulose rich portion of the corn cob in this work has considerably lower MUP compared to other corn cob films except Heated_CC. A similar result was also seen by Abdulkhani et al. (2013) as lignocellulosic composite films fabricated from different biomass have quite different MUP values. Different free hydroxyl groups which are reported as the positions capable of association with water were hold accountable for this result (Abdulkhani et al., 2013). Measured MUP values were greater than many studies in the literature. This finding might be attributed to the microporous structure which can be inferred from the layered structure in the SEM images of the films. On the other hand, films were fabricated from the fully dissolved corn cob-ionic liquid solution in this study, whereas produced films in the literature were cast from suspensions. This might also caused to measure higher MUP values than MUP values reported in the literature.

4.8. Mechanical properties of corn cob based films

Another targeted property related to polymeric films to be used for applications such as packaging, coating and biomedicine due to the compatibility of these compounds is their mechanical properties. For instance, considering the packaging applications, the packaging should remain undamaged during application, consecutive transportation and handling and therefore, must be able to withstand a particular mechanical strength to protect the packaged product (Mikkonen and Tenkanen, 2012).

The most common mechanical features reported in studies where the films produced from synthetic polymer or fractioned/unfractioned lignocellulosic biomass for numerous purposes found in literature are the tensile strength, elongation at break, and Young’s modulus.

The figures below illustrate related mechanical properties (ultimate tensile strength (UTS), elastic modulus (E), elongation at break (e_b)) of the films produced in this thesis work.

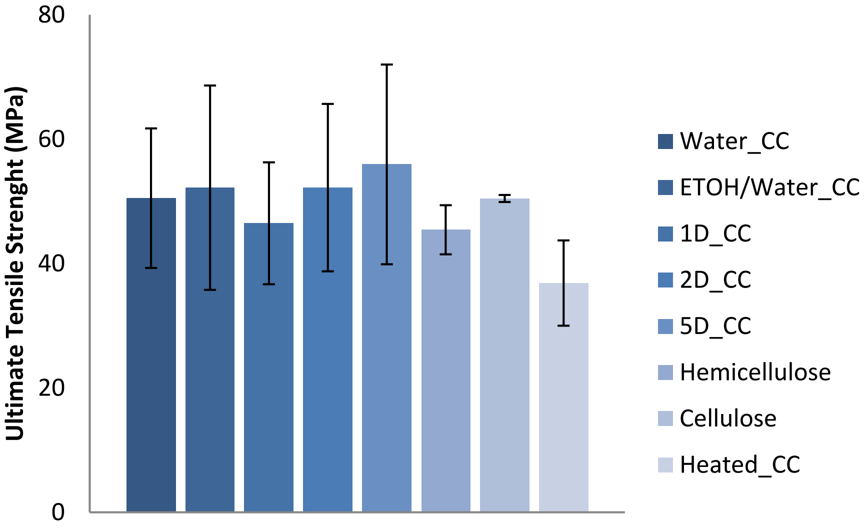

Figure 4.14. Ultimate tensile strength of corn cob based films

All the films produced illustrated a low elongation at break and rather high ultimate tensile strength values. UTS and E values are in the range of 36.9-56.0 MPa and 1700-3449 MPa, respectively (Figures 4.14 and 4.15). Films produced in this study also illustrated low per cent elongation at break values as the lowest e_b value is 1.4% found for Heated_CC and the highest e_b value is 3.8% found for 5D_CC film (Figure 4.16).

Conditioning the films produced from unfractioned corn cob in 100% RH desiccator with different times did not produce a significant change in mechanical properties due to the absence of a consistent trend that is valid for UTS, e_b and E values of the1D_CC, 2D_CC and 5D_CC films. In fact, no noteworthy difference

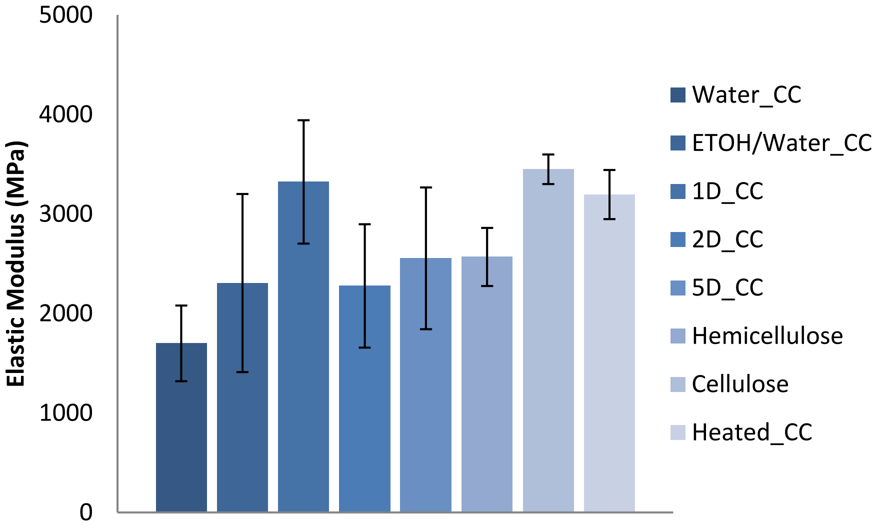

Figure 4.15. Elastic Modulus of corn cob based film

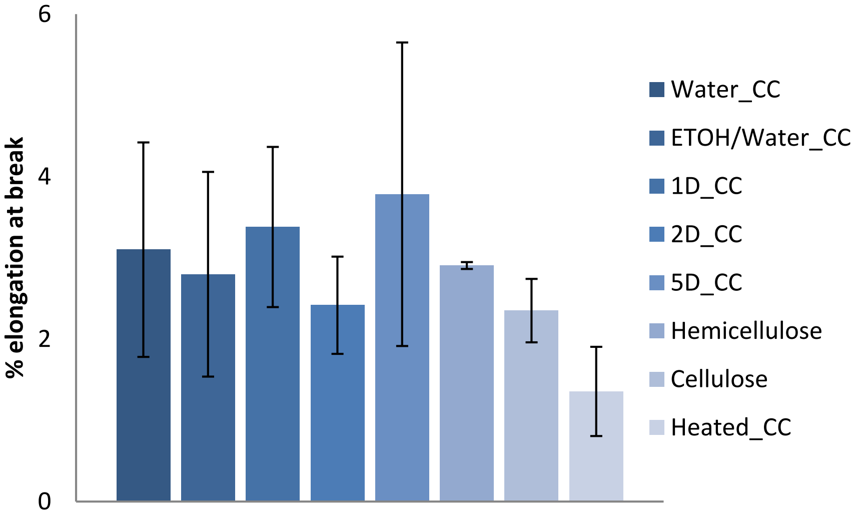

Figure 4.16. % elongation at break of corn cob based films

was observed for UTS for the films produced directly from corn cob itself.

E value for Heated_CC film was noticeably higher than E value of Water_CC film which was also close to E value of cellulose film together with 1D_CC film. E for other films was similar ranging between 1700-2555 MPa approximately.

Percent elongation at break value was found to be similar for the entire corn cob based films with the exception of e_b value of Heated_CC film that had the lowest e_b value as 1.4%.

Effects of heating unfractionated corn cob film to 200^0C for 24 hours observed on e_b and E of the films were larger than on UTS values of the films. Considering the results, heating unfractionated corn cob film to 200^0C for 24 hours led to produce stiffer films. Furthermore, after heating the sample, the obtained films are less stretchable as they illustrate a substantially lower e_b value measured as 1.4% on average. These results might be suggesting the existence of cross-linking between the polymer chains of the film fabricated. In a support of this inference, Molton and Demmitt (1977) showed that simple heating that is 170-200^0C up to 40 hr caused to depolymerization and cross-linking of cellulose. They explained and discussed various mechanisms may lead to cross-linking in cellulose. Mechanisms are explained through ether and ester formation between chains. Ester formation is defined with the carboxyl group requirement that may esterify with a hydroxyl group on an adjacent molecule. On the other hand, an acidic degradation product is shown to be an alternative that can cause the linkage of chains, cross-linking in other words. In a study of Rodrig et al. (1975) they propose the cross-linking of cellulose through ester formation with a decomposition product. Besides, cross-linking of cellulose which is explained by the mechanisms including free radicals are also take part in the literature. When the number of radicals generated upon heating is sufficient, free radicals are proven to cause cross-linking of cellulose chains (Molton and Demmitt, 1977). Radical formation in cellulose is reported by Arthur and Hinojosa (1966) to initiate between the temperature ranges of 250-

300^0C. Overall, Molton and Demmitt (1977) introduced two mechanisms that might lead to cross-linking upon heating as; initial carbonium ion-mediated dehydration mechanism that predominates at temperatures below 250^0C and another mechanism that yields to free radical chain reactions at temperatures 300^0C and higher and discussed the routes of these mechanisms explained in their paper.

Other studies in the literature also confirmed that cross-linking causes to measure lower percent elongation at break values. Sirviö et al. (2014) produced biocomposite films based on cellulose and alginate and found out that the e_b values of the biocomposite films were slightly decreased during the cross-linking. Furthermore, Guo and coworkers (2014) have reported remarkably less extensible edible gelatin films as a result of cross-linking. In a study of Mu et al. (2012) lower e_b values were measured for glycerol-plasticized gelatin edible films cross-linked by heat curing and cross-linking is reported to result in harder and tougher film structure.

Fractioning hemicellulosic portion of corn cob to produce films as well as isolation of the cellulosic portion, did not lead to a major differentiation in tensile testing measurements. Cellulose film gives only slightly higher results for E value through the films produced from fractionated/unfractionated corn cob. Therefore, it can be said that UTS and e_b results were almost independent of fractioning the corn cob since hemicellulose and cellulose films do not have noticeable different results in terms of these values. E value only was found to be dependent on fractioning the cellulosic portion of the corn cobs as a noticeable increase was observed in this value for cellulose film.

Table 4.2 contains the studies reported in the literature and enables to make a comparison of the mechanical properties between the corn cob films produced in this thesis and films found in the literature to be used for the same purposes. Basically, the mechanical properties of four different kind of film which are chitosan, starch or hemicellulose based and composite lignocellulosic films are provided in the Table 4.2 with the intention of making a comparison.

The mechanical properties of the films produced in this work from corn cob and hemicellulose based films reported in the literature seem to be comparable. Similar to the films produced in this study, UTS, e_b and E values of pure hemicellulose films tabulated below are in the range of 12-58 MPa, 3-12% and 735-3100 MPa respectively. Films fabricated from chitosan only had lower UTS while e_b values of these films are apparently higher than the films of the present work and the literature reaching up to 33% in a study provided in the Table 4.2 (Mali et al., 2006). On the other hand, pure starch based film is not superior in terms of its mechanical features to the films included in the Table 4.2 and films' of this work.

Actually, films derived from renewable materials are not adequate to compete with conventional packaging materials considering their mechanical behaviors. Poor mechanical properties are common problem that circumvent the use of these films in various applications instead of the films produced from commercial polymers. In many studies, mechanical performance of the films mentioned above was tried to be enhanced by different means either by compounding with a plasticizer or other polymers or by the addition of nano-sized components, for instance, cellulose nano fibers, cellulose nano crystals, etc.

Mechanical performance of the films provided in the table seems to be affected by the addition of reinforcement materials. For instance, in the case of the film produced from hemicellulose extracted from rye endosperm, addition of nanocomponent sepiolite obviously strengthens the film since its UTS and E value increased from 42.5 MPa to 74 MPa and 2300 MPa to 3900 MPa respectively while addition of this component does not have an important influence on e_b value, fluctuating between 10 and 12% (Sárossy, 2011). Using another reinforcement which is microfibrillated cellulose has better effect on UTS since it

Table 4.2. Tensile testing results of biodegradable and non-biodegradable films in the literature

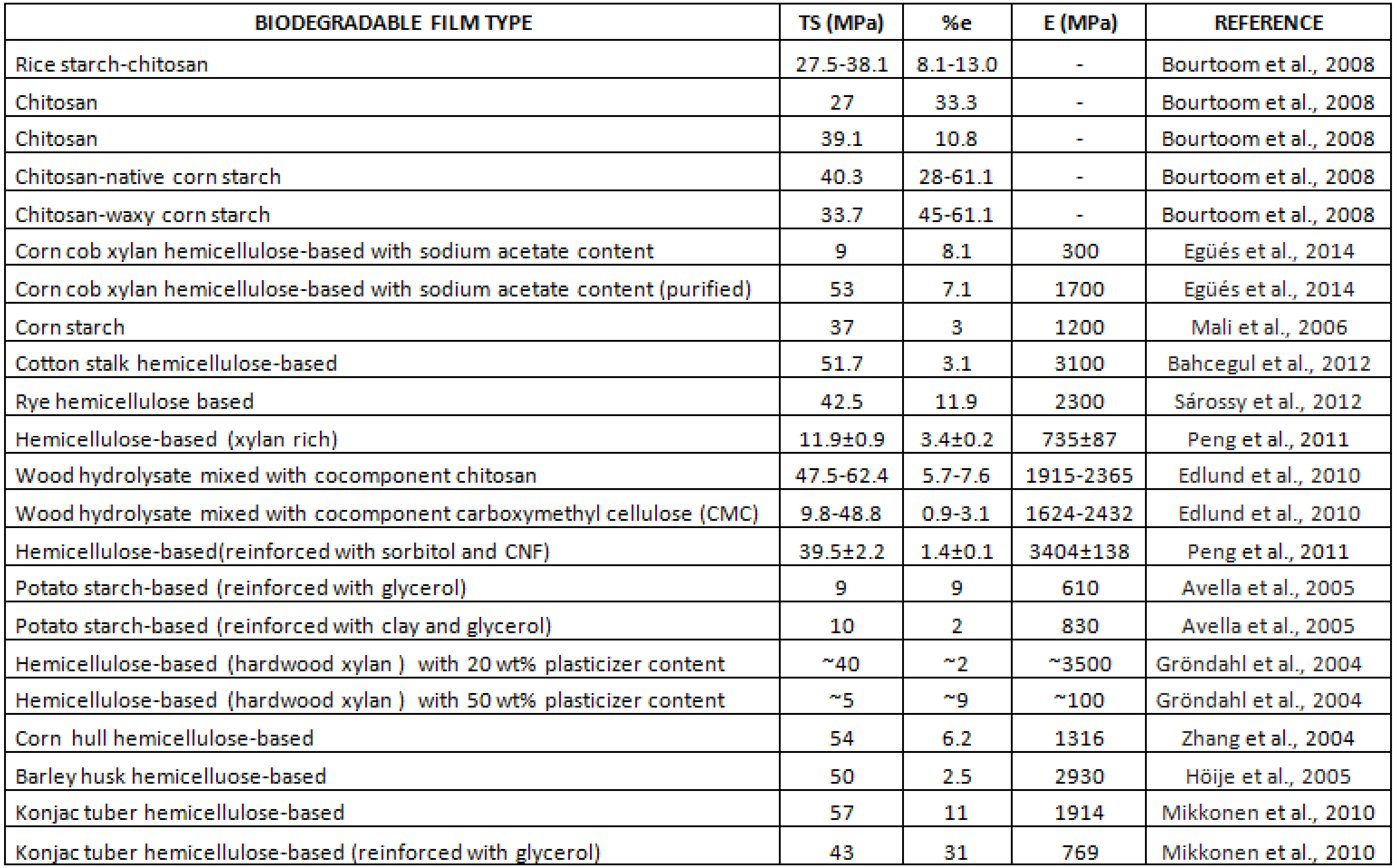

BIODEGRADABLE FILM TYPE	TS (MPa)	%e	E (MPa)	REFERENCE
Rice starch-chitosan	27.5-38.1	8.1-13.0	-	Bourtoom et al., 2008
Chitosan	27	33.3	-	Bourtoom et al., 2008
Chitosan	39.1	10.8	-	Bourtoom et al., 2008
Chitosan-native corn starch	40.3	28-61.1	-	Bourtoom et al., 2008
Chitosan-waxy corn starch	33.7	45-61.1	-	Bourtoom et al., 2008
Corn cob xylan hemicellulose-based with sodium acetate content	9	8.1	300	Egüés et al., 2014
Corn cob xylan hemicellulose-based with sodium acetate content (purified)	53	7.1	1700	Egüés et al., 2014
Corn starch	37	3	1200	Mali et al., 2006
Cotton stalk hemicellulose-based	51.7	3.1	3100	Bahcegul et al., 2012
Rye hemicellulose based	42.5	11.9	2300	Sárossy et al., 2012
Hemicellulose-based (xylan rich)	11.9±0.9	3.4±0.2	735±87	Peng et al., 2011
Wood hydrolysate mixed with cocomponent chitosan	47.5-62.4	5.7-7.6	1915-2365	Edlund et al., 2010
Wood hydrolysate mixed with cocomponent carboxymethyl cellulose (CMC)	9.8-48.8	0.9-3.1	1624-2432	Edlund et al., 2010
Hemicellulose-based(reinforced with sorbitol and CNF)	39.5±2.2	1.4±0.1	3404±138	Peng et al., 2011
Potato starch-based (reinforced with glycerol)	9	9	610	Avella et al., 2005
Potato starch-based (reinforced with clay and glycerol)	10	2	830	Avella et al., 2005
Hemicellulose-based (hardwood xylan) with 20 wt% plasticizer content	~40	~2	~3500	Gröndahl et al., 2004
Hemicellulose-based (hardwood xylan) with 50 wt% plasticizer content	~5	~9	~100	Gröndahl et al., 2004
Corn hull hemicellulose-based	54	6.2	1316	Zhang et al., 2004
Barley husk hemicelluose-based	50	2.5	2930	Höije et al., 2005
Konjac tuber hemicellulose-based	57	11	1914	Mikkonen et al., 2010
Konjac tuber hemicellulose-based (reinforced with glycerol)	43	31	769	Mikkonen et al., 2010

Table 4.2. Tensile testing results of biodegradable and non-biodegradable films in the literature (continued)

BIODEGRADABLE FILM TYPE	**TS (MPa)**	**%e**	**E (MPa)**	**REFERENCE**
Konjac tuber hemicellulose-based (reinforced with chitosan)	88	33	-	Ye et al., 2006
Spruce wood hemicellulose-based (reinforced with glyoxal)	23	3.7	684	Mikkonen et al., 2012
Rye endosperm hemicellulose-based film with 2.5 wt% sepiolite content	74	10	3900	Sárossy et al., 2011
Oat spell hemicellulose-based (reinforced with cellulose nano crystals and sorbitol)	5	30	-	Saxena et al., 2009
Rye endosperm hemicellulose-based	58	8.1	2500	Mikkonen et al., 2011
Rye endosperm hemicellulose-based (reinforced with microfibrillated cellulose)	95	11	2522	Mikkonen et al., 2012
Lignocellulosic composite film_- cotton linter(unfractionated biomass)	129.7	24.7	115.6	Abdulkhani et al., 2013
Lignocellulosic composite film_- poplar wood(unfractionated biomass)	17.8	1.2	41.7	Abdulkhani et al., 2013
Lignocellulosic composite film_- chemi-mechanical pulp (unfractionated biomass)	61.3	3.9	25.7	Abdulkhani et al., 2013
Synthetic wood composite film	61.7	-	-	Simmons et al., 2011
Polylactic acid	42	7.2	1400	Abdelwahab et al., 2011
NON-BIODEGRADABLE FILM TYPE	**TS (MPa)**	**%e**	**E (MPa)**	**REFERENCE**
Polypropylene	151-270	32-150	2800-5000	Yuksekkalayci et al., 1999
Polystyrene (PS)	55-82	3-40	3200	Auras et al., 2003
Polyethylene terephthalate (PET)	275	60-165	2800-4100	Auras et al., 2003

increased that value from 42.5 MPa to 95 MPa (Mikkonen et al., 2012). Addition of these reinforcement materials resulted in one of the best mechanical performances among the studies presented in the Table 4.2.

Peng et al. (2011) measured somewhat lower tensile strength and elastic modulus and comparable elongation at break values with those of the corn cob based films in our study for their sorbitol added bamboo hemicellulose based films. UTS and E values measured for corn cob based films is roughly 3 times higher than the reported UTS and E values of their hemicellulose based films which were reported as 12 MPa and 735 MPa, respectively. UTS and E values increased to 40 MPa and 3404 MPa when microfibrillated cellulose is used together with sorbitol while the films become less ductile with this alteration Peng et al. (2011).

On the whole, interactions of reinforcement component (cellulose or other materials) with the polymer matrix of the films seem to contribute a noticeable improvement in mechanical features of the materials. Similar to the authors of the mentioned studies who enable us to make this deduction, Sárossy (2011) also relates the superior mechanical properties of reinforced hemicellulose based films to pure ones with favored interaction due to the well dispersion of the reinforcement material between the polymer matrix and reinforcement component.

The highest UTS value included in the Table 4.2 belongs to the study of Abdulkhani et al. (2013) where the films are produced from lignocellulosic materials with using an ionic liquid as the solvent. In this study, three different lignocellulosic materials which are ball-milled poplar wood, chemi-mechanical pulp and cotton linter were mixed with ionic liquid, [BMIM][Cl], and the films were fabricated from the suspension. The ultimate tensile strength reached to 129.7 MPa which was approximately 2.3 times larger than the maximum UTS value measured in this study when cotton linter is used as the raw material of the composite film. The tensile testing results of other films produced from ball -

milled poplar wood and chemi-mechanical pulp are not superior to the films produced from corn cob in this thesis. UTS and e_b results of the poplar wood film were worse while these two values of chemi-mechanical pulp film were comparable with the tensile testing results of this study. Elastic modulus values of poplar wood and chemi-mechanical pulp film are clearly lower than corn cob films which are reported as 41.7 and 25.7 MPa respectively. They related the cotton linter film's high mechanical performance to high cellulose content of cotton linter film. They define cotton linter film as the 'self-reinforced' material due to its high cellulose content and presence of hemicellulose and lignin were accepted as impurities that worsen the mechanical performance of the lignocellulosic composite film. Cotton linter's high cellulose content is verified by Sczostak et al. (2009) and Morais et al. (2013) since they reported that the cotton linter is a potential source of nanocellulose crystals with more than 80% of cellulose content. Similar to Abdulkhani's view (2013), Bahcegul et al. (2012) reported that presence of lignin together with hemicellulose result in poor mechanical properties for hemicellulose based films which was found to be likely attributable to the agglomeration mechanism, promoted by the presence of lignin together with hemicellulose, explained by Westbye et al. (2007).

According to these interpretations, cellulose films were expected to have better mechanical features than other films produced in this study since hemicellulose and lignin content together was lower. However, mechanical performance of cellulose films' was not better than films produced from unfractionated corn cob or fractionated hemicellulose films of the present study in terms of E and UTS properties. Comparable mechanical properties can be related to the homogeneity of the films resulting from the full dissolution of corn cob in this study as opposed to these studies in the literature. Poly (lactic acid) (PLA) is a well-known biodegradable polymer employed to fabricate films for packaging purposes (Yuksekkalayci et al., 1999; Abdelwahab et al., 2012). Measured UTS in this study was nearly the same with the UTS of PLA film which was reported as 42 MPa by Abdelwahab et al. (2012). E value of corn cob based films of this study was approximately 1.8 times higher than E value of PLA film. e_b value of PLA film 2.9 times higher than that of e_b value of corn cob based films in general. Tensile properties of corn cob based films seemed to be comparable with PLA films tensile properties. On the other hand, tensile properties of conventional non-biodegradable polymer which is polypropylene (PP) were far better than corn cob based films mechanical properties. Reported UTS, E and e_b values by Yuksekkalayci et al. (1999) were 4-7, and 13-60 times higher than UTS and e_b of corn cob based films, respectively, whereas E values were similar.

By and large, the mechanical properties of the corn cob based films of this study seemed to be comparable with the mechanical properties of the films reported in the literature produced. In the literature commonly, films for packaging purposes are produced by fractioning the biomass as is often fractioning the hemicellulosic portion of the related biomass by different methods. According to the tensile testing results gathered in this work, fractioning the biomass did not lead to a vital difference in terms of mechanical features since the tensile testing results of this work seemed to be as good as most of the tensile testing results of the films derived from extracted hemicelluloses from different biomass. The mechanical properties of the films in this study were good and additional polymers or plasticizers were needed to obtain similar mechanical properties in the literature. On the other hand, fractionating the biomass and enhancing the mechanical properties with the compounds defined before require the consumption of chemicals, which may be considered as a drawback.

4.9. Membrane Studies

4.9.1. Evaluation of the corn cob based films as a membrane

It was concluded that uniform film formation is possible with the dissolution of corncob or cellulose rich portion of corn cob extracted by alkaline extraction in ionic liquid, [EMIM][Ac] at determined conditions. On the other hand, as highlighted by Xing et al. (2011), fabrication of membranes with greener solvents and technologies is also important considering environmental issues. Ionic liquids employed in this study to prepare films were also started to be nominated as a new generation of solvents to replace the traditional organic solvents currently used in membrane preparation (Xing et al., 2010; Li et al., 2011). Therefore, during the characterization of the corn cob based films, the studies were carried out to explore whether these films may have membrane properties as well.

4.9.2. Evaluation of morphology of corn cob based films as a membrane

In the SEM analysis of the films prepared by dissolving 4 wt% corn cobs in [EMIM][Ac] and dissolving 4 wt % cellulose extracted from corn cob in [EMIM][Ac], a nodular structure throughout the whole cross-section was observed. Similar morphology was reported by almost all researchers using ionic liquids as phase inversion solvents.

The layered relatively dense images observed with SEM might arise from the distinctive precipitation path takes place with the use of ionic liquid as the solvent (Xing et al., 2010). In the study of Xing and coworkers (2010), the cross-sections of membranes cast from cellulose acetate (CA)/1-butyl-3-methylimidazolium thiocyanate ([BMIM][SCN]) was found to be macrovoid-free, dense and full of nodules, whereas other CA membranes fabricated with different conventional solvents, i.e., N-methyl-2-pyrrolidinone (NMP) and acetone had relatively porous. SEM images which were similar to the cross-sectional images observed in this study were reported to be the result of high solvent outflow to the coagulant inflow ratio and ionic liquid’s inherently high viscosity (Xing et al., 2010).

Macrovoid-free and relatively dense, layered structure was also confirmed by Li et al., (2011) when ionic liquid was employed to fabricate cellulose membranes by phase inversion method (Li et al., 2011).

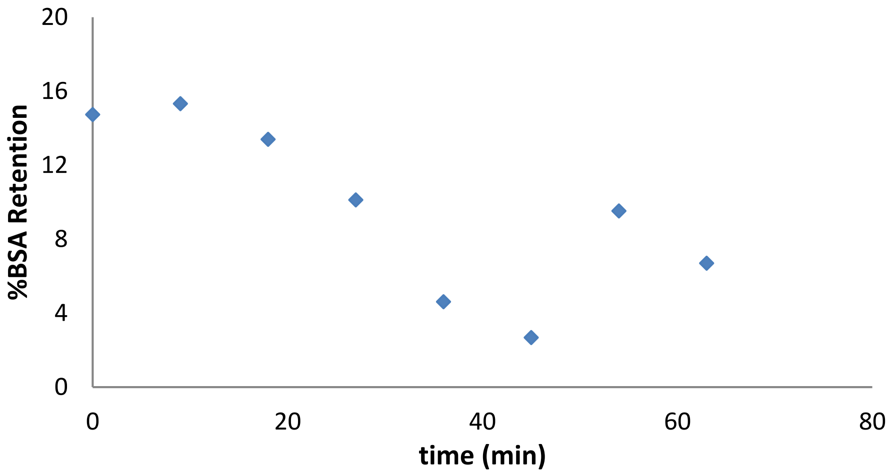

Figure 4.17. BSA retention of RG cellulose membrane

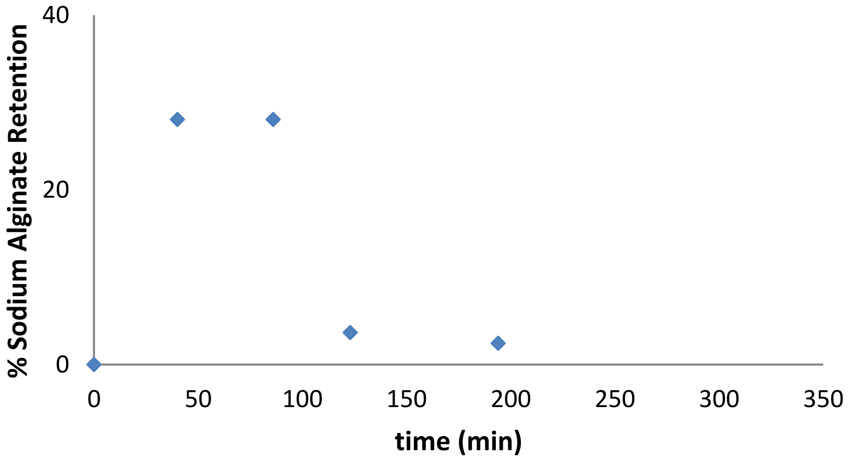

Figure 4.18. Sodium alginate retention of RG cellulose membrane

4.9.3. Pure Water Permeabilities of corn cob based films

Pure water permeability of the film prepared with 4 wt% cellulose-rich portion of corn cob cast on nonwoven support was measured as 85 L/m^2.bar.h. Film fabricated from cellulose extracted by alkaline extraction from corn cob (cellulose film) was renamed as regenerated (RG) cellulose membrane in the rest of the membrane studies.

4.9.4. Performance of RG cellulose film as a membrane in BSA and sodium alginate separation

Separation of bovine serum albumin (BSA) and sodium alginate from their aqueous solutions using RG cellulose membrane was also investigated. As illustrated in Figure 4.17 and Figure 4.18 that RG cellulose membrane showed no retention for both BSA and sodium alginate. Although the RG cellulose membrane showed resistance to water permeation, it did not have any selectivity for the two probe macromolecules while SEM images show a quite dense structure. It is possible that cellulose swells extensively in water preventing the retention of BSA or sodium alginate by the membrane.

CHAPTER 5

CONCLUSION AND RECOMMENDATIONS

This study investigated the capability of lignocellulosic agricultural residue, namely corn cobs, as the raw material to fabricate films in the absence of any additional film-forming additives. Environmental sensitivity of the film production process was enhanced through the selection of ionic liquid as solvent. Films were achieved to be fabricated directly from corn cob-ionic liquid solution. 140°C and 60 min were selected as optimum dissolution temperature and time to prepare film forming solution out of various experimental conditions. Films were also fabricated from the fractions (i.e., cellulosic and hemicellulosic portions) of corn cob.

Bubble-like features that cause local color differences monitored via optical microscope images of the films disappeared through conditioning the films at 100% RH environment prior to coagulation. A nodular, layered and macrovoid-free structure throughout the whole cross-section of the films was observed with the morphological property studies.

One limitation of this study was the water sensitivity of the films fabricated that could influence their potential application. Heat treatment performed at 200°C for 24 h was found to be effective and reduced the water sensitivity of corn cob based films by maintaining their integrity even after one week of immersion in water. On the other hand, discoloration was observed when the film was subjected to heat treatment. Accordingly, the optical property studies revealed that all films were essentially transparent with the exception of Heated_CC film transmitting only 30% of incident light.

An additional limitation of the work is related to the moisture uptake of the films. All the films fabricated, except heat-treated film (with 26% MUP), were found to be hygroscopic and absorb significant amount of moisture (ranged from 46% to 104%) in high humidity environment (100% RH). Isolation of the cellulosic portion of the biomass to fabricate the films was found to reduce the percent moisture uptake by half.

On the other hand, WVP results showed that it is possible to measure lower or at least comparable WVP values compared to fractionated corn cob films with the films fabricated directly from corn cob solutions in [EMIM][Ac] without the support of additional film-forming additives or chemical modifications commonly employed for hemicellulose based films. Corn cob cellulose and hemicellulose based films had higher water vapor permeabilities than films produced directly from corn cobs (27-40$\times10^{-12}$ vs. 3-13$\times10^{-12}$ g.m^{-1}.Pa^{-1}.s^{-1}).

Additionally, films that were made from corn cob itself or its components as the raw material, showed promising mechanical properties. UTS and E values were in the range of 36.9-56.0 MPa and 1700-3449 MPa, respectively while illustrating a low percent elongation at break values (1.4-3.8%). Heat treatment led to produce stiffer and less stretchable films than the other films produced in this study considering E and e_b values.

The studies were further conducted to explore whether these films may have membrane properties as well via pure water permeability and retention tests by the filtration of bovine serum albumin and sodium alginate. Membrane (RG Cellulose) was fabricated by dissolution of the cellulose-rich portion of corn cob in [EMIM][Ac] at predetermined conditions through phase inversion method. Pure water permeability of the resultant membrane cast on nonwoven support was determined as 85 L/m^2.bar.h. Performance of corn cob cellulose film as a membrane in BSA and sodium alginate separation was also investigated. Although a resistance was shown by the membrane to water permeation and relatively dense morphology was monitored via SEM, no selectivity for the selected two probe macromolecules was determined through the retention tests performed.

Recommendations for future studies may include the production of membranes from celluloses with different molecular weights obtained from different forms (fibers, microcrystalline cellulose, etc.). Another recommendation can be about the recycling of the ionic liquid used in the process since ionic liquids are very expensive solvents. The effect of recycling the ionic liquid on the properties of the films and membranes produces can be investigated and an optimum number of recycling step can be determined.

REFERENCES

Abdelwahab, M. A., Flynn, A., Chiou, B. S., Imam, S., Orts, W., & Chiellini, E. (2012). Thermal, mechanical and morphological characterization of plasticized PLA–PHB blends. *Polymer Degradation and Stability*, *97*(9), 1822

Abdulkhani, A., Hojati Marvast, E., Ashori, A., & Karimi, A. N. (2013). Effects of dissolution of some lignocellulosic materials with ionic liquids as green solvents on mechanical and physical properties of composite films. *Carbohydrate polymers*, *95*(1), 57-63.

Akgül, M., & Tozluoğlu, A. Kimyasal termomekanik hamur yöntemi. Süleyman Demirel Üniversitesi Orman Fakültesi Dergisi Seri: A, Sayı: 2, Yıl: 2006, ISSN: 1302-7085, Sayfa: 156-174

Amass, W., Amass, A., & Tighe, B. (1998). A review of biodegradable polymers: uses, current developments in the synthesis and characterization of biodegradable polyesters, blends of biodegradable polymers and recent advances in biodegradation studies. *Polymer International*, *47*(2), 89-144.

Arthur, J. C., & Hinojosa, O. (1966). Thermal initiation of free radicals in cotton cellulose. *Textile Research Journal*, *36*(4), 385-387.

Auras, R. A., Harte, B., Selke, S., & Hernandez, R. (2003). Mechanical, physical, and barrier properties of poly (lactide) films. *Journal of Plastic Film and Sheeting*, *19*(2), 123-135.

Auras, R., Singh, S. P., & Singh, J. (2006). Performance evaluation of PLA against existing PET and PS containers. *Journal of Testing and Evaluation*,*34*(6), 530.

Avella, M., De Vlieger, J. J., Errico, M. E., Fischer, S., Vacca, P., & Volpe, M. G. (2005). Biodegradable starch/clay nanocomposite films for food packaging applications. *Food chemistry*, *93*(3), 467-474.

Bahcegul, E., Toraman, H. E., Ozkan, N., & Bakir, U. (2012). Evaluation of alkaline pretreatment temperature on a multi-product basis for the co-production of glucose and hemicellulose based films from lignocellulosic biomass.*Bioresource technology*, *103*(1), 440-445.

Bourtoom, T., & Chinnan, M. S. (2008). Preparation and properties of rice starch–chitosan blend biodegradable film. *LWT-Food Science and Technology*,*41*(9), 1633-1641.

Bozdemir, Ö. A., & Tutas, M. (2003). Plasticiser Effect on Water Vapour Permeability Properties of Locust bean gum-Based Edible Films. *Turkish Journal of Chemistry*, *27*(6).

Brandt, A., Gräsvik, J., Hallett, J. P., & Welton, T. (2013). Deconstruction of lignocellulosic biomass with ionic liquids. *Green chemistry*, *15*(3), 550-583.

Broido, A., Javier-Son, A. C., Ouano, A. C., & Barrall, E. M. (1973). Molecular weight decrease in the early pyrolysis of crystalline and amorphous cellulose.*Journal of Applied Polymer Science*, *17*(12), 3627-3635.

Callister, W. D., & Rethwisch, D. G. (2007). *Materials science and engineering: an introduction* (Vol. 7, pp. 665-715). New York: Wiley.

Chen, M., Zhang, X., Liu, C., Sun, R., & Lu, F. (2014). Approach to Renewable Lignocellulosic Biomass Film Directly from Bagasse. *ACS Sustainable Chemistry & Engineering*, *2*(5), 1164-1168.

Coma, V., Sebti, I., Pardon, P., Pichavant, F. H., & Deschamps, A. (2003). Film properties from crosslinking of cellulosic derivatives with a polyfunctional carboxylic acid. *Carbohydrate polymers*, *51*(3), 265-271.

Dadi, A. P., Varanasi, S., & Schall, C. A. (2006). Enhancement of cellulose saccharification kinetics using an ionic liquid pretreatment step. *Biotechnology and Bioengineering*, *95*(5), 904-910.

Edlund, U., Ryberg, Y. Z., & Albertsson, A. C. (2010). Barrier films from renewable forestry waste. *Biomacromolecules*, *11*(9), 2532-2538.

Egüés, I., Stepan, A. M., Eceiza, A., Toriz, G., Gatenholm, P., & Labidi, J. (2014). Corncob arabinoxylan for new materials. *Carbohydrate polymers*, *102*, 12-20.

Farris, S., Introzzi, L., & Piergiovanni, L. (2009). Evaluation of a bio-coating as a solution to improve barrier, friction and optical properties of plastic films.*Packaging technology and science*, *22*(2), 69-83.

FitzPatrick, M., Champagne, P., Cunningham, M. F., & Falkenburger, C. (2012). Application of optical microscopy as a screening technique for cellulose and lignin solvent systems. *The Canadian Journal of Chemical Engineering,90*(5), 1142-1152.

Gao, J., Luo, Z. G., & Luo, F. X. (2012). Ionic liquids as solvents for dissolution of corn starch and homogeneous synthesis of fatty-acid starch esters without catalysts. *Carbohydrate polymers*, *89*(4), 1215-1221.

Gaudin, S., Lourdin, D., Forssell, P. M., & Colonna, P. (2000). Antiplasticisation and oxygen permeability of starch–sorbitol films.*Carbohydrate Polymers*, *43*(1), 33-37.

Godbillot, L., Dole, P., Joly, C., Rogé, B., & Mathlouthi, M. (2006). Analysis of water binding in starch plasticized films. *Food Chemistry*, *96*(3), 380-386.

Goksu, E. I., Karamanlioglu, M., Bakir, U., Yilmaz, L., & Yilmazer, U. (2007). Production and characterization of films from cotton stalk xylan. *Journal of agricultural and food chemistry*, *55*(26), 10685-10691.

Gröndahl, M., Eriksson, L., & Gatenholm, P. (2004). Material properties of plasticized hardwood xylans for potential application as oxygen barrier films.*Biomacromolecules*, *5*(4), 1528-1535.

Guo, J., Ge, L., Li, X., Mu, C., & Li, D. (2014). Periodate oxidation of xanthan gum and its crosslinking effects on gelatin-based edible films. *Food Hydrocolloids*, *39*, 243-250.

Hansen, N. M., & Plackett, D. (2008). Sustainable films and coatings from hemicelluloses: a review. *Biomacromolecules*, *9*(6), 1493-1505.

Heikkinen, S. L., Mikkonen, K. S., Koivisto, P., Heikkilä, M. I., Pirkkalainen, K., Liljeström, V.,& Tenkanen, M. (2013). Long-Term Physical Stability of Plasticized Hemicellulose Films. *BioResources*, *9*(1), 906-921.

Hou, X. D., Smith, T. J., Li, N., & Zong, M. H. (2012). Novel renewable ionic liquids as highly effective solvents for pretreatment of rice straw biomass by selective removal of lignin. *Biotechnology and bioengineering*, *109*(10), 2484-2493.

Höije, A., Gröndahl, M., Tømmeraas, K., & Gatenholm, P. (2005). Isolation and characterization of physicochemical and material properties of arabinoxylans from barley husks. *Carbohydrate Polymers*, *61*(3), 266-275.

Huijgen, W., Bermudez, L., & Bakker, R. (2010). *Literature review of physical and chemical pretreatment processes for lignocellulosic biomass* (pp. 978-9).

Karatzos, S. K., Edye, L. A., & Doherty, W. O. S. (2012). Sugarcane bagasse pretreatment using three imidazolium-based ionic liquids; mass balances and enzyme kinetics. *Biotechnology for biofuels*, *5*(1), 62.

Kester, J. J., & Fennema, O. R. (1986). Edible films and coatings: a review.*Food technology (USA)*.

Kilpeläinen, I., Xie, H., King, A., Granstrom, M., Heikkinen, S., & Argyropoulos, D. S. (2007). Dissolution of wood in ionic liquids. *Journal of Agricultural and Food Chemistry*, *55*(22), 9142-9148.

Kim, K. W., Ko, C. J., & Park, H. J. (2002). Mechanical Properties, Water Vapor Permeabilities and Solubilities of Highly Carboxymethylated Starch-Based Edible Films. *Journal of Food Science*, *67*(1), 218-222.

Kirk-Othmer, E. (1983). of Chem. *Tech.*,, *1*, 733-739.

Li, W., Sun, N., Stoner, B., Jiang, X., Lu, X., & Rogers, R. D. (2011). Rapid dissolution of lignocellulosic biomass in ionic liquids using temperatures above the glass transition of lignin. *Green Chemistry*, *13*(8), 2038-2047.

Li, X. L., Zhu, L. P., Zhu, B. K., & Xu, Y. Y. (2011). High-flux and anti-fouling cellulose nanofiltration membranes prepared via phase inversion with ionic liquid as solvent. *Separation and Purification Technology*, *83*, 66-73.

Lynd et al. (2002) Lynd, L. R., Weimer, P. J., Van Zyl, W. H., & Pretorius, I. S. (2002). Microbial cellulose utilization: fundamentals and biotechnology. *Microbiology and molecular biology reviews*, *66*(3), 506-577.

Ma, H., Hsiao, B. S., & Chu, B. (2011). Thin-film nanofibrous composite membranes containing cellulose or chitin barrier layers fabricated by ionic liquids. *Polymer*, *52*(12), 2594-2599.

Mali, S., Grossmann, M. V. E., García, M. A., Martino, M. N., & Zaritzky, N. E. (2006). Effects of controlled storage on thermal, mechanical and barrier properties of plasticized films from different starch sources. *Journal of Food Engineering*, *75*(4), 453-460.

Mikkonen, K. S., Heikkinen, S., Soovre, A., Peura, M., Serimaa, R., Talja, R. A., & Tenkanen, M. (2009). Films from oat spelt arabinoxylan plasticized with glycerol and sorbitol. *Journal of applied polymer science*, *114*(1), 457-466.

Mikkonen, K. S., & Tenkanen, M. (2012). Sustainable food-packaging materials based on future biorefinery products: Xylans and mannans. *Trends in Food Science & Technology*, *28*(2), 90-102.

Mikkonen, K. S., Heikkilä, M. I., Helén, H., Hyvönen, L., & Tenkanen, M. (2010). Spruce galactoglucomannan films show promising barrier properties.*Carbohydrate polymers*, *79*(4), 1107-1112.

Mikkonen, K. S., Heikkilä, M. I., Willför, S. M., & Tenkanen, M. (2012). Films from glyoxal-crosslinked spruce galactoglucomannans plasticized with sorbitol.*International Journal of Polymer Science*, *2012*.

Mikkonen, K. S., Mathew, A. P., Pirkkalainen, K., Serimaa, R., Xu, C., Willför, S.,& Tenkanen, M. (2010). Glucomannan composite films with cellulose nanowhiskers. *Cellulose*, *17*(1), 69-81.

Mikkonen, K. S., Pitkänen, L., Liljeström, V., Bergström, E. M., Serimaa, R., Salmén, L., & Tenkanen, M. (2012). Arabinoxylan structure affects the reinforcement of films by microfibrillated cellulose. *Cellulose*, *19*(2), 467-480.

Mikkonen, K. S., Stevanic, J. S., Joly, C., Dole, P., Pirkkalainen, K., Serimaa, R.,& Tenkanen, M. (2011). Composite films from spruce galactoglucomannans with microfibrillated spruce wood cellulose. *Cellulose*,*18*(3), 713-726.

Mikkonen, K. S., Yadav, M. P., Cooke, P., Willför, S., Hicks, K. B., & Tenkanen, M. (2008). Films from spruce galactoglucomannan blended with poly (vinyl alcohol), corn arabinoxylan, and konjac glucomannan. *BioResources*,*3*(1), 178-191.

Mohanty, A. K., Misra, M., & Hinrichsen, G. (2000). Biofibres, biodegradable polymers and biocomposites: an overview. *Macromolecular Materials and Engineering*, *276*(1), 1-24.

Molton, P. M., & Demmitt, T. F. (1977). *Reaction mechanisms in cellulose pyrolysis: a literature review* (No. BNWL-2297). Battelle Pacific Northwest Labs., Richland, WA (USA).

Morais, J. P. S., Rosa, M. D. F., Nascimento, L. D., do Nascimento, D. M., & Cassales, A. R. (2013). Extraction and characterization of nanocellulose structures from raw cotton linter. *Carbohydrate polymers*, *91*(1), 229-235.

Mora-Pale, M., Meli, L., Doherty, T. V., Linhardt, R. J., & Dordick, J. S. (2011). Room temperature ionic liquids as emerging solvents for the pretreatment of lignocellulosic biomass. *Biotechnology and bioengineering*, *108*(6), 1229-1245.

Mu, C., Guo, J., Li, X., Lin, W., & Li, D. (2012). Preparation and properties of dialdehyde carboxymethyl cellulose crosslinked gelatin edible films. *Food Hydrocolloids*, *27*(1), 22-29.

Muhammad, N., Man, Z., & Khalil, M. A. B. (2012). Ionic liquid—a future solvent for the enhanced uses of wood biomass. *European Journal of Wood and Wood Products*, *70*(1-3), 125-133.

Pacault A., & Sauret G.,(1958). Study of the Thermal De-polymerization of Cellulose," Compt. Rend. Acad. Sci., 246, 608-611.

Peng, X. W., Ren, J. L., Zhong, L. X., & Sun, R. C. (2011). Nanocomposite films based on xylan-rich hemicelluloses and cellulose nanofibers with enhanced mechanical properties. *Biomacromolecules*, *12*(9), 3321-3329.

Péroval, C., Debeaufort, F., Despré, D., & Voilley, A. (2002). Edible arabinoxylan-based films. 1. Effects of lipid type on water vapor permeability, film structure, and other physical characteristics. *Journal of Agricultural and Food Chemistry*, *50*(14), 3977-3983.

Phan The, D., Debeaufort, F., Peroval, C., Despre, D., Courthaudon, J. L., & Voilley, A. (2002). Arabinoxylan-lipid-based edible films and coatings. 3. Influence of drying temperature on film structure and functional properties.*Journal of agricultural and food chemistry*, *50*(8), 2423-2428.

Rhim, J. W., & Ng, P. K. (2007). Natural biopolymer-based nanocomposite films for packaging applications. *Critical reviews in food science and nutrition*,*47*(4), 411-433.

Rindlav-Westling, A. S., Stading, M., Hermansson, A. M., & Gatenholm, P. (1998). Structure, mechanical and barrier properties of amylose and amylopectin films. *Carbohydrate Polymers*, *36*(2), 217-224.

Rodrig, H., Basch, A., & Lewin, M. (1975). Crosslinking and pyrolytic behavior of natural and man-made cellulosic fibers. *Journal of Polymer Science: Polymer Chemistry Edition*, *13*(8), 1921-1932.

Sannigrahi, P., Ragauskas, A. J., & Tuskan, G. A. (2010). Poplar as a feedstock for biofuels: a review of compositional characteristics. *Biofuels, Bioproducts and Biorefining*, *4*(2), 209-226.

Sárossy, Z. (2011). Production and utilization of hemicelluloses from renewable resources for sustainable advanced products. Technical University of DenmarkDanmarks Tekniske Universitet, Risø National Laboratory for Sustainable EnergyRisø Nationallaboratoriet for Bæredygtig Energi.

Sárossy, Z., Blomfeldt, T. O., Hedenqvist, M. S., Koch, C. B., Ray, S. S., & Plackett, D. (2012). Composite films of arabinoxylan and fibrous sepiolite: Morphological, mechanical, and barrier properties. *ACS applied materials & interfaces*, *4*(7), 3378-3386.

Sárossy, Z., Tenkanen, M., Pitkänen, L., Bjerre, A. B., & Plackett, D. (2013). Extraction and chemical characterization of rye arabinoxylan and the effect of β-glucan on the mechanical and barrier properties of cast arabinoxylan films.*Food hydrocolloids*, *30*(1), 206-216.

Saxena, A., Elder, T. J., Pan, S., & Ragauskas, A. J. (2009). Novel nanocellulosic xylan composite film. *Composites Part B: Engineering*, *40*(8), 727-730.

Sczostak, A. (2009, June). Cotton linters: an alternative cellulosic raw material. In *Macromolecular symposia* (Vol. 280, No. 1, pp. 45-53). WILEY-VCH Verlag.

Simmons, T. J., Lee, S. H., Miao, J., Miyauchi, M., Park, T. J., Bale, S. S., ... & Linhardt, R. J. (2011). Preparation of synthetic wood composites using ionic liquids. *Wood Science and Technology*, *45*(4), 719-733.

Sinha Ray, S., & Bousmina, M. (2005). Biodegradable polymers and their layered silicate nanocomposites: in greening the 21st century materials world.*Progress in Materials Science*, *50*(8), 962-1079.

Sirviö, J. A., Kolehmainen, A., Liimatainen, H., Niinimäki, J., & Hormi, O. E. (2014). Biocomposite cellulose-alginate films: Promising packaging materials.*Food chemistry*, *151*, 343-351.

Spiridon, I., & Popa, V. I. (2008). Hemicelluloses: major sources, properties and applications. *Monomers, polymers and composites from renewable resources*,*1*, 289.

Stevanic, J. S., Bergström, E. M., Gatenholm, P., Berglund, L., & Salmén, L. (2012). Arabinoxylan/nanofibrillated cellulose composite films. *Journal of Materials Science*, *47*(18), 6724-6732.

Sun, N., Rahman, M., Qin, Y., Maxim, M. L., Rodríguez, H., & Rogers, R. D. (2009). Complete dissolution and partial delignification of wood in the ionic liquid 1-ethyl-3-methylimidazolium acetate. *Green Chemistry*, *11*(5), 646-655.

Sun, N., Rodríguez, H., Rahman, M., & Rogers, R. D. (2011). Where are ionic liquid strategies most suited in the pursuit of chemicals and energy from lignocellulosic biomass?. *Chemical Communications*, *47*(5), 1405-1421.2011

Sun, S. N., Li, M. F., Yuan, T. Q., Xu, F., & Sun, R. C. (2012). Effect of ionic liquid pretreatment on the structure of hemicelluloses from corncob. *Journal of agricultural and food chemistry*, *60*(44), 11120-11127.

Sun, Y., & Cheng, J. (2002). Hydrolysis of lignocellulosic materials for ethanol production: a review. *Bioresource technology*, *83*(1), 1-11.

Swatloski, R. P., Spear, S. K., Holbrey, J. D., & Rogers, R. D. (2002). Dissolution of cellose with ionic liquids. *Journal of the American Chemical Society*, *124*(18), 4974-4975.

Tejinder, S. (2003). Preparation and characterization of films using barley and oat β-glucan extracts. *Cereal chemistry*, *80*(6), 728-731.

Thermowood handbook, Finnish Thermowood Association, 2003.

Toraman, E (2012). 'Investigation of alkaline pretreatment parameters on a multi-product basis for the co-productıon of glucose and hemicellulose based fılms from corn cobs.' A master thesis submitted to Middle East Technical University.

Turhan, K. N., & Şahbaz, F. (2001). A simple method for determining light transmittance of polymer films used for packaging foods. *Polymer international*,*50*(10), 1138-1142.

Westbye, P., Köhnke, T., Glasser, W., & Gatenholm, P. (2007). The influence of lignin on the self-assembly behaviour of xylan rich fractions from birch (Betula pendula). *Cellulose*, *14*(6), 603-613.

Xing, D. Y., Peng, N., & Chung, T. S. (2010). Formation of cellulose acetate membranes via phase inversion using ionic liquid,[BMIM] SCN, as the solvent.*Industrial & Engineering Chemistry Research*, *49*(18), 8761-8769.

Xing, D. Y., Peng, N., & Chung, T. S. (2011). Investigation of unique interactions between cellulose acetate and ionic liquid [EMIM] SCN, and their influences on hollow fiber ultrafiltration membranes. *Journal of Membrane Science*, *380*(1), 87-97.

Van de Ven, W. J. C., Sant, K. V. T., Pünt, I. G. M., Zwijnenburg, A., Kemperman, A. J. B., van der Meer, W. G. J., & Wessling, M. (2008). Hollow fiber dead-end ultrafiltration: influence of ionic environment on filtration of alginates. *Journal of Membrane Science*, *308*(1), 218-229.

Yaich, A. I., Edlund, U., & Albertsson, A. C. (2014). Adapting wood hydrolysate barriers to high humidity conditions. *Carbohydrate polymers*, *100*, 135-142.

Ye, X., Kennedy, J. F., Li, B., & Xie, B. J. (2006). Condensed state structure and biocompatibility of the konjac glucomannan/chitosan blend films.*Carbohydrate Polymers*, *64*(4), 532-538.

Yuksekkalayci, C., Yilmazer, U., & Orbey, N. (1999). Effects of nucleating agent and processing conditions on the mechanical, thermal, and optical properties of biaxially oriented polypropylene films. *Polymer Engineering & Science, 39*(7), 1216-1222.

Zavrel, M., Bross, D., Funke, M., Büchs, J., & Spiess, A. C. (2009). High-throughput screening for ionic liquids dissolving (ligno-) cellulose. *Bioresource Technology*, *100*(9), 2580-2587.

Zhang, L., Ruan, D., & Zhou, J. (2001). Structure and properties of regenerated cellulose films prepared from cotton linters in NaOH/urea aqueous solution.*Industrial & engineering chemistry research*, *40*(25), 5923-5928.

Zhang, P., & Whistler, R. L. (2004). Mechanical properties and water vapor permeability of thin film from corn hull arabinoxylan. *Journal of applied polymer science*, *93*(6), 2896-2902.

Zhang, Y. H. P., Ding, S. Y., Mielenz, J. R., Cui, J. B., Elander, R. T., Laser, M., & Lynd, L. R. (2007). Fractionating recalcitrant lignocellulose at modest reaction conditions. *Biotechnology and Bioengineering*, *97*(2), 214-223.

Zhang, Y., Pitkänen, L., Douglade, J., Tenkanen, M., Remond, C., & Joly, C. (2011). Wheat bran arabinoxylans: Chemical structure and film properties of three isolated fractions. *Carbohydrate Polymers*, *86*(2), 852-85

APPENDIX A

CALCULATION OF LIGHT TRANSMITTANCE OF CORN COB BASED FILMS

Percent light transmittance and opaqueness for unit thickness of the films were calculated by the formulas given below.

$$\%Light\ Transmittance\ = \frac{Measured\ value\ of\ sample\ by\ lightmeter\ (Lux)}{Measured\ value\ of\ glass\ substrate\ (reference)(Lux)}$$

$$Opaqueness/Film\ thickness\ = \frac{1-(\%Light\ transmittance/100)}{Film\ thickness(\mu m)}$$

A sample calculation for Water_CC film

$$\%Light\ Transmittance\ = \frac{54.3\ (Lux)\times 100}{81.9\ (reference)(Lux)} = 66.3$$

$$\frac{Opaqueness}{Film\ thickness}\ = \frac{1-\left(\frac{66.3}{100}\right)}{13.6\ (\mu m)} = 0.025\ \mu\mathrm{m}^{-1}$$

Table A.1. Recorded data for % light transmittance

Sample	Light Transmittance (Lux)	Reference (Lux)	%Light Transmittance	Average %Light Transmittance
Water_CC	54.3	81.9	66.30037	65.84±2.41
Water_CC	50.9	81.9	62.14896	
Water_CC	53.5	81.9	65.32357	
Water_CC	56.3	81.9	68.74237	
Water_CC	54.6	81.9	66.66667	
1D_CC	58.1	81.9	70.94017	73.50±3.63
1D_CC	62.3	81.9	76.06838	
2D_CC	62.4	81.9	76.19048	76.19±0.35
2D_CC	62.8	81.9	76.67888	
5D_CC	68.4	81.9	83.51648	82.78±1.04
5D_CC	67.2	81.9	82.05128	
ETOH/Water_CC	66.1	81.9	80.70818	79.52±1.45

Table A.1. Recorded data for % light transmittance (continued)

Sample	Light Transmittance (Lux)	Reference (Lux)	%Light Transmittance	Average %Light Transmittance
ETOH/Water_CC	66.2	81.9	80.83028	
ETOH/Water_CC	64.1	81.9	78.26618	
ETOH/Water_CC	64.1	81.9	78.26618	
Hemicellulose_CC	87	114	76.31578947	78.84±4.86
Hemicellulose_CC	95	114	83.33333333	
Hemicellulose_CC	94	114	82.45614035	
Hemicellulose_CC	83.5	114	73.24561404	
Cellulose_CC	102	114	89.47368421	89.25±1.10
Cellulose_CC	100	114	87.71929825	
Cellulose_CC	102	114	89.47368421	
Cellulose_CC	103	114	90.35087719	
Heated_CC	35	108	32.40740741	30.32±5.87
Heated_CC	39	108	36.11111111	
Heated_CC	33	108	30.55555556	
Heated_CC	24	108	22.22222222	

Table A.2. Recorded data for opaqueness/film thickness

Sample	(%Light Transmittance)/100	Opaqueness /Film Thickness	Average Opaqueness/Film Thickness
Water_CC	0.663004	0.024779	0.025±0.001
Water_CC	0.62149	0.027832	
Water_CC	0.653236	0.025497	
Water_CC	0.687424	0.022984	
Water_CC	0.666667	0.02451	
1D_CC	0.709402	0.032289	0.029±0.004
1D_CC	0.760684	0.026591	
2D_CC	0.761905	0.016732	0.017±0.00024
2D_CC	0.766789	0.016389	
5D_CC	0.835165	0.014088	0.0147±0.0009
5D_CC	0.820513	0.015341	
ETOH/Water_CC	0.807082	0.027959	0.03±0.002
ETOH/Water_CC	0.808303	0.027782	
ETOH/Water_CC	0.782662	0.031498	
ETOH/Water_CC	0.782662	0.031498	
Hemicellulose_CC	0.763158	0.01149719	0.010±0.002
Hemicellulose_CC	0.833333	0.00809061	
Hemicellulose_CC	0.824561	0.00851643	

Table A.2. Recorded data for opaqueness/film thickness (continued)

Sample	**(%Light Transmittance)/100**	**Opaqueness/Film Thickness**	**Average Opaqueness/Film Thickness**
Hemicellulose_CC	0.732456	0.01298756	
Cellulose_CC	0.894737	0.00683527	0.007±0.0007
Cellulose_CC	0.877193	0.00797448	
Cellulose_CC	0.894737	0.00683527	
Cellulose_CC	0.903509	0.00626566	
Heated_CC	0.32407	0.05572382	0.057±0.005
Heated_CC	0.361111	0.05267015	
Heated_CC	0.305556	0.05725015	
Heated_CC	0.222222	0.06412018	

APPENDIX B

CALCULATION OF WATER VAPOR PERMEABILITY (WVP) OF CORN COB BASED FILMS

Table B.1. Recorded data for WVP calculations

RECORDED DATA	conditioned weight of the film tested (dried in 50°C oven for 24h)
	film weight after different periods of time
	time
	film thickness
	film area
	saturation vapor pressure of water at 30°C

A sample calculation for hemicellulose film

Table B.2. Recorded weight (gr) of the test assembly at different time periods

	0h	2h	4h	5h	6h	24 h	48 h	120 h	168 h
Hemicellulose	7.58	7.65	7.76	7.73	7.75	8.01	8.08	8.19	8.24
Hemicellulose	7.67	7.75	7.81	7.83	7.86	8.05	8.11	8.22	8.26

Table B.3. Recorded data for total grams of vapor permeated at different time periods

	0h	2h	4h	5h	6h	24 h	48 h	120 h	168 h
Hemicellulose	0	0.071	0.18	0.14	0.16	0.43	0.49	0.61	0.65
Hemicellulose	0	0.079	0.13	0.16	0.18	0.38	0.44	0.54	0.59

Step #1

$$transpiration\ rate\left(\frac{g}{h} * m^2\right) = \frac{slope\ of\ total\ grams\ of\ water\ permeated\ vs\ time\ graph}{film\ area\ (m^2)}$$

Table B.4. Recorded Data for calculating the water vapor permeability for hemicellulose samples

sample	slopes	R-squared value	area(m2)	transpiration rate (g/h.m^2)
Hemicellulose-1	0.0322	0.8353	0.001256	25.63694268
Hemicellulose-2	0.033	0.9875	0.001256	26.27388535

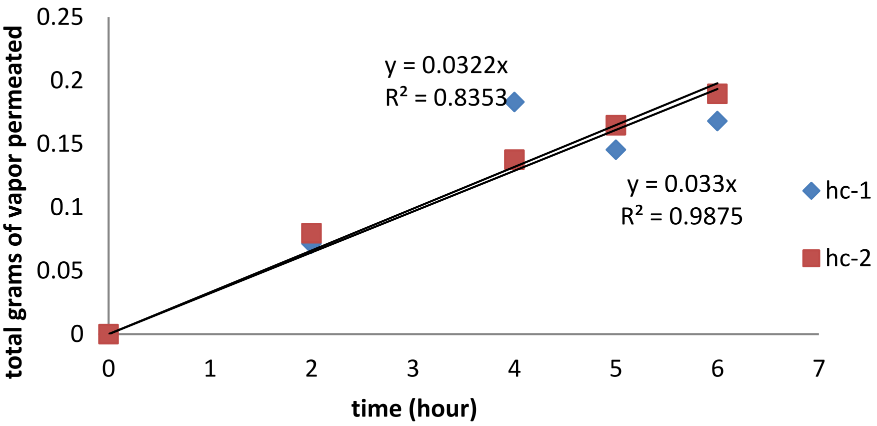

Figure B.1. Total grams of water permeated vs. time

Step #2

$$WVP\left(\frac{g}{m.Pa.sec}\right) = \frac{transpiration\ rate * film\ thickness}{saturation\ vapor\ pressure\ of\ water\ at\ 30℃}$$

sample	thickness (µm)	saturation vapor pressure of water at 30°C (Pa)
Hemicellulose	23	4240
Hemicellulose	24	4240

sample	water vapor permeability (g/.Pa.sec)
Hemicellulose	38.6301×10^{-12}
Hemicellulose	41.3111×10^{-12}

Water vapor permeability of hemicellulose film	**average**	39.9706×10^{-12}
	stdev	1.89579×10^{-12}

Table B.5. Transpiration rates of the film produced

Sample	slope	Area (m^2)	Transpiration rate ($g/h.m^2$)
Water_CC	0.0167	0.001256	13.29617834
Water_CC	0.0161	0.001256	12.81847134
ETOH/Water_CC	0.0164	0.001256	13.05732484
ETOH/Water_CC	0.0161	0.001256	12.81847134
1D_CC	0.0166	0.001256	13.21656051
1D_CC	0.0148	0.001256	11.78343949
2D_CC	0.0147	0.001256	11.70382166
2D_CC	0.0137	0.001256	10.90764331
5D_CC	0.014	0.001256	11.14649682
5D_CC	0.136	0.001256	10.82802548
Hemicellulose	0.0322	0.001256	25.63694268
Hemicellulose	0.033	0.001256	26.27388535
Cellulose	0.0171	0.001256	13.61464968
Cellulose	0.0236	0.001256	18.78980892
Heated_CC	0.0258	0.001256	20.54140127
Heated_CC	0.0237	0.001256	18.86942675

Table B.6. Water vapor permeability of the films

Sample	Film thickness (µm)	saturation vapor pressure of water at 30°C (Pa)	Water vapor permeability ($g.m^{-1}.Pa^{-1}.s^{-1}$)
Water_CC	14	4240	1.22E-11
Water_CC	12	4240	1.18E-11
ETOH/Water_CC	4	4240	3.42E-12
ETOH/Water_CC	4.6	4240	3.36E-12
1D_CC	8	4240	6.93E-12
1D_CC	9.2	4240	6.18E-12
2D_CC	17	4240	1.30E-11
2D_CC	18.3	4240	1.21E-11
5D_CC	12	4240	8.51E-12
5D_CC	10.1	4240	8.76E-12
Hemicellulose	23	4240	3.86301E-11
Hemicellulose	24	4240	4.13111E-11
Cellulose	23	4240	2.05147E-11
Cellulose	21	4240	2.58508E-11
Heated_CC	20	4240	2.69148E-11
Heated_CC	22	4240	2.71965E-11

APPENDIX C

CALCULATION OF MOISTURE UPTAKE (MUP) OF CORN COB BASED FILMS

Moisture uptake values of the corncob based films were calculated according to the given formula below where W_{sample} (gr) is the weight of sample at the time of exposure to moisture, $W_{conditioned}$ (gr) is the weight of the conditioned sample.

$$\frac{W_{sample} - W_{conditioned}}{W_{conditioned}} * 100$$

<u>A sample calculation for 1D/CC film</u>

Table C.1. Recorded weight (gr) of the sample at different time periods in 100% RH desiccator

$W_{conditioned}$	24 hr	96h	120h
0.0641	0.1021	0.1092	0.11

$$Water\ Uptake\%\ at\ 24\ h = \frac{0.1021 - 0.0641}{0.0641} \times 100 = 59.28\%$$

Table C.2. Recorded data for moisture uptake% at different time periods:

Moisture Uptake%	24 hr	96h	120h
	59.28237129	70.35881435	71.60686427

Table C.3. Moisture uptake of the films against time

Sample	MUP at 24h	MUP at 48h	MUP at 96h	MUP at 120h
Water_CC		58.08		
Water_CC	68.51	45.41	78.33	94.03
Water_CC	70.88	38.20	88.60	85.18
1D_CC	66.93	39.68	83.27	82.59
1D_CC	59.28	60.65	70.36	71.60
2D_CC				111.24
2D_CC	72.10	50.88	92.39	103.32
2D_CC	70.12	74.54	86.70	95.45
5D_CC	70.18	85.3	84.40	83.49
5D_CC	73.23	72.4	82.37	74.69
5D_CC			80.63	
ETOH/Water_CC			90.69	
ETOH/Water_CC	85.90	78.10	101.95	101.37
ETOH/Water_CC	74.88	70.29	92.49	120.39

Table C.4. Average moisture uptake% values of the films

Sample	MUP at 0h	MUP at 24h	MUP at 48h	MUP at 96h	MUP at 120h
Water_CC	0	57.84±20.6	47.23±10.1	83.47±7.3	89.61±6.3
1D_CC	0	63.11±5.4	50.17±14.8	76.81±9.13	77.10±7.77
2D_CC	0	71.12±1.40	62.71±16.7	89.55±4.02	109.78±14.4
5D_CC	0	71.71±2.16	78.85±9.12	82.47±1.89	79.09±6.22
ETOH/Water_CC	0	66.80±24.2	74.20±5.52	83.97±22.7	87.85±41.01
Hemicellulose	0	79.73±2.85	78.71±4.28	96.12±5.27	
Cellulose	0	49.42±1.29	43.25±5.96	46.10±5.27	
Heated_CC	0	24.27±11.9	19.24±3.81	35.61±6.24	

APPENDIX D

TENSILE TESING DATA OF CORN COB BASED FILMS

Table D.1. Mechanical properties recorded for the films

Sample	E (MPa)	UTS (MPa)	%e_b
Water_CC	1950	57.9	4.3
	1800	59	3.1
	1600	53.4	2.9
	2250	25.4	1.4
	2080	59.4	2.2
	1270	53.1	5.3
	1240	45.1	1.8
	1410	50.9	3.8
1D_CC	2820	37.8	2.2
	4360	62.7	4.7
	2900	41.3	4
	3160	42.4	3.2
	3370	48.2	2.8
2D_CC	2370	40.8	2.7
	2460	40.3	2.5
	3770	48.2	2
	2220	59.3	1.7
	1510	75.8	3.4
	1330	48.9	2.2
5D_CC	3430	48.9	3.1
	2620	34.5	2.3
	3370	42.5	1.8
	1770	68	5.1
	1980	72.8	6.8
	2160	69	3.6
ETOH/Water_CC	3210	30.1	0.98
	3280	42.2	1.7
	3360	44.4	1.9
	1640	71.6	3.8
	1200	76.1	4.1
	1280	56	4.2
	2180	37.4	2.1
	2300	59.9	3.6

Table D.1. Mechanical properties recorded for the films (continued)

Sample	E (MPa)	UTS (MPa)	%e_b
Hemicellulose	2500	45.23	2.87
	2317.33	41.6	2.9
	2887.5	49.48	2.95
Cellulose	3293.333	50.4	2.6
	3465	51.05	2.55
	3590	48.93	1.9
Heated_CC	3443.333	38.6	1.2
	2950	29.3	0.9
	3193.333	42.7	1.97

Table D.2. Average values of mechanical properties of corn cob based films

Sample	UTS (MPa)	E (MPa)	% e_b
Water_CC	50.5 ± 11.2	1700 ± 378.8	3.1 ± 1.3
ETOH/Water_CC	52.2 ± 16.4	2306.3 ± 895.4	2.79 ± 1.3
1D_CC	46.5 ± 9.8	3322 ± 619.7	3.4 ± 0.99
2D_CC	52.1 ± 13.5	2276.7 ± 867.1	2.4 ± 0.6
5D_CC	56 ± 16.1	2555 ± 712.3	3.8 ± 1.9
Hemicellulose	45.4 ± 3.9	2568.3 ± 291.2	2.9 ± 0.04
Cellulose	50.5 ± 0.6	3449.4 ± 149	2.4 ± 0.4
Heated_CC	36.9 ± 6.7	3195.6 ± 246.7	1.4 ± 0.6

APPENDIX E

PURE WATER PERMEABILITY OF RG CELLULOSE MEMBRANE

PWP was calculated by the following equation where Q, A and ΔP denote the water permeation rate (L/h), effective filtration area of membrane (m^2) and pressure difference (bar), respectively.

$$PWP = \frac{Q}{A * \Delta P}$$

Table E.1. Recorded data for the test performed at 0.5 bar (run 1)

m(kg)	water density (kg/m3)	1/density (m3/kg)	m*1/density*1000 (L)	time(min)	time(hr)
0	1000	0.001	0	0	0.166667
0.00247	1000	0.001	0.00247	10	0.166667
0.00152	1000	0.001	0.00152	20	0.166667
0.00152	1000	0.001	0.00152	30	0.166667
0.00152	1000	0.001	0.00152	40	0.166667
0.00156	1000	0.001	0.00156	50	0.166667
0.00152	1000	0.001	0.00152	60	0.166667
0.00153	1000	0.001	0.00153	70	0.166667
0.00154	1000	0.001	0.00154	80	0.166667
0.00149	1000	0.001	0.00149	90	0.166667
0.00154	1000	0.001	0.00154	100	0.166667
0.00151	1000	0.001	0.00151	110	0.166667
0.00149	1000	0.001	0.00149	120	0.166667
0.00148	1000	0.001	0.00148	130	0.166667
0.0015	1000	0.001	0.0015	140	0.166667
0.00154	1000	0.001	0.00154	150	0.166667
0.00151	1000	0.001	0.00151	160	0.166667
0.00159	1000	0.001	0.00159	170	0.166667
0.00161	1000	0.001	0.00161	180	0.166667
0.00159	1000	0.001	0.00159	190	0.166667
0.00149	1000	0.001	0.00149	200	0.166667
0.00233	1000	0.001	0.00233	210	0.166667
0.00152	1000	0.001	0.00152	220	0.166667
0.00152	1000	0.001	0.00152	230	0.166667

Table E.1. Recorded data for the test performed at 0.5 bar (run 1) (continued)

m(kg)	water density (kg/m3)	1/density (m3/kg)	m*1/density*1000 (L)	time(min)	time(hr)
0.0015	1000	0.001	0.0015	240	0.166667
0.0016	1000	0.001	0.0016	250	0.166667
0.00156	1000	0.001	0.00156	260	0.166667
0.00152	1000	0.001	0.00152	270	0.166667
0.00152	1000	0.001	0.00152	280	0.166667
0.00148	1000	0.001	0.00148	290	0.166667
0.00148	1000	0.001	0.00148	300	0.166667
0.00152	1000	0.001	0.00152	310	0.166667
0.00141	1000	0.001	0.00141	320	0.166667
0.00149	1000	0.001	0.00149	330	0.166667
0.00142	1000	0.001	0.00142	340	0.166667
0.00149	1000	0.001	0.00149	350	0.166667
0.00143	1000	0.001	0.00143	360	0.166667

Table E.2. Flux and permeance of the membrane (run 1)

membrane area (m2)	presssure (bar)	flux	permeance
0.000314	0.5	0	0
0.000314	0.5	47.19745	94.3949
0.000314	0.5	29.04459	58.08917
0.000314	0.5	29.04459	58.08917
0.000314	0.5	29.04459	58.08917
0.000314	0.5	29.80892	59.61783
0.000314	0.5	29.04459	58.08917
0.000314	0.5	29.23567	58.47134
0.000314	0.5	29.42675	58.8535
0.000314	0.5	28.47134	56.94268
0.000314	0.5	29.42675	58.8535
0.000314	0.5	28.8535	57.70701
0.000314	0.5	28.47134	56.94268
0.000314	0.5	28.28025	56.56051
0.000314	0.5	28.66242	57.32484
0.000314	0.5	29.42675	58.8535
0.000314	0.5	28.8535	57.70701
0.000314	0.5	30.38217	60.76433
0.000314	0.5	30.76433	61.52866
0.000314	0.5	30.38217	60.76433
0.000314	0.5	28.47134	56.94268
0.000314	0.5	44.52229	89.04459
0.000314	0.5	29.04459	58.08917

Table E.2. Flux and permeance of the membrane (continued)

membrane area (m2)	presssure (bar)	flux	permeance
0.000314	0.5	29.04459	58.08917
0.000314	0.5	28.66242	57.32484
0.000314	0.5	30.57325	61.1465
0.000314	0.5	29.80892	59.61783
0.000314	0.5	29.04459	58.08917
0.000314	0.5	29.04459	58.08917
0.000314	0.5	28.28025	56.56051
0.000314	0.5	28.28025	56.56051
0.000314	0.5	29.04459	58.08917
0.000314	0.5	26.94268	53.88535
0.000314	0.5	28.47134	56.94268
0.000314	0.5	27.13376	54.26752
0.000314	0.5	28.47134	56.94268
0.000314	0.5	27.32484	54.64968

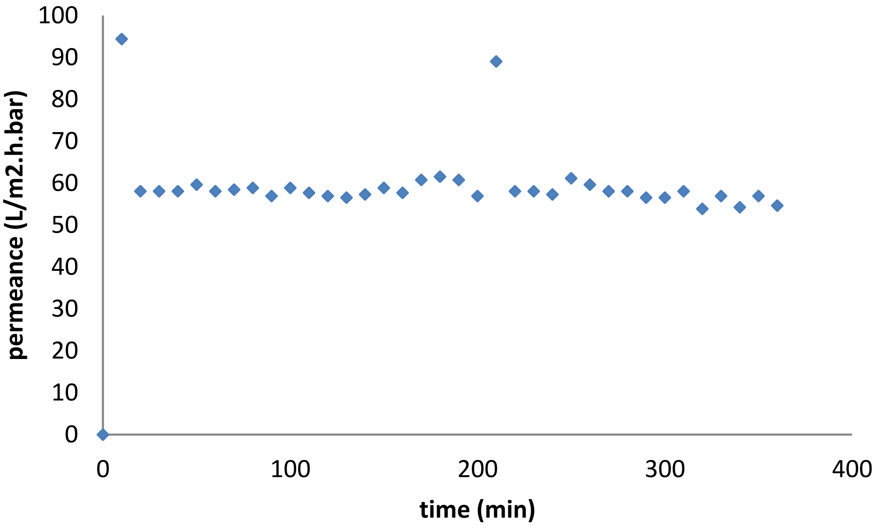

Figure E.1. Permeance of the membrane (run 1)

Table E.3. Recorded data for the test performed at 0.5 bar (run 2)

m(kg)	water density (kg/m3)	1/density (m3/kg)	m*1/density*1000 (L)
0	1000	0.001	0
0.00204	1000	0.001	0.00204

Table E.3. Recorded data for the test performed at 0.5 bar (run 2) (continued)

m(kg)	water density (kg/m3)	1/density (m3/kg)	m*1/density*1000 (L)
0.00105	1000	0.001	0.00105
0.00109	1000	0.001	0.00109
0.00141	1000	0.001	0.00141
0.0012	1000	0.001	0.0012
0.00132	1000	0.001	0.00132
0.00131	1000	0.001	0.00131
0.00136	1000	0.001	0.00136
0.00143	1000	0.001	0.00143
0.00138	1000	0.001	0.00138
0.0015	1000	0.001	0.0015
0.00135	1000	0.001	0.00135
0.00146	1000	0.001	0.00146
0.00145	1000	0.001	0.00145
0.0015	1000	0.001	0.0015
0.00142	1000	0.001	0.00142
0.00144	1000	0.001	0.00144
0.00148	1000	0.001	0.00148
0.00143	1000	0.001	0.00143
0.00144	1000	0.001	0.00144
0.00147	1000	0.001	0.00147

Table E.4. Flux and permeance of the membrane (run 2)

time(min)	time(hr)	membrane area (m2)	presssure (bar)	flux	permeance
0	0.166666667	0.000314	0.5	0	0
10	0.166666667	0.000314	0.5	38.98089164	77.96178
20	0.166666667	0.000314	0.5	20.06369423	40.12739
30	0.166666667	0.000314	0.5	20.82802544	41.65605
40	0.166666667	0.000314	0.5	26.94267511	53.88535
50	0.166666667	0.000314	0.5	22.92993626	45.85987
60	0.166666667	0.000314	0.5	25.22292989	50.44586
70	0.166666667	0.000314	0.5	25.03184708	50.06369
80	0.166666667	0.000314	0.5	25.98726109	51.97452
90	0.166666667	0.000314	0.5	27.32484071	54.64968
100	0.166666667	0.000314	0.5	26.3694267	52.73885
110	0.166666667	0.000314	0.5	28.66242032	57.32484
120	0.166666667	0.000314	0.5	25.79617829	51.59236
130	0.166666667	0.000314	0.5	27.89808912	55.79618
140	0.166666667	0.000314	0.5	27.70700631	55.41401
150	0.166666667	0.000314	0.5	28.66242032	57.32484
160	0.166666667	0.000314	0.5	27.13375791	54.26752
170	0.166666667	0.000314	0.5	27.51592351	55.03185

Table E.4. Flux and permeance of the membrane (run 2) (continued)

time(min)	time(hr)	membrane area (m2)	presssure (bar)	flux	permeance
180	0.166666667	0.000314	0.5	28.28025472	56.56051
190	0.166666667	0.000314	0.5	27.32484071	54.64968
200	0.166666667	0.000314	0.5	27.51592351	55.03185
210	0.166666667	0.000314	0.5	28.08917192	56.17834

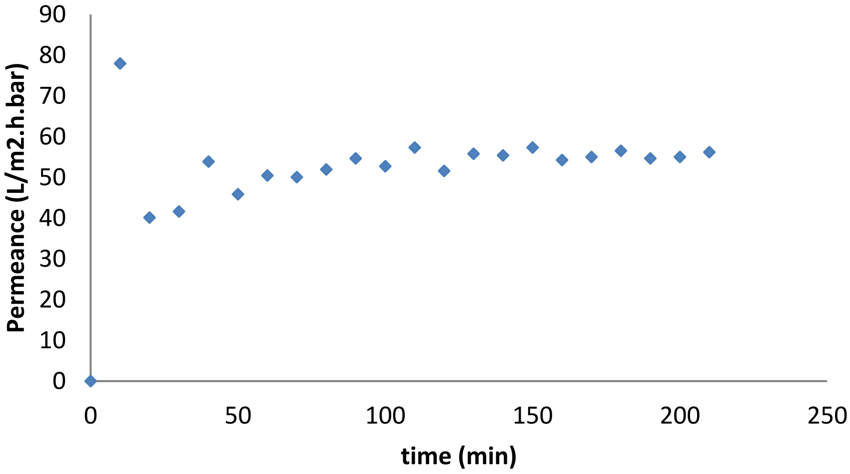

Figure E.2 Permeance of the membrane (run 2)

Table E.5. Recorded data for the test performed at 0.5 bar (run 3)

m(kg)	water density (kg/m3)	1/density (m3/kg)	m*1/density*1000 (L)
0	1000	0.001	0
0.00061	1000	0.001	0.00061
0.0012	1000	0.001	0.0012
0.0013	1000	0.001	0.0013
0.00136	1000	0.001	0.00136
0.00124	1000	0.001	0.00124
0.0012	1000	0.001	0.0012
0.00123	1000	0.001	0.00123
0.00116	1000	0.001	0.00116
0.00123	1000	0.001	0.00123
0.00125	1000	0.001	0.00125
0.00123	1000	0.001	0.00123
0.00124	1000	0.001	0.00124

Table E.5. Recorded data for the test performed at 0.5 bar (run 3) (continued)

0.00121	1000	0.001	0.00121
0.00123	1000	0.001	0.00123
0.00122	1000	0.001	0.00122
0.00128	1000	0.001	0.00128
0.00134	1000	0.001	0.00134
0.00135	1000	0.001	0.00135
0.00117	1000	0.001	0.00117
0.00123	1000	0.001	0.00123
0.00116	1000	0.001	0.00116
0.00122	1000	0.001	0.00122
0.00118	1000	0.001	0.00118
0.00122	1000	0.001	0.00122
0.00124	1000	0.001	0.00124
0.00132	1000	0.001	0.00132
0.00126	1000	0.001	0.00126
0.00123	1000	0.001	0.00123
0.00111	1000	0.001	0.00111
0.00114	1000	0.001	0.00114
0.00119	1000	0.001	0.00119
0.00115	1000	0.001	0.00115
0.00118	1000	0.001	0.00118
0.00123	1000	0.001	0.00123
0.00126	1000	0.001	0.00126
0.00121	1000	0.001	0.00121

Table E.6. Flux and permeance of the membrane (run 3)

time(min)	time(hr)	membrane area (m2)	pressure (bar)	flux	permeance
0	0.166667	0.000314	0.5	0	0
10	0.166667	0.000314	0.5	11.65605	23.3121
20	0.166667	0.000314	0.5	22.92994	45.85987
30	0.166667	0.000314	0.5	24.84076	49.68153
40	0.166667	0.000314	0.5	25.98726	51.97452
50	0.166667	0.000314	0.5	23.69427	47.38853
60	0.166667	0.000314	0.5	22.92994	45.85987
70	0.166667	0.000314	0.5	23.50318	47.00637
80	0.166667	0.000314	0.5	22.16561	44.33121
90	0.166667	0.000314	0.5	23.50318	47.00637
100	0.166667	0.000314	0.5	23.88535	47.7707
110	0.166667	0.000314	0.5	23.50318	47.00637
120	0.166667	0.000314	0.5	23.69427	47.38853
130	0.166667	0.000314	0.5	23.12102	46.24204

Table E.6. Flux and permeance of the membrane (run 3) (continued)

time(min)	time(hr)	membrane area (m2)	pressure (bar)	flux	permeance
140	0.166667	0.000314	0.5	23.50318	47.00637
150	0.166667	0.000314	0.5	23.3121	46.6242
160	0.166667	0.000314	0.5	24.4586	48.9172
170	0.166667	0.000314	0.5	25.6051	51.21019
180	0.166667	0.000314	0.5	25.79618	51.59236
190	0.166667	0.000314	0.5	22.35669	44.71338
200	0.166667	0.000314	0.5	23.50318	47.00637
210	0.166667	0.000314	0.5	22.16561	44.33121
220	0.166667	0.000314	0.5	23.3121	46.6242
230	0.166667	0.000314	0.5	22.54777	45.09554
240	0.166667	0.000314	0.5	23.3121	46.6242
250	0.166667	0.000314	0.5	23.69427	47.38853
260	0.166667	0.000314	0.5	25.22293	50.44586
270	0.166667	0.000314	0.5	24.07643	48.15287
280	0.166667	0.000314	0.5	23.50318	47.00637
290	0.166667	0.000314	0.5	21.21019	42.42038
300	0.166667	0.000314	0.5	21.78344	43.56688
310	0.166667	0.000314	0.5	22.73885	45.47771
320	0.166667	0.000314	0.5	21.97452	43.94904
330	0.166667	0.000314	0.5	22.54777	45.09554
340	0.166667	0.000314	0.5	23.50318	47.00637
350	0.166667	0.000314	0.5	24.07643	48.15287
360	0.166667	0.000314	0.5	23.12102	46.24204

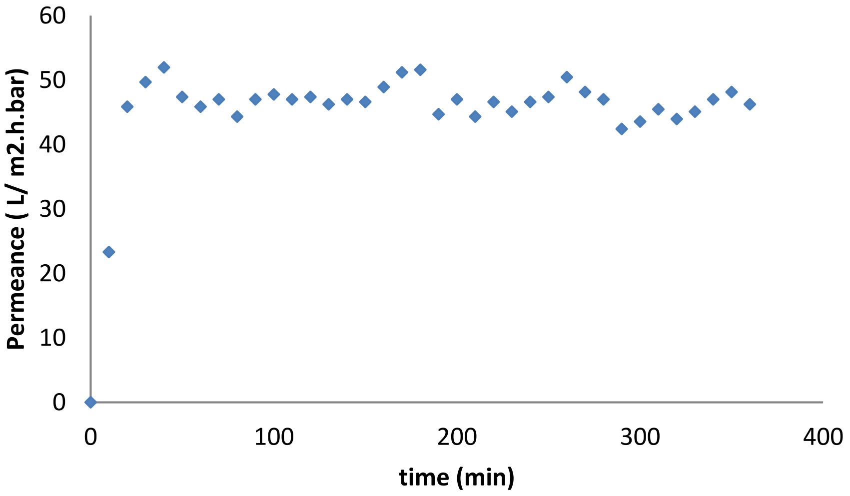

Figure E.3. Permeance of the membrane (run 3)

Table E.7. Recorded data for the test performed at 1 bar (run 4)

m(kg)	water density (kg/m3)	1/density (m3/kg)	m*1/density*1000 (L)
0	1000	0.001	0
0.0289	1000	0.001	0.0289
0.02194	1000	0.001	0.02194
0.01677	1000	0.001	0.01677
0.0144	1000	0.001	0.0144
0.01248	1000	0.001	0.01248
0.01156	1000	0.001	0.01156
0.01049	1000	0.001	0.01049
0.00961	1000	0.001	0.00961
0.0093	1000	0.001	0.0093
0.00918	1000	0.001	0.00918
0	1000	0.001	0
0.00754	1000	0.001	0.00754
0.00718	1000	0.001	0.00718
0.00677	1000	0.001	0.00677
0.00678	1000	0.001	0.00678
0.00666	1000	0.001	0.00666
0.00637	1000	0.001	0.00637
0.00643	1000	0.001	0.00643
0.00632	1000	0.001	0.00632
0.00598	1000	0.001	0.00598
0.00554	1000	0.001	0.00554
0.00544	1000	0.001	0.00544
0.00566	1000	0.001	0.00566
0.0056	1000	0.001	0.0056
0.00527	1000	0.001	0.00527
0.00509	1000	0.001	0.00509
0.005	1000	0.001	0.005
0.00507	1000	0.001	0.00507

Table E.8. Flux and permeance of the membrane (run 4)

time(min)	time(hr)	membrane area (m2)	presssure (bar)	flux	permeance
0	0.166667	0.000314	1	0	0
10	0.166667	0.000314	1	552.2293	552.2293
20	0.166667	0.000314	1	419.2357	419.2357
30	0.166667	0.000314	1	320.4459	320.4459
40	0.166667	0.000314	1	275.1592	275.1592
50	0.166667	0.000314	1	238.4713	238.4713
60	0.166667	0.000314	1	220.8917	220.8917
70	0.166667	0.000314	1	200.4459	200.4459

Table E.8. Flux and permeance of the membrane (run 4) (continued)

time(min)	time(hr)	membrane area (m2)	presssure (bar)	flux	permeance
80	0.166667	0.000314	1	183.6306	183.6306
90	0.166667	0.000314	1	177.707	177.707
100	0.166667	0.000314	1	175.414	175.414
110	0.166667	0.000314	1	144.0764	144.0764
120	0.166667	0.000314	1	137.1975	137.1975
130	0.166667	0.000314	1	129.3631	129.3631
140	0.166667	0.000314	1	129.5541	129.5541
150	0.166667	0.000314	1	127.2611	127.2611
160	0.166667	0.000314	1	121.7197	121.7197
170	0.166667	0.000314	1	122.8662	122.8662
180	0.166667	0.000314	1	120.7643	120.7643
190	0.166667	0.000314	1	114.2675	114.2675
200	0.166667	0.000314	1	105.8599	105.8599
210	0.166667	0.000314	1	103.949	103.949
220	0.166667	0.000314	1	108.1529	108.1529
230	0.166667	0.000314	1	107.0064	107.0064
240	0.166667	0.000314	1	100.7006	100.7006
250	0.166667	0.000314	1	97.26115	97.26115
260	0.166667	0.000314	1	95.5414	95.5414
270	0.166667	0.000314	1	96.87898	96.87898

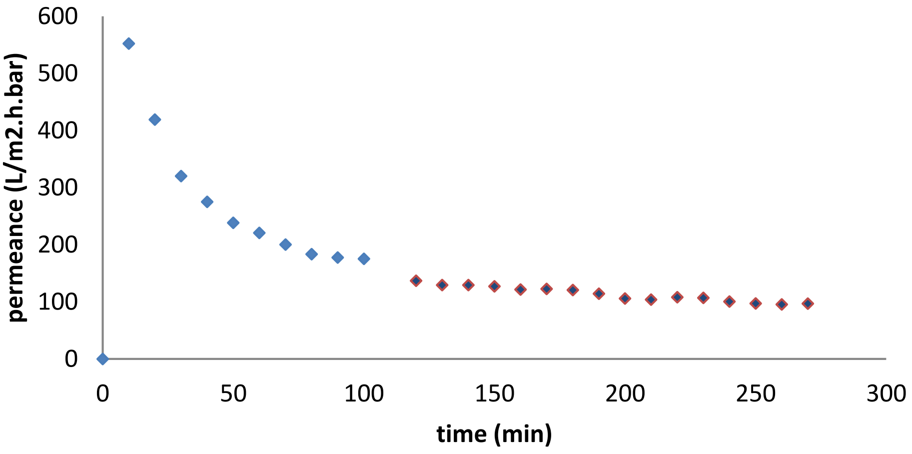

Figure E.4. Permeance of the membrane (run 4)

Table E.9. Recorded data for the test performed at 1 bar (run 5)

m(kg)	water density (kg/m3)	1/density (m3/kg)	m*1/density*1000 (L)
0	1000	0.001	0
0.00298	1000	0.001	0.00298
0.0037	1000	0.001	0.0037
0.004	1000	0.001	0.004
0.00428	1000	0.001	0.00428
0.00439	1000	0.001	0.00439
0.00433	1000	0.001	0.00433
0.00438	1000	0.001	0.00438
0.00439	1000	0.001	0.00439
0.00425	1000	0.001	0.00425
0.00431	1000	0.001	0.00431
0.0043	1000	0.001	0.0043
0.00415	1000	0.001	0.00415
0.00427	1000	0.001	0.00427
0.00419	1000	0.001	0.00419
0.00413	1000	0.001	0.00413
0.00409	1000	0.001	0.00409
0.00396	1000	0.001	0.00396
0.00374	1000	0.001	0.00374
0.00396	1000	0.001	0.00396

Table E.10. Flux and permeance of the membrane (run 5)

time(min)	time(hr)	membrane area (m2)	presssure (bar)	flux	permeance
0	0.166667	0.000314	1	0	0
10	0.166667	0.000314	1	56.94268	56.94268
20	0.166667	0.000314	1	70.70064	70.70064
30	0.166667	0.000314	1	76.43312	76.43312
40	0.166667	0.000314	1	81.78344	81.78344
50	0.166667	0.000314	1	83.88535	83.88535
60	0.166667	0.000314	1	82.73885	82.73885
70	0.166667	0.000314	1	83.69427	83.69427
80	0.166667	0.000314	1	83.88535	83.88535
90	0.166667	0.000314	1	81.21019	81.21019
100	0.166667	0.000314	1	82.35669	82.35669
110	0.166667	0.000314	1	82.16561	82.16561
120	0.166667	0.000314	1	79.29936	79.29936
130	0.166667	0.000314	1	81.59236	81.59236
140	0.166667	0.000314	1	80.06369	80.06369
150	0.166667	0.000314	1	78.9172	78.9172
160	0.166667	0.000314	1	78.15287	78.15287

Table E.10. Flux and permeance of the membrane (run 5) (continued)

time(min)	time(hr)	membrane area (m2)	presssure (bar)	flux	permeance
170	0.166667	0.000314	1	75.66879	75.66879
180	0.166667	0.000314	1	71.46497	71.46497
190	0.166667	0.000314	1	75.66879	75.66879

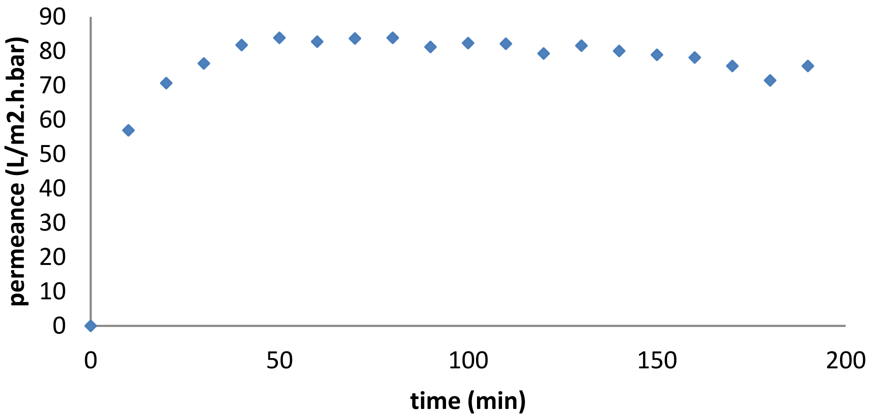

Figure E.5. Permeance of the membrane (run 5)

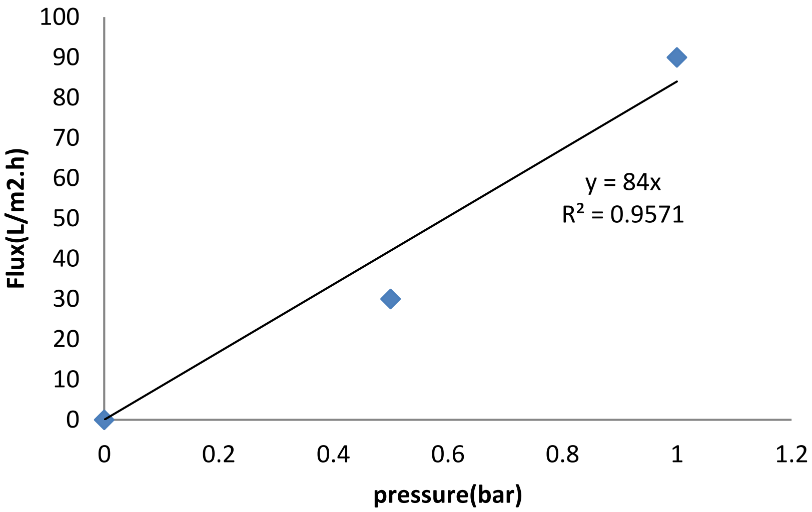

Figure E.6. Flux vs. pressure graph of the membrane

APPENDIX F

BSA AND SODIUM ALGINATE SEPARATION RG CELLULOSE MEMBRANE

A sample calculation for BSA retention at 9 min

The BSA rejection was calculated by the following equation where C_p and C_f are the solute concentrations in the permeate and feed solutions, respectively.

$$Rejection\ (R) = \left(1 - \frac{C_P}{C_F}\right) * 100$$

$$C_P = 0.573\ at\ 220\ nm\ vavelenght$$

$$C_F = 0.672\ at\ 220\ nm\ vavelenght$$

$$Rejection\ (R) = \left(1 - \frac{0.573}{0.672}\right) * 100 = 14.73\%$$

Table F.1. Recorded data for BSA retention

CODE	duratıon (min)	Wbeaker+tube (gr)	Wbeaker+tube (gr)	Weight difference (gr)	PRESSURE (BAR)
P1	8	53.0771	56.4201	3.343	0.3
P2	8.42	52.9953	56.5769	3.5816	0.25
P3	9.12	53.06	56.715	3.655	0.25
P4	9.27	53.0686	56.8602	3.7916	0.25
P5	9	53.0412	56.0732	3.032	0.25
P6	9	53.0485	56.5633	3.5148	0.25
P7	9	53.0354	56.6459	3.6105	0.25
P8	9	52.9837	56.7067	3.723	0.25
P9	9	53.0086	56.6394	3.6308	0.25
R (retentate)		52.9568	56.5236	3.5668	
I (initial)		52.9556	57.5879	4.6323	

Table F.2. BSA retention of the membrane

CODE	ABS	%retention	time (min)
PBS	reference (buffer solution)		
Initial	0.672		
P1	0.573	0	0
P2	0.569	14.7321429	9
P3	0.582	15.327381	18
P4	0.604	13.3928571	27
P5	0.641	10.1190476	36
P6	0.654	4.61309524	45
P7	0.608	2.67857143	54
P8	0.627	9.52380952	63
P9	0.683	6.69642857	72
R	1	-1.6369048	81

Table F.3. Recorded data for sodium alginate retention

Weight difference (gr)	Weight difference (kg)	DURATION (min)	DURATION (H)	PRESSURE (BAR)
0	0	0	0	0.3
4.1	0.0041	14	0.233333333	0.3
3.41	0.00341	14	0.233333333	0.25
3.53	0.00353	15	0.25	0.25
3.18	0.00318	15	0.25	0.25
3.15	0.00315	15	0.25	0.25
2.73	0.00273	15	0.25	0.25
2.6	0.0026	15	0.25	0.25
3.08	0.00308	20	0.333333333	0.25
2.85	0.00285	20	0.333333333	0.25

Table F.4. Sodium alginate retention of the membrane

CODE	ABS	%retention	time (min)
FEED	0.082	0	0
P1	0.112	-36.58536585	15
P2	0.059	28.04878049	40
P3	0.059	28.04878049	86

Table F.4. Sodium alginate retention of the membrane (continued)

CODE	ABS	%retention	time (min)
P4	0.079	3.658536585	123
P5	0.103	-25.6097561	158
P6	0.08	2.43902439	194
P7	0.088	-7.317073171	229
P8	0.087	-6.097560976	269
P9	0.091	-10.97560976	302

Determining the UV-vis wavelength to detect concentrations in the permeate and feed solutions

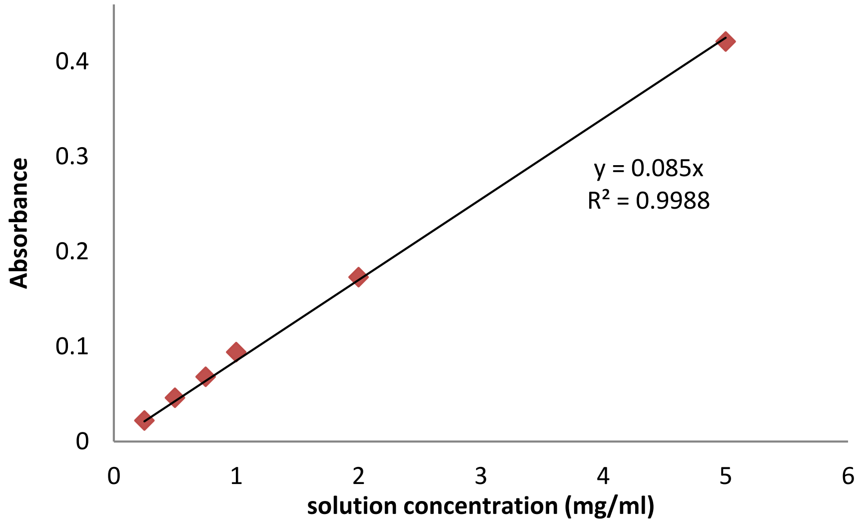

Figure F.1. Absorbance vs. solution concentration

Table F.5. Absorbance values of sodium alginate solutions with different concentration at 260 nm wavelength

concentration (mg/ml)	wavelenght (nm)	absorbance (A)
5	260	0.421
2	260	0.173
1	260	0.094

Table F.5. Absorbance values of sodium alginate solutions with different concentration at 260 nm wavelength (continued)

concentration (mg/ml)	wavelenght (nm)	absorbance (A)
0.75	260	0.068
0.5	260	0.046
0.25	260	0.022

APPENDIX G

XRD PATTERNS OF CORN COB, ITS CELLULOSE RICH PORTION AND 1D_CC FILM

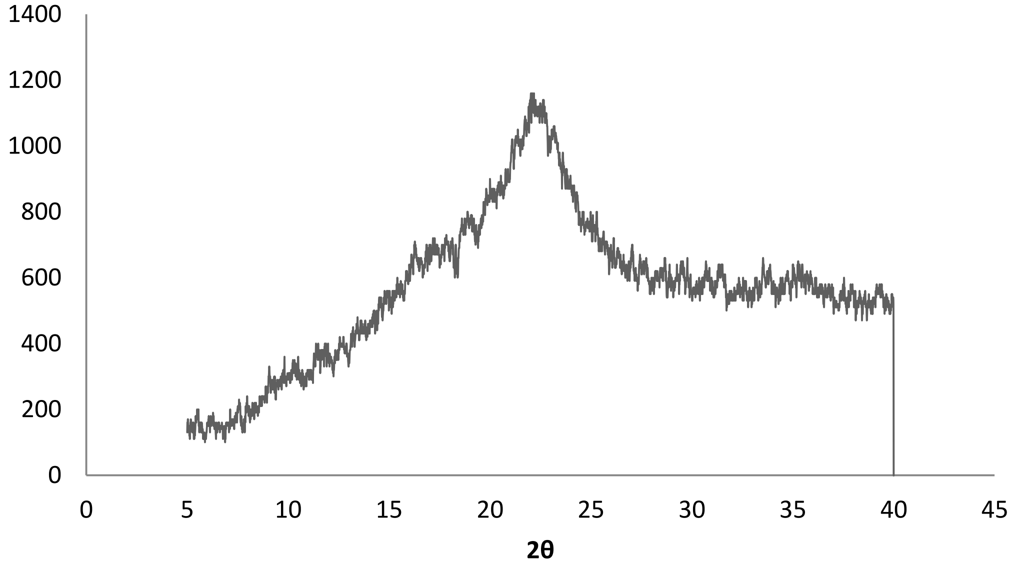

Figure G.1. XRD pattern of corn cob

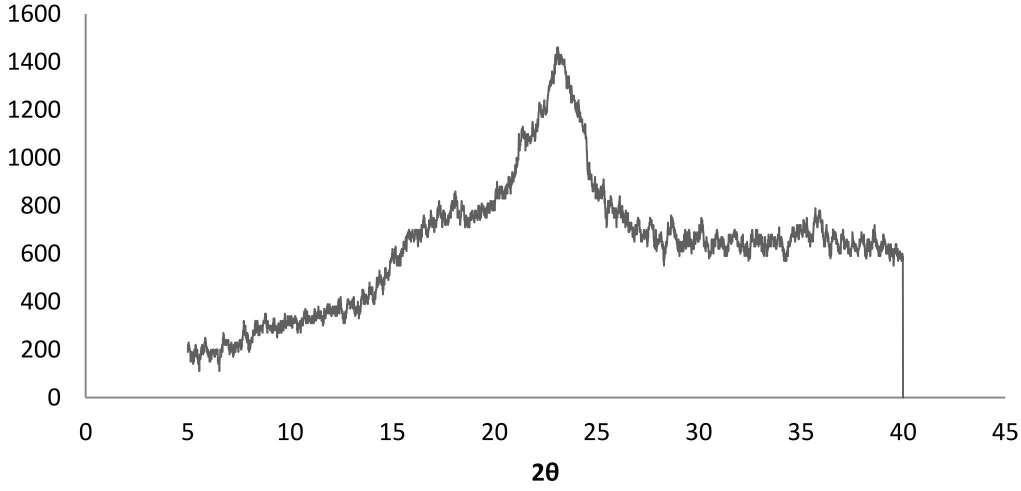

Figure G.2. XRD pattern of cellulose rich portion of corn cob

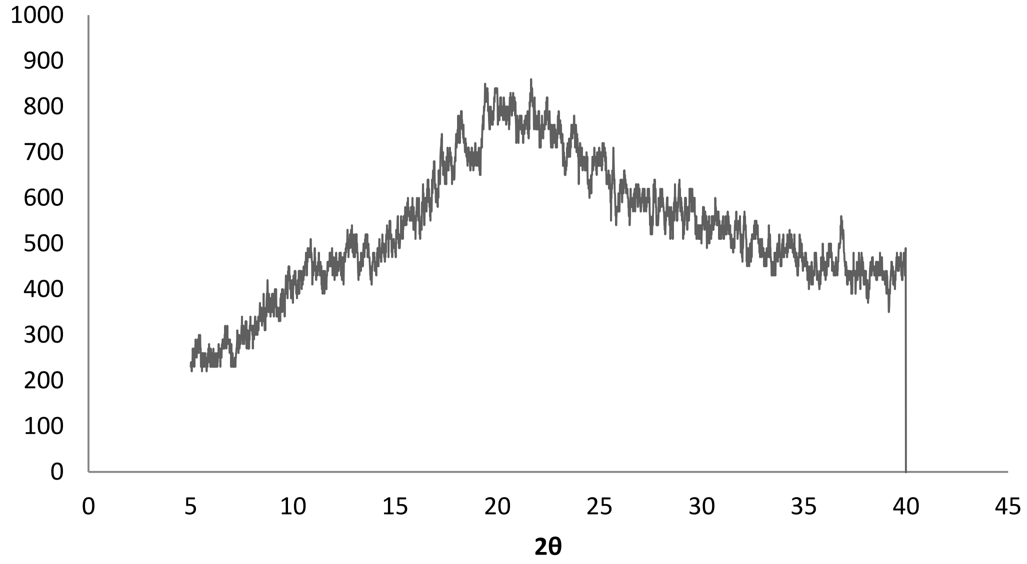

Figure G.3. XRD pattern 1D_CC film

APPENDIX H

FT-IR SPECTRA OF THE FILMS

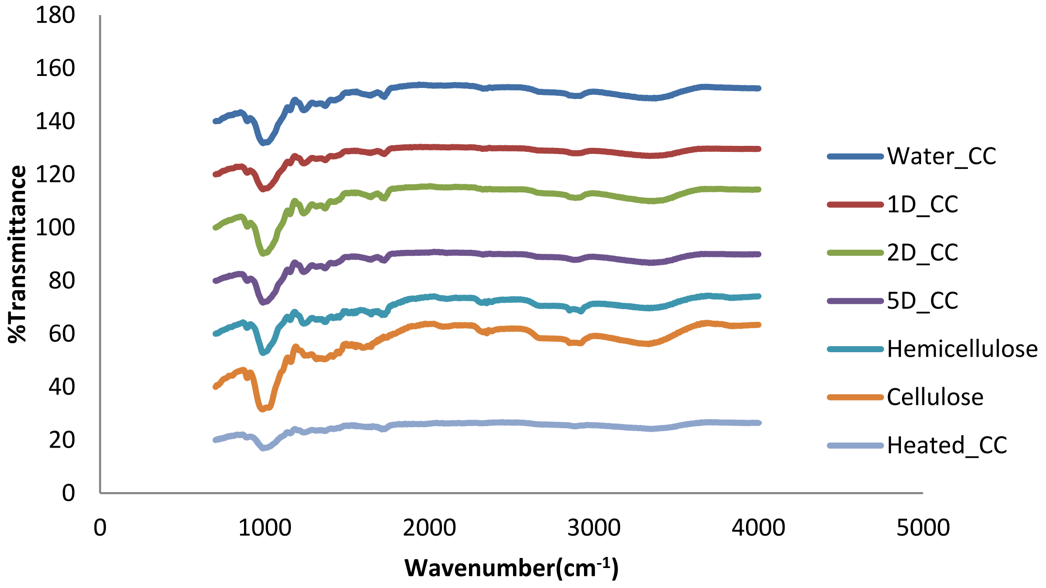

Figure H.1. FT-IR spectra of the films.